UNIVERSIDADE ESTADUAL PAULISTA - UNESP

Faculdade de Engenharia - Campus de Bauru

THALITA LACERDA DOS SANTOS

DOMESTIC WASTEWATER TREATMENT IN ALGAL-BACTERIAL COLUMN PHOTOBIOREACTORS:

IMPACTS OF OPERATIONAL CONDITIONS AND SUPPORT MEDIA

Bauru

2026

THALITA LACERDA DOS SANTOS

DOMESTIC WASTEWATER TREATMENT IN ALGAL-BACTERIAL COLUMN PHOTOBIOREACTORS:

IMPACTS OF OPERATIONAL CONDITIONS AND SUPPORT MEDIA

Tese apresentada à Universidade Estadual Paulista (UNESP), Faculdade de Engenharia, Bauru, para obtenção do título Doutora em Engenharia Civil e Ambiental.

Área de Concentração: Saneamento ambiental

Orientador(a): Prof. Dr. Gustavo Henrique Ribeiro da Silva

Coorientador(a): Prof. Dr. Raúl Muñoz Torre

Bauru

2026

S237d

Santos, Thalita Lacerda dos
Domestic wastewater treatment in algal-bacterial column photobioreactors : impacts of operational conditions and support media / Thalita Lacerda dos Santos. -- Bauru, 2026
151 p. : il., tabs., fotos

Tese (doutorado) - Universidade Estadual Paulista (UNESP), Faculdade de Engenharia, Bauru
Orientador: Gustavo Henrique Ribeiro da Silva
Coorientador: Raúl Muñoz Torre

1. Single-stage photobioreactor. 2. Nutrient recovery. 3. Domestic wastewater treatment. 4. Biomass production. I. Título.

Sistema de geração automática de fichas catalográficas da Unesp. Dados fornecidos pelo autor(a).

IMPACTO POTENCIAL DESTA PESQUISA

O foco dessa tese foi o desenvolvimento de um fotobiorreator tubular vertical de estágio único para remoção de carbono e nutrientes em efluente doméstico, gerando impactos em diferentes áreas.

Do ponto de vista técnico-científico, a tese avançou no conhecimento sobre as interações entre microalgas e bactérias em sistemas de estágio único, otimizando parâmetros operacionais e investigando o uso de um meio suporte (mini-Biobob). O aspecto inovador no âmbito socioambiental se destaca pelo avanço no desenvolvimento de tecnologia compacta para saneamento descentralizado, com potencial para inserção em espaços urbanos densos, carentes de infraestrutura e com restrição de área, alinhando o tratamento de efluentes à visão da economia circular. No âmbito econômico, a recuperação de carbono, nitrogênio e fósforo via produção de biomassa pode gerar insumos com potencial biotecnológico. A pesquisa também contribui para a formação educacional e cultural de recursos humanos na interface entre engenharia sanitária, biotecnologia e sustentabilidade, integrando o saneamento como vetor de saúde pública, justiça ambiental e economia circular.

O estudo se alinha com os Objetivos de Desenvolvimento Sustentável (ODS) da ONU, contribuindo para: (i) água potável e saneamento (ODS 6), pela melhoria da eficiência do tratamento de efluentes e (ii) proteção da vida aquática (ODS 14), ao reduzir a descarga de nutrientes eutrofizantes. Desta forma, os resultados oferecem soluções para mitigação da poluição hídrica e promoção do desenvolvimento sustentável.

POTENTIAL IMPACT OF THIS RESEARCH

This thesis focused on the development of a single-stage column photobioreactor aimed at removing carbon and nutrients from domestic wastewater, with implications for several fields. From a scientific and technical perspective, the thesis advances knowledge on microalgal-bacterial interactions in single-stage systems, optimizes operational parameters, and investigates the use of support media (mini-Biobob). The socio-environmental innovative aspect lies in the application of single-stage column photobioreactors as a compact technology for decentralized sanitation, with potential for deployment in dense, infrastructure-poor urban areas with space constraints, enabling wastewater treatment through a circular economy approach. From an economic standpoint, nutrient recovery via biomass production can generate valuable inputs with biotechnological potential. The research also contributes to the educational and cultural formation of human resources at the interface between sanitary engineering, biotechnology, and sustainability, integrating sanitation as a vector for public health, environmental justice, and circular economy.

The study aligns with the United Nations Sustainable Development Goals (SDGs), contributing to: (i) clean water and sanitation (SDG 6) by improving wastewater treatment efficiency; and (ii) life below water (SDG 14) by reducing the discharge of eutrophication nutrients. The results provide solutions to mitigate water pollution and to promote sustainable development.

UNIVERSIDADE ESTADUAL PAULISTA

Câmpus de Bauru

DEFESA DE TESE DE DOUTORADO DO PROGRAMA DE PÓS-GRADUAÇÃO EM ENGENHARIA CIVIL E AMBIENTAL

DISCENTE: THALITA LACERDA DOS SANTOS

TÍTULO: DOMESTIC WASTEWATER TREATMENT IN ALGAL-BACTERIAL COLUMN PHOTOBIOREACTORS: IMPACTS OF OPERATIONAL CONDITIONS AND SUPPORT MEDIA

Data: 16 de julho de 2026

Local: https://meet.google.com/zvi-gtqr-rdz

APROVADO (X) REPROVADO ( )

PARECER CIRCUNSTANCIADO:

A candidata apresentou sua tese de doutorado de forma clara, objetiva e organizada, respeitando o tempo estabelecido para a defesa. Demonstrou domínio do tema, da metodologia empregada e dos resultados obtidos. Durante a arguição, respondeu às questões formuladas pela banca com segurança, clareza e embasamento científico, evidenciando maturidade acadêmica e capacidade de discussão crítica.

Diante da qualidade do trabalho e do excelente desempenho na apresentação e na defesa, manifesto parecer favorável à

Bauru, 16 de julho de 2026

Documento assinado digitalmente
GUSTAVO HENRIQUE RIBEIRO DA SILVA
Data: 17/07/2026 13:19:09-0300
Verifique em https://validar.iti.gov.br

Prof. Dr. Gustavo Henrique Ribeiro da Silva

TORRES FRANCO ANDRES FELIPE - 60457325P
Firmado digitalmente por TORRES FRANCO ANDRES FELIPE - 60457325P
Fecha: 2026.07.17 22:05:58 +02'00'

Prof. Dr. Andres Felipe Torres Franco

Documento assinado digitalmente
MARIA DE LOURDES FLORENCIO DOS SANTOS
Data: 20/07/2026 17:16:12-0300
Verifique em https://validar.iti.gov.br

Profª. Drª. Maria de Lourdes Florencio dos Santos

Profª. Drª. Rosana de Cassia de Souza Schneider

Prof. Dr. Cesar Rossas Mota Filho

Documento assinado digitalmente
ROSANA DE CASSIA DE SOUZA SCHNEIDER
Data: 21/07/2026 19:12:16-0300
Verifique em https://validar.iti.gov.br

Documento assinado digitalmente
CESAR ROSSAS MOTA FILHO
Data: 04/08/2026 16:13:37-0300
Verifique em https://validar.iti.gov.br

Para Loriza e Luiza, por quem e com quem tudo é possível

AGRADECIMENTOS

A realização deste trabalho é resultado da parceria e suporte de tantas pessoas e instituições que, de diferentes maneiras, contribuíram para que eu chegasse até aqui.

Agradeço à Coordenação de Aperfeiçoamento de Pessoal de Nível Superior (CAPES) – Código de Financiamento 001 e no âmbito do Programa CAPES-PrInt (Projeto nº 88887.194785/2018-00; Processo nº 88887.892272/2023-00). Agradeço o Conselho Nacional de Desenvolvimento Científico e Tecnológico (CNPq; Processo nº 308663/2021–7). Agradeço à Fundação de Amparo à Pesquisa do Estado de São Paulo (FAPESP), pelo apoio financeiro, concedido por meio do Processo nº 2024/09344-9.

Ao Prof. Dr. Gustavo Henrique Ribeiro da Silva, meu sincero agradecimento pela orientação segura, pelos ensinamentos que vão além da ciência e pelos momentos de aprendizado genuíno que levarei comigo.

Al Prof. Dr. Raúl Muñoz, mi sincera gratitud, no solo por la co-orientación y la dedicación, sino por haber reavivado en mí el orgullo de ser ingeniera química. Gracias por las discusiones técnicas que siempre fueron mucho más que eso, y por la inspiración personal que trasciende lo académico. Es, sin duda, uno de los científicos más brillantes y productivos que he conocido.

I would like to express my special gratitude to Laura, my tutor, for all her dedication and attention to my training as a scientist. Her participation in this process was a turning point, a mark that will remain forever in my development.

Estendo meus agradecimentos ao DAE Bauru e aos técnicos do Laboratório de Saneamento da Unesp, pelo suporte essencial ao longo dos experimentos. Aos colegas da pós-graduação da UNESP Bauru e do *Institute of Sustainable Processes* (ISP) da Universidade de Valladolid, pela convivência, pelas trocas e pelo companheirismo.

Aos amigos do "nosso país" Pernambuco, guardo com especial carinho: Micaías e Hortência, o bonde afetuoso que torna meus dias mais leves; Luciana, a mana cujas palavras de incentivo sempre chegam como brisa na hora exata; e Igor, cujo cuidado e amizade verdadeira são porto seguro. A Pedro, Fab, Mihai e Sol, agradeço pelas parcerias acadêmicas que suavizaram o percurso e pelas trocas que embelezaram cada descoberta. *En español, quiero agradecer especialmente a Elisa, por su cálida amistad y sus divertidas clases de español, que trascendieron el idioma y se convirtieron en abrazos en forma de palabras.*

Bruna e Nataliia, a Espanha jamais seria a mesma sem vocês!!! Obrigada por cada risada, cada conversa, cada momento partilhado. É uma honra ser chamada de amiga por vocês.

Que essa parceria tão bonita, dentro e fora do laboratório, continue florescendo em todos os continentes!

(*In English to my Bestie Nat: Bruna and Nataliia, Spain would never be the same without you!!! Thank you for every laugh, every conversation, every shared moment. It's an honour to be called a friend by you. May this special partnership inside and outside the lab continue to bear beautiful fruits on every continent!*)

À minha Amiga Débora, com A maiúsculo, meu reconhecimento por uma amizade que é farol, porto e casa ao mesmo tempo.

A todos os amigos e colegas, que embora não citados nominalmente, significaram apoio ao longo desta importante etapa.

E agradeço de maneira muito especial o apoio, o incentivo e o amor da parte mais importante da minha vida:

Ao Zeus, meu parceirinho especialista em fazer sorrir, quanta leveza você traz aos meus dias, quanta alegria em forma de olhar e rabinho ‘abanante’.

À minha vó Luiza... ah que saudade, vozinha... Sua força, sua doçura e sua determinação permanecem em mim como herança e inspiração. Esta conquista também é sua!

E à minha mãe Loriza, minha base, minha dupla, minha conexão mais profunda. Mãe, cada página escrita tem um pouco do seu apoio e do seu amor incondicional. Sou o que sou porque você é quem é. Sua filha é doutora! E isso é tão seu quanto meu. Te amo!

“A reta é uma curva que não sonha”

(Manoel de Barros)

RESUMO

O saneamento global enfrenta desafios ambientais, sociais e tecnológicos, agravados pelo crescimento populacional e pelas mudanças climáticas, evidenciando a necessidade de transição para estruturas resilientes baseadas na bioeconomia circular. Esta pesquisa investigou o uso de fotobiorreatores tubulares verticais para o cultivo de microalgas e bactérias como uma estratégia sustentável para o tratamento de esgoto doméstico e produção de biomassa.

O trabalho foi dividido em três estudos complementares. O primeiro avaliou os efeitos operacionais no desempenho do fotobiorreator, demonstrando que a redução do tempo de detenção hidráulica aumentou significativamente a remoção de carbono total e nitrogênio, enquanto a redução do tempo de retenção de sólidos preveniu o acúmulo de nitrito e resultou em níveis indetectáveis de N_2O. O segundo aprofundou a investigação dos mecanismos de remoção de nitrogênio, adicionando a alil-tioureia como uma ferramenta para inibir seletivamente a nitrificação bacteriana. Os resultados revelaram que a inibição da nitrificação reduziu a taxa de remoção de NH_4^+ e aumentou a contribuição da assimilação microalgal, evidenciando que a assimilação é a rota dominante no sistema estudado, embora a via bacteriana seja necessária para a elevar os níveis globais de remoção. Adicionalmente, as mudanças na estrutura da comunidade microbiana decorrentes da inibição reduziram a eficiência de remoção de carbono orgânico total e aumentaram a assimilação de carbono na biomassa. O terceiro avaliou o uso de um meio suporte (mini-Biobob) para a fixação de biomassa. Apesar do aumento da biomassa aderida, os resultados não demonstraram ganhos relevantes na remoção de carbono, nitrogênio e fósforo, sugerindo que o uso de meio suporte pode causar atenuação de luz e limitações hidrodinâmicas, comprometendo o desempenho global do processo.

A tese demonstra que fotobiorreatores tubulares verticais de estágio único são uma tecnologia promissora para o tratamento descentralizado de esgoto doméstico, podendo figurar como uma alternativa em áreas com restrição de espaço. A elucidação das rotas microbiológicas reforça o papel da assimilação algal, enquanto os testes com meio suporte indicam que fatores foto-hidrodinâmicos são críticos e devem ser equilibrados. Em suma, a pesquisa avança no conhecimento das interações microalga-bactéria e fornece diretrizes operacionais para o escalonamento do processo.

***Palavras-chave*:** fotobiorreator de estágio único, recuperação de nutrientes, tratamento de efluentes domésticos, produção de biomassa.

ABSTRACT

Global sanitation faces environmental, social, technological challenges, which are exacerbated by population growth and climate change, highlighting the urgent need to transition towards resilient framework based on circular bioeconomy. This research investigated the use of column photobioreactor for the cultivation of microalgal–bacterial consortium as a sustainable strategy for domestic wastewater treatment and biomass production.

The work was divided into three complementary studies. The first study evaluated the operational effects on photobioreactor performance, demonstrating that reducing the hydraulic retention time significantly increased total carbon and nitrogen removal, whilst reducing the solids retention time prevented nitrite accumulation and resulted in undetectable levels of N_2O. The second study deepened the investigation into nitrogen removal mechanisms by using allylthiourea as an operational tool to selectively inhibit bacterial nitrification. The results revealed that nitrification inhibition reduced the NH_4^+ removal rate and increased the contribution of microalgal assimilation, demonstrating that assimilation is the dominant pathway in the studied system, although the bacterial pathway is necessary to raise removal levels. Additionally, shifts in the microbial community structure resulting from this inhibition reduced total organic carbon removal efficiency and increased carbon assimilation into biomass. The third study evaluated the use of a support media (mini-Biobob) for biomass attachment. Despite the increased in attached biomass, the results showed no significant improvements in carbon, nitrogen and phosphorus removal efficiencies, suggesting that the use of support media may cause light attenuation and hydrodynamic limitations, thereby compromising the overall treatment performance.

This thesis demonstrates that single-stage column photobioreactors are a promising technology for decentralised domestic wastewater treatment, potentially serving as an alternative in space-constrained areas. The elucidation of microbiological pathways reinforces the role of algal assimilation, while the use of support media indicate that photo-hydrodynamic factors are critical and must be balanced. This research contributes to advancing knowledge on microalgae-bacteria interactions and provides operational guidelines for process scale-up.

***Keywords*:** single-stage photobioreactor, nutrient recovery, domestic wastewater treatment, biomass production.

LIST OF FIGURES

LIST OF TABLES

TABLE OF CONTENTS

1. Introduction and thesis outline

1.1. THESIS SCOPE AND OUTLINE

The focus of this thesis is the development and optimization of microalgae-based systems for nutrient recovery from domestic wastewater, aiming to support sustainable sanitation practices and the transition towards a circular economy. In densely populated urban settlements (e.g., favelas), where space is severely limited and conventional sanitation infrastructure is often lacking, compact and high-productivity technologies are urgently needed. Column PBR offer a promising pathway for decentralized treatment due to their high nutrient removal rates per unit area, potential for biomass valorisation, and suitability for modular, space-efficient deployment.

This thesis addresses four key areas of innovation in microalgae-based wastewater treatment: advancements in column PBR design, elucidation of algal-bacterial symbioses, process optimization and identification of operational challenges. These knowledge gaps are summarized visually in Figure 1. The specific objectives of this research are: (1) to utilize microalgae as a tool to recover nitrogen and phosphorus from domestic wastewater and (2) to improve the operational performance of PBR systems by maximizing nutrient removal and the biomass productivity, thereby contributing to the development of decentralized sanitation solutions for underserved urban communities.

- Chapter 1 presents the state of the art on microalgae-based wastewater treatment systems, including a comprehensive review of nutrient removal mechanisms, current technological configurations, and operational bottlenecks.
- Chapter 2 describes the two studied systems: the single-stage column PBR and the column PBR with support media. The mains objectives of each study and the analytical procedures, and calculations are explained.
- Chapter 3 evaluates the effects of HRT, biomass concentration and illuminated surface area (S/V) ratio on the performance of a single-stage PBR.
- Chapter 4 investigates the mechanisms of nitrogen removal. In this experiment, allylthiourea, a selective nitrification inhibitor, was added to suppress bacterial activity and investigate the interplay between nutrient and carbon removal pathways in the single-stage microalgal-bacterial photobioreactor treating domestic wastewater.

- Chapter 5 examines the use of a support media (mini-Biobob) in vertical column PBR to assess its effects on nutrient removal. To evaluate the impact of increased surface area on biomass production and nutrient removal, three reactor configurations were tested: Control (no support media), ½ BB and ⅓ BB, with increasing surface area.
- Chapter 6 presents the overall conclusions of the thesis, its contribution to understanding microalgae-bacteria interactions, and research perspectives.

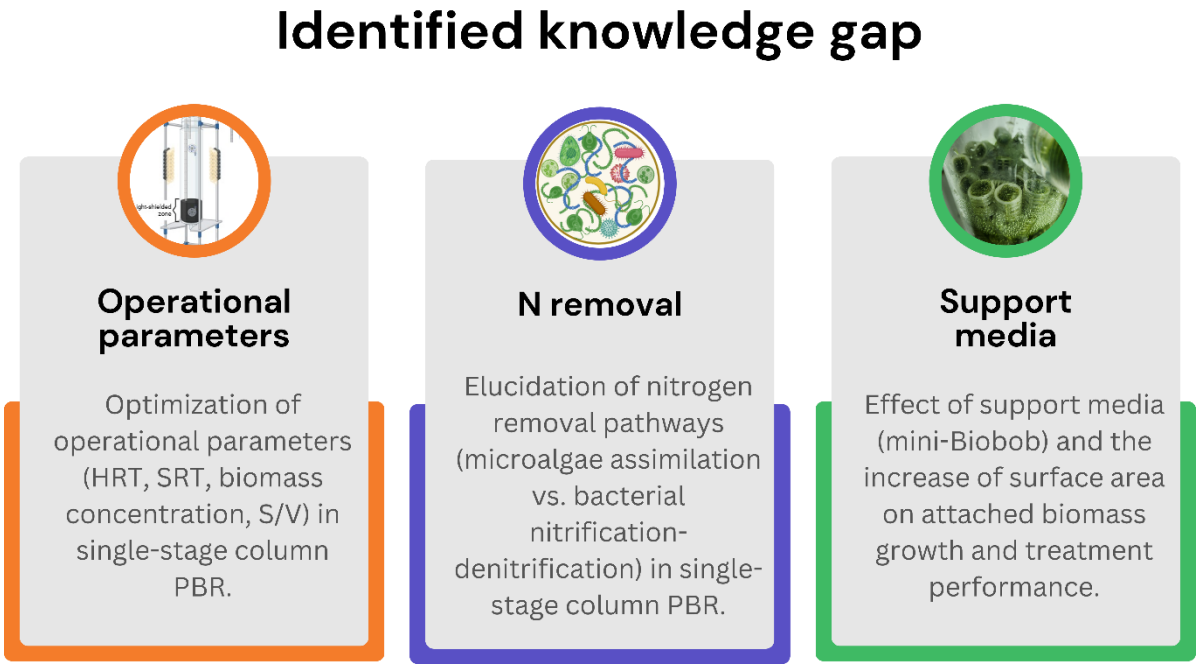

Figure 1: Knowledge gaps have been identified which will be addressed throughout the thesis. Drawing from Canva.

1.2. INTRODUCTION: THE WASTEWATER CHALLENGE

Despite their critical economic and ecological value, water resources face severe quantitative and qualitative threats, compounded by rising demand across agro-industrial and domestic sectors, driven by anthropogenic activities (Ossai et al., 2026). The problem is exacerbated by inadequate water sanitation: approximately 2.1 billion people still lacked access to safely managed drinking water, and a further 3.4 billion lack safely managed sanitation in the World (Pratap et al., 2023; WHO, 2025). This deficit contributes to depletion of source water quality. Combined with increasing wastewater generation from population growth (Pratap et al., 2023), this factors creates a vicious cycle that further undermines water security.

Beyond human access, the environmental impacts are also wide-reaching. Biodiversity loss, ecosystem degradation, trophic bioaccumulation, and widespread eutrophication are all directly linked to three major sectors: agriculture, industry, and domestic sectors (Mohsenpour et al., 2021; Mustafa et al., 2021; Ossai et al., 2026). Agriculture, the largest freshwater consumer (approximately 70% of global withdrawals), returns runoff rich in nutrients and persistent pesticides (Pratap et al., 2023; Sepúlveda-Muñoz et al., 2023). Industry, responsible for approximately 22% of freshwater use, discharges toxic heavy metals and recalcitrant synthetic compounds, while domestic wastewater adds pathogens, emerging pollutants (particularly pharmaceuticals and microplastics) accelerating ecosystem degradation and human health risks (Mustafa et al., 2021; Ossai et al., 2026; Pratap et al., 2023; Sepúlveda-Muñoz et al., 2023).

In response to these environmental pressures, although conventional wastewater treatment systems effectively reduce biochemical oxygen demand (BOD), nutrients and pathogens, they operate on a linear model designed primarily to protect public health and the environment, failing to recover valuable nutrients such as nitrogen and phosphorus (Oruganti et al., 2022; Ossai et al., 2026; Pratap et al., 2023; WHO & UN-Habitat, 2024). This represents a missed opportunity for a circular economy, where wastewater is reimagined as a resource rather than a waste to be treated (Acién et al., 2016; Sepúlveda-Muñoz et al., 2023).

Addressing this multifaceted crisis requires not only efficient treatment but also sustainable wastewater management strategies, designed according to the characteristics of the effluents involved for nutrient recovery that align with circular principles (Mohsenpour et al., 2021; Oruganti et al., 2022; WHO & UN-Habitat, 2024). In this context, microalgae-based wastewater treatment has gained attention since microalgae can assimilate nutrients into biomass while producing oxygen through photosynthesis, thus reducing the need for external aeration (Acién et al., 2016; Kwon et al., 2019; Oruganti et al., 2022; Sepúlveda-Muñoz et al., 2023). Therefore, the understanding of nutrient recovery mechanisms and the choice of appropriate cultivation systems and operational parameters are critical for optimizing performance.

Following this scenario, the Section 1.3 details the definitions and composition of domestic wastewater, which is the main contributor to municipal loads.

1.3. THE COMPLEXITY OF DOMESTIC WASTEWATER

Definitions of domestic wastewater vary across regions and regulatory frameworks yet share fundamental aspects. The United Nations Human Settlements Programme (UN-Habitat) and the World Health Organization (WHO) (2024) described domestic wastewater as “wastewater from residential settlements and services which originates predominantly from the human metabolism and from household activities”. In turn, urban or municipal wastewater is defined as “domestic wastewater or the mixture of domestic wastewater with industrial wastewater and/or runoff rainwater” (WHO & UN-Habitat, 2024). Similarly, the Brazilian technical standard NBR 9648 (ABNT, 1986) characterises municipal wastewater as "liquid effluent consisting of domestic and industrial wastewater, infiltration water, and parasitic rainwater inflow". While the terminology differs slightly, all definitions acknowledge the heterogeneous origins and composition of domestic wastewater.

The specific characteristics of domestic wastewater vary depending on several factors, including water usage patterns, climate, infrastructure, socioeconomic conditions, and population behaviours (Mustafa et al., 2021; Ossai et al., 2026; WHO & UN-Habitat, 2024). The physicochemical composition of wastewater reflects the technological development level and daily habits of contributing populations, resulting in a complex mixture of organic and inorganic matter, nutrients (notably nitrogen and phosphorus), oxygen-demanding compounds, solids and pathogenic microorganisms (Chai et al., 2021; Mustafa et al., 2021; Ossai et al., 2026; Pratap et al., 2023).

The organic fraction, accounting for approximately 75% of total carbon, originates primarily from human excreta, food waste and personal care products (Acién et al., 2016; Mohsenpour et al., 2021). While this proportion can vary, typical composition ranges include approximately 25–50% carbohydrates, 40% proteins and amino acids and 10% fats and oils, contributing to a BOD that typically maintains a chemical oxygen demand (COD)/BOD_5 ratio between 1.7 and 2.4 (Von Sperling, 2007).

The inorganic constituents are equally diverse, including cations such as sodium, calcium, potassium, and magnesium as well as anions like chloride, sulphate, phosphate, and bicarbonate (Acién et al., 2016; Mohsenpour et al., 2021). Additional constituents include ammonium compounds, trace heavy metals and emerging compounds such as cosmetics, pharmaceuticals and surfactants (Acién et al., 2016; Mustafa et al., 2021).

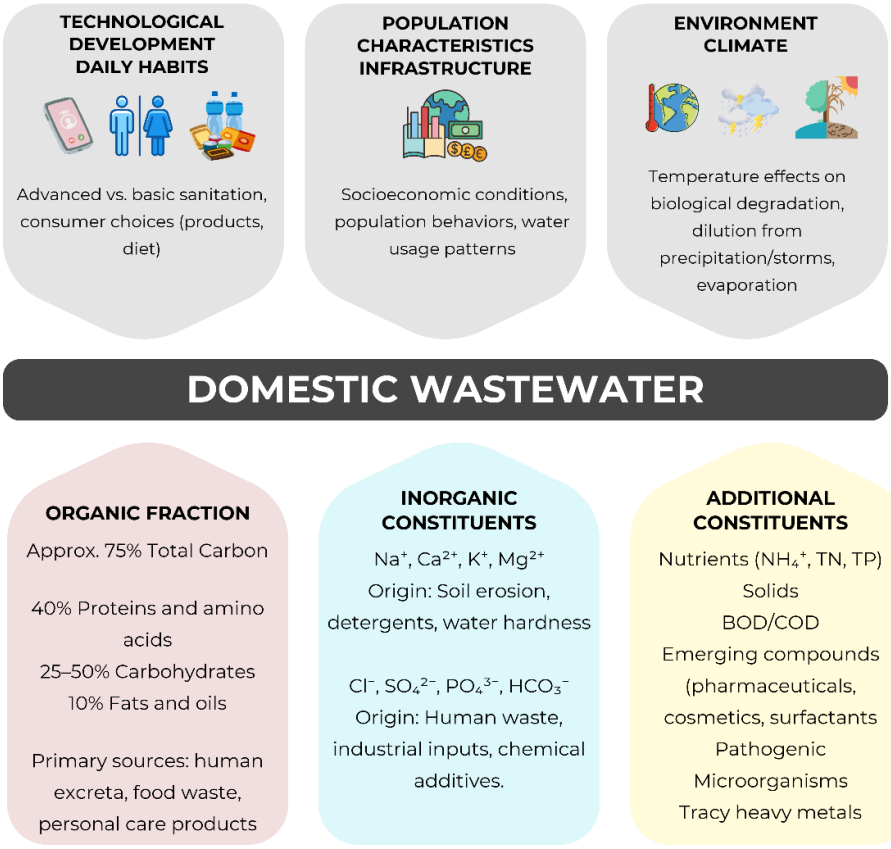

Figure 2: Influences and physicochemical composition of domestic wastewater. Drawings from Canva.

1.3.1. NITROGEN AND PHOSPHORUS IN DOMESTIC WASTEWATER

The nutrient content, particularly nitrogen and phosphorus, requires careful consideration due to their significant environmental impact when discharged into aquatic ecosystems (Acién et al., 2016; Mohsenpour et al., 2021).

The primary sources of nitrogen in domestic wastewater are human excretion, food waste, and inputs associated with the Haber-Bosch process (Han & Zhou, 2022; Mohsenpour et al., 2021; Ossai et al., 2026; WHO & UN-Habitat, 2024). In raw domestic wastewater, nitrogen exist in two main forms: organic and inorganic. Organic nitrogen is bound to carbon-based compounds and represents the initial form of much of the nitrogen excreted (Xu et al., 2024). Urea, proteins, amino acids, purines, nucleosides, and other complex organic materials constitute this fraction (Mohsenpour et al., 2021; Xu et al., 2024). On the other hand, inorganic nitrogen appears in different oxidation states, related to the continuous biochemical and chemical processes of the nitrogen cycle, with ample variation from -3 (ammonium) to +5 (nitrate) (Han & Zhou, 2022; Rahimi et al., 2020). In domestic wastewater, the majority of inorganic nitrogen is in the form of ammonium (NH_4^+). This occurs because urea and proteins are converted rapidly into ammonium by mineralisation/ammonification, via enzymes such as urease (Xu et al., 2024). A small fraction may exist as free ammonia (NH_3) or as ionised NH_4^+, the distribution of which is pH-dependent, with NH_3-N predominates at pH values above 9.25 (Acién et al., 2016; Chai et al., 2021; Von Sperling, 2007). Nitrite (NO_2^-) and nitrate (NO_3^-) are typically present at very low concentrations in raw domestic wastewater (unless industrial nitrate discharge are present), although they may become the predominant forms after secondary biological treatment (nitrification), where bacteria oxidise ammonium (Chai et al., 2021; González-Camejo et al., 2022). Therefore, the two dominant nitrogen forms in raw domestic wastewater are organic nitrogen and ammonium. Total nitrogen (TN) concentrations in untreated domestic wastewater vary significantly depending on socioeconomic and geographical factors (Abdel-Raouf et al., 2012). In treatment systems, the influent entering tertiary (polishing) treatment typically presents lower nitrogen concentrations, in the range of 20 to 80 mg L^{-1}, depending on the efficiency of previous stages (González-Camejo et al., 2022; Xu et al., 2024). In recognition of the environmental significance of nitrogen emissions, the United Nations Environment Assembly adopted the “Sustainable Nitrogen Management” resolution (UNEP/EA.5/2), to enhance N-use efficiency and reduce global N waste (Han & Zhou, 2022).

Phosphorus in domestic wastewater is primarily derived from anthropogenic activities, with synthetic detergents accounting for over 50% of total phosphorus (Mustafa et al., 2021; Sepúlveda-Muñoz et al., 2023). Like nitrogen, phosphorus speciation is pH-dependent and the most common forms include orthophosphate (PO_4^{3-}), polyphosphate and organic phosphate (Mohsenpour et al., 2021; Mustafa et al., 2021). The prevalence of PO_4^{3-} is particularly relevant due to its high solubility and bioavailability, representing both a pollution risk and a strategic opportunity for nutrient recovery, notably considering global phosphorus reserves are non-renewable (El Wali et al., 2021; van der Wiel et al., 2019).

1.3.2. MICROBIOLOGICAL HAZARDS

Microbiologically, domestic wastewater provides an ideal environment for a diverse range of microorganisms, many of which are beneficial for biological treatment processes (Mohsenpour et al., 2021; Von Sperling, 2007). However, raw domestic wastewater also acts as a massive reservoir of pathogenic microorganisms, representing a significant public health concern (Pratap et al., 2023; Von Sperling, 2007). The type, quantity and severity of these pathogens vary with region, hygienic habits, and socioeconomic status, with concentrations in low-income regions reaching levels 10 to 1000 times higher than those in developed countries, reflecting disparities in sanitation infrastructure, health coverage, and disease prevalence (Pratap et al., 2023). These pathogens are broadly classified into three categories: bacteria, viruses and protozoa/helminths, summarized in Table 1.

Table 1: Main pathogens, possible disease or symptoms, and number of cases annually worldwide.

Principal pathogens	Disease/symptoms	Total infection (per year)
Bacterial		
Escherichia coli pathotypes: enterotoxigenic (ETEC), enteropathogenic (EPEC), enterohemorrhagic (EHEC), enteroaggregative (EAEC), and enteroinvasive (EIEC)	Diarrheal disease, inflammatory bowel disease, abdominal pain, fever, intestinal obstruction	2.8 million cases
Campylobacter spp. (*Campylobacter jejuni, Campylobacter coli*)	Campylobacteriosis, enteritis with diarrhoea, abdominal pain, fever, nausea, vomiting, bloody stool. Complications can include Guillain-Barré syndrome and reactive arthritis	230,000 to 2 million cases
Salmonella spp.	Typhoid, salmonellosis (acute diarrheal), fever, headache, malaise, cough	200 million to 1 billion cases
Enterococcus spp. (*E. faecalis*, *E. faecium*)	Urinary tract infections, bacteraemia, bacterial endocarditis, diverticulitis, meningitis	100,000 to 250,000 deaths
Clostridium botulinum, *Clostridium perfringes*	Botulism, slurred speech, blurred vision, descending flaccid paralysis, respiratory failure, gastroenteritis	100 million cases
Vibrio spp. (*Vibrio cholerae*, *Vibrio parahaemolyticus)*	Cholera, bloody diarrhoea, gastroenteritis, extraintestinal infections	1.3 to 4 million cases 14,000 to 21,000 deaths
Other common bacteria include: *Shigella* spp., *Leptospira* spp*., Pseudomonas aeruginosa, Staphylococcus aureus, Helicobacter pylori, Yersinia enterocolitica, Aeromonas spp., Klebsiella pneumoniae.*		

(Continued)

Table 1: Main pathogens, possible disease or symptoms, and number of cases annually worldwide – cont'd

Principal pathogens	Disease/symptoms	Total infection (per year)
Viruses		
Norovirus	Acute gastroenteritis, diarrhoea, nausea, vomiting.	685 million cases
Rotavirus	Severe diarrhoea and vomiting	25 million cases 527,000 deaths
Enterovirus	Fever, cough, body and muscle aches	1 billion cases
Hepatitis A and E	Fatigue, fever, nausea, diarrhoea, acute pancreatitis, encephalitis, meningitis, myocarditis	Hepatitis A: 1.5 million cases Hepatitis E: 15 to 110 million cases
Adenovirus	Fever, sore throat, bronchitis, pneumonia, diarrhoea	20 million cases
Other common viruses include: astrovirus, SARS-CoV-2, JC polyomavirus, and human polyomaviruses.		
Protozoa		
Giardia intestinalis	Giardiasis, abdominal cramps, diarrhoea, nausea.	200 to 300 million cases 500,000 deaths
Cryptosporidium parvum and *Cryptosporidium hominis*	Cryptosporidiosis/ intestinal infection	3 cases per 100,000 people 48,000 deaths
Entamoeba histolytic	Amoebic dysentery/ intestinal and extraintestinal infection	100,000 deaths

(Continued)

Table 1: Main pathogens, possible disease or symptoms, and number of cases annually worldwide – cont'd

Principal pathogens	Disease/symptoms	Total infection (per year)
Protozoa		
Blastocystis	Diarrhoea, abdominal pain, weight loss	1 billion cases
Cyclospora cayetanensis	Cyclosporiasis, diarrhoea, weight loss, cramps, fatigue, nausea	50 million cases 40,000 to 100,000 deaths
Helminths		
Ancylostoma duodenale and Necator americans	Hookworm disease, hypochromic anemia, fatigue, skin problems	470 million
Ascaris lumbricoides	Ascariasis, abdominal pain, malnutrition, intestinal obstruction	732 million to 1.2 billion
Enterobius vermicularis	Pinworm disease, sleep disorder, insomnia	1 billion cases
Taenia spp.	Taeniasis and cysticercosis, abdominal pain, nausea, diarrhoea	40 to 60 million cases
Tricchuris trichura	*Trichuriais* (whipworm disease), abdominal pain, diarrhoea, rectal prolapse	460 to 800 million cases

Source: Data compiled and processed from the World Health Organization (WHO), National Center for Biotechnology Information (NCBI), Centers for Disease Control and Prevention (CDC), and European Centre for Disease Prevention and Control (ECDC) databases (https://www.who.int; https://www.ncbi.nlm.nih.gov; https://www.cdc.gov; https://www.ecdc.europa.eu), accessed in April 2026.

Bacterial pathogens are responsible for some of the most severe waterborne diseases (Pratap et al., 2023). Enteric viruses are particularly concerning due to their small size, low infectious dose, and resistance to conventional treatment processes (Pratap et al., 2023). Parasitic protozoa and helminths produce oocysts, cysts and eggs that are highly resistant to conventional treatment processes, surviving conditions that effectively eliminate bacterial pathogens (Pratap et al., 2023; WHO, 2022).

The presence of these microbial communities, combined with the complex chemical composition, makes untreated domestic wastewater a significant potential hazard to both ecosystem and human health (Ossai et al., 2026; Pratap et al., 2023).For this reason, disinfection efficiency is typically assessed via the removal of indicator organisms (Ossai et al., 2026).

1.3.3. EXPERIMENTAL CONSIDERATIONS AND SYNTHETHIC WASTEWATER

To address the complexity of domestic wastewater, synthetic wastewater (SWW) is frequently employed in experimental studies to overcome the inherent variability of real wastewater. By enabling precise control of parameters such as organic load, nutrient concentration, and inhibitory substance levels, SWW serves as a valuable tool for investigating treatment mechanisms under reproducible laboratory conditions. The diverse and complex composition of domestic wastewater, including biodegradable organics, essential nutrients, emerging contaminants, and microbial hazards, necessitates robust and flexible treatment strategies that can address this heterogeneity (Acién et al., 2016; Ossai et al., 2026).

1.4. CONVENTIONAL WASTEWATER TREATMENT: LIMITATIONS OF THE LINEAR MODEL

The formal recognition of water and sanitation as fundamental human rights by the United Nations General Assembly in 2010 (Resolution A/RES/64/292) institutionalized the global imperative to expand the treatment infrastructure, supported by Sustainable Development Goal Target 6.3 (WHO, 2025). This effort addresses the environmental consequences of discharge untreated wastewater, notably the acceleration of eutrophication,

which in turn compromises the life of aquatic biota and drives systemic biodiversity loss (Mohsenpour et al., 2021; Ossai et al., 2026; Pratap et al., 2023).

Despite technological progress, the overall performance and accessibility of conventional wastewater treatment systems remain limited globally. According to the WHO & UN-Habitat report (2024), 58% of domestic wastewater was safely treated globally in 2022 (estimated representative of 89% of the global population and 92% of the global volume of household wastewater generated). In Brazil, the safe treatment of domestic wastewater, which requires at least secondary treatment, is estimated at 43.4% (WHO & UN-Habitat, 2024). Of this volume, only 54.3% of the wastewater collected through sewer system receives effective treatment before disposal (SINISA, 2025; WHO & UN-Habitat, 2024).

Compounding this challenge, conventional wastewater treatment plants contribute to environmental impacts due to their substantial energy demands (approximately 3% of global electricity) and greenhouse gas (GHG) emissions (Mohsenpour et al., 2021; Oruganti et al., 2022; WHO & UN-Habitat, 2024). Treatment coverage remain alarmingly low in low-income countries (approx. 8%), while even in Latin America and Caribbean only 46% of household wastewater is treated (Pratap et al., 2023; WHO & UN-Habitat, 2024). This creates a complex technological and economic challenge, requiring solutions that balance treatment efficacy with sustainability considerations (Abdel-Raouf et al., 2012; Acién et al., 2016; Pratap et al., 2023; WHO & UN-Habitat, 2024).

1.4.1. CONVENTIONAL WASTEWATER TREATMENT

Conventional wastewater treatment systems are primarily designed to achieve three core objectives: (1) the reduction of carbonaceous organic matter, (2) the removal of nutrients (particularly nitrogen and phosphorus), and (3) the elimination of pathogens and suspended solids to meet regulatory discharge standards (Acién et al., 2016; Metcalf & Eddy Inc et al., 2013; Mohsenpour et al., 2021; Oruganti et al., 2022; Ossai et al., 2026). These systems are typically structured in a multi-stage sequence comprising preliminary treatment, primary, secondary, and tertiary treatment processes, and sludge treatment which employ both physicochemical and biological mechanisms to progressively convert pollutants into inert compounds to enabling safe water discharge or reuse (Acién et al., 2016; Metcalf & Eddy Inc et al., 2013; Silva, 2023; Von Sperling, 2007). This constitute a linear approach, where

wastewater is viewed primarily as waste to be treated and discarded rather than as a resource to be recovered.

Primary treatment is primarily physical, relying on sedimentation to remove settleable solids and floatable materials. This stage commonly achieves the removal of 50-70% of suspended solids and 25-40% of BOD (Metcalf & Eddy Inc et al., 2013; Von Sperling, 2007). Secondary treatment employs biological processes to degrade organic matter, with the activated sludge process representing the most widely adopted technology globally, capable of achieving 85-95% BOD removal and 70-90% of suspended solid (Metcalf & Eddy Inc et al., 2013; Silva, 2023; Von Sperling, 2007).

Tertiary treatment provides further polishing through nutrient removal (typically via chemical precipitation or biological nitrification-denitrification) and disinfection (Abdel-Raouf et al., 2012; Metcalf & Eddy Inc et al., 2013; Von Sperling, 2007). Nitrogen is typically removed via biological nitrification–denitrification, physicochemical methods, or assimilation (Han & Zhou, 2022; Torres-Franco et al., 2021). Nitrogen compounds, particularly ammonia, pose additional risks including toxicity to aquatic life and interference with disinfection processes, while nitrate contamination in drinking water sources raises public health concerns (Abdel-Raouf et al., 2012; Foladori et al., 2020). Phosphorus is typically removed either by chemical precipitation (commonly using ferric or aluminium salts) or through enhanced biological uptake (Metcalf & Eddy Inc et al., 2013; Ossai et al., 2026). In some cases, quaternary treatment is distinguished as a separate stage aimed at removing emerging pollutants such as pharmaceuticals, personal care products, and heavy metals (Abdel-Raouf et al., 2012). A summary of the main characteristics of these treatment stages is presented in Figure 3.

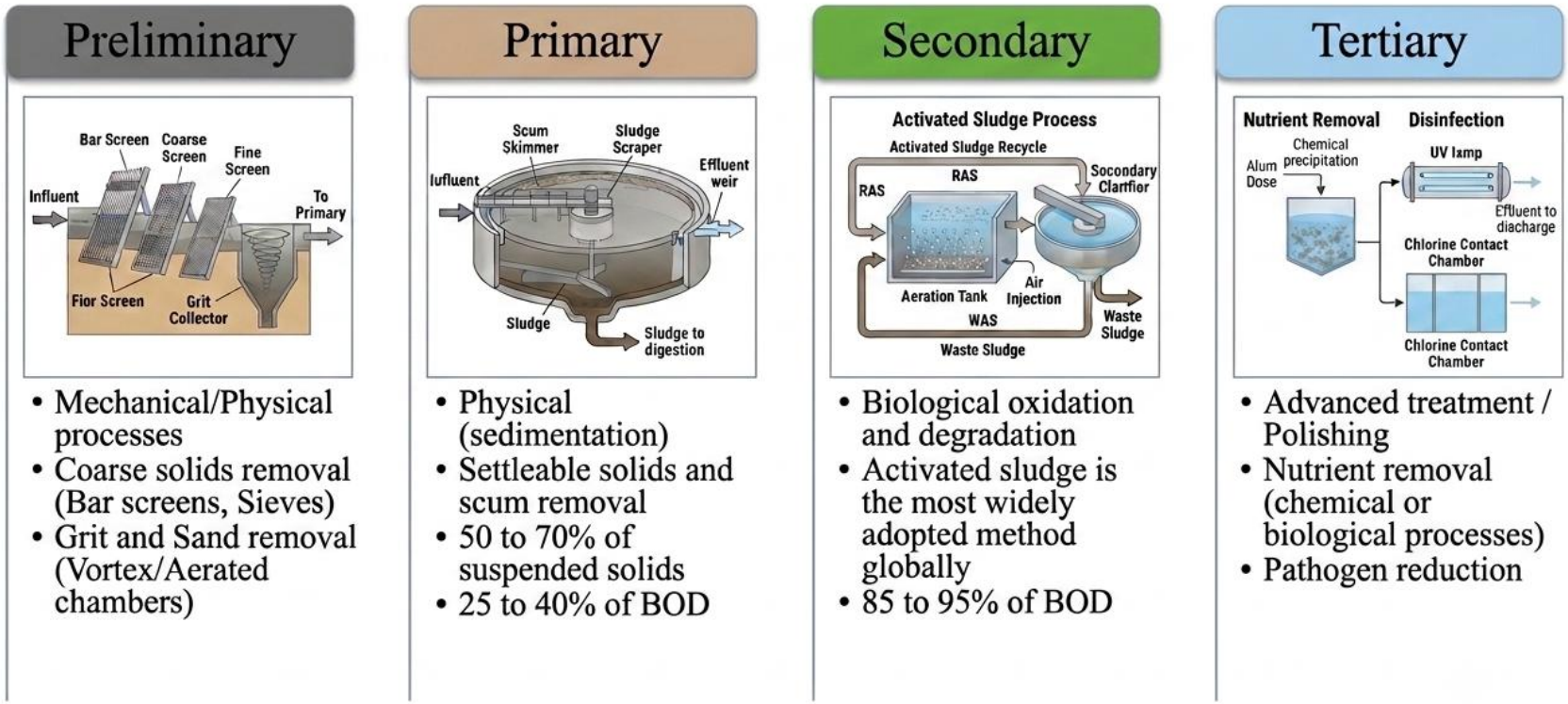

Figure 3: Stages of conventional wastewater treatment. Drawings from Gemini.

Numerous physicochemical technologies have been employed to enhance nutrient and contaminant removal efficiency, including coagulation-flocculation, ion exchange, advanced oxidation processes (AOPs), membrane filtration, solid-phase extraction, nanofiltration, and photocatalytic/electrochemical degradation (Gonçalves et al., 2017; Han & Zhou, 2022; Mustafa et al., 2021). However, their technical viability is frequently compromised by intrinsic limitations of each process. Coagulation-flocculation and chemical precipitation result in generation of high volume of hazardous sludge and the continuous and expensive addition of chemical reagents (Acién et al., 2016). Ion exchange, although efficient in ammonium and metal removal, faces the challenges of rapid chemical equilibrium depleting the resins, the high costs of its regeneration, and the risk of pollutant desorption in the final effluent (Chai et al., 2021).

Among more advanced techniques, AOPs are extremely effective at degrading recalcitrant pollutants, but their application is limited by energy intensity and the potential formation of toxic byproducts (Acién et al., 2016; Ossai et al., 2026). Similarly, membrane technologies offer superior clarification yet suffer from frequent fouling, which increases maintenance costs and requires high hydraulic pressures, contributing to the high electricity consumption of the sector (Acién et al., 2016; Ossai et al., 2026). While these methods are capable of achieving high effluent standards, their limitations reinforce the need for strategies that balance treatment effectiveness with environmental and economic sustainability. (Acién et al., 2016; Gonçalves et al., 2017; Mustafa et al., 2021)

This linear treatment model has proved to be particularly problematic from an operational perspective, as it focuses on removing pollutants rather than recovering them (Abdel-Raouf et al., 2012; Bux & Chisti, 2016; Silva, 2023). Conventional biological nutrient removal systems are energy-intensive, particularly due to aeration, which typically account for 45% to 75% of the total energy demand (Abdel-Raouf et al., 2012; Kwon et al., 2019; Tang et al., 2025). This mechanical aeration is required to support the metabolic activity of heterotrophic and nitrifying bacteria to oxidize organic matter and ammonia (Mohsenpour et al., 2021; Oruganti et al., 2022). Furthermore, conventional systems, particularly activated sludge, generate high quantities of sludge, whose handling and disposal can lead to secondary pollution and high management costs (Kwon et al., 2019; Mohsenpour et al., 2021). These factors combined with the high capital and operational costs associated with tertiary treatment create substantial economic barriers to implementation, particularly in developing regions (Acién et al., 2016; Oruganti et al., 2022; Pratap et al., 2023).

To overcome these limitations of the linear system, the sanitation sector is shifting toward a circular economy model, an innovative approach that transforms wastewater from a liability into an asset, driving the development of resource-recovery technologies designed to extract nutrients and clean water (Silva, 2023).

1.4.2. THE CIRCULAR APPROACH TO WASTEWATER

To mitigate the sustainable limitations of conventional wastewater treatment systems, there is growing interest in alternative strategies aligned with the principles of the circular economy. Transitioning a from linear to a circular approach necessitates a substantial restructuring of conventional concepts, techniques, and technologies (Langergraber et al., 2021). As highlight in the literature, future wastewater systems must balance technological feasibility, economic viability and environmental sustainability. This requires a paradigm shift: the focus is no longer strictly on pollutant removal but on the valorisation and recovery of resources, transforming effluent from an environmental liability into a strategic source of water, energy, and nutrients to alleviate pressures on natural resources (Oruganti et al., 2022; Ossai et al., 2026; Silva, 2023; WHO & UN-Habitat, 2024).

This circular vision of sanitation, increasingly consolidated within circular bioeconomy frameworks, positions wastewater not as a waste stream to be treated and then discarded, but as an untapped strategic resource containing water, energy, and valuable nutrients, closing resource cycles addressing global water security and sanitation challenges (Mohsenpour et al., 2021; Ossai et al., 2026; Pratap et al., 2023; WHO & UN-Habitat, 2024). Consequently, traditional sanitation infrastructures are evolving into Water Resource Recovery Facilities (WRRFs) (Devos et al., 2023; Ossai et al., 2026). Within these facilities, operational objectives transcend pollutant removal to integrate water reuse, nutrient recovery (specifically N and P), and bioenergy extraction (biogas) (Ossai et al., 2026; WHO & UN-Habitat, 2024). Ultimately, closing these resource cycles is vital to aligning the sanitation sector with the Sustainable Development Goals (SDGs) and the mitigation of global climate impacts (WHO & UN-Habitat, 2024).

For small towns and rural areas, the cost of conventional centralised systems is often prohibitive, while their technical complexity frequently results in operational failures (Acién et al., 2016; Pratap et al., 2023). In parallel, decentralized treatment assumes a strategic role, offering cost-effective alternatives by eliminating the need to connect extensive networks of

households (Pratap et al., 2023; Silva, 2023). Instead, communities can deploy multiple small-scale treatment plants, thereby enhancing local access to sustainable sanitation solutions (Silva, 2023).

However, the current reliance on rudimentary alternative solutions highlights a critical infrastructure gap. For instance, onsite systems like septic tanks serve 13.8% of the urban population and 36.2% of the rural population, yet less than 40% of these individual systems are considered safely managed. Posing substantial environmental and public health risks (SINISA, 2025; WHO & UN-Habitat, 2024).

To address these operational and safety deficiencies without incurring the high costs of conventional infrastructure, recent academic and technological interest has shifted towards nature-based, low-cost decentralised solutions (Langergraber et al., 2021). Among these, algal-bacterial treatment systems have emerged as particularly promising in this context. By harnessing the complementary metabolic functions of microalgae and bacteria, these systems enable simultaneous oxygenation, nutrient uptake, and biomass production, offering a closed-loop solution that is both ecologically and operationally sustainable (García et al., 2017; Noyola et al., 2012).

In summary, the transition from conventional treatment plants to WRRFs represents a necessary evolution for the sanitation sector. These solutions must prioritise effective nutrient recovery while balancing energy consumption, cost-efficiency, and environmental sustainability (Foladori et al., 2020; Mohsenpour et al., 2021; Ossai et al., 2026). Among the available alternatives, microalgae-based treatment addresses the main limitations of conventional systems: reducing the energy consumption on aeration (via photosynthetic oxygen) and allowing nutrient recovery in the form of biomass, enabling a circular approach to the management of domestic wastewater. The following section discusses the cultivation strategies and nutrient recovery mechanisms that make microalgae particularly suitable for this task.

1.5. MICROALGAE AND WASTEWATER TREATMENT

The increasing threat of resource depletion, coupled with the ecological and public health impacts of nutrient pollution in aquatic ecosystems, has intensified scientific efforts to develop sustainable technologies for carbon and nutrient recovery from wastewater (Acién et al., 2016; Devos et al., 2023; Ossai et al., 2026; Sepúlveda-Muñoz et al., 2023). In this

context, microalgae-based systems have emerged as a promising alternative, capable of simultaneously addressing conventional wastewater treatment challenges and emerging environmental concerns (Chai et al., 2021; Torres-Franco et al., 2021). These systems integrate pollutant removal with carbon sequestration, nutrient recovery and bioremediation of persistent pollutants, including pharmaceuticals, personal care products, plasticisers, and heavy metals, compounds typically resistant to conventional treatment technologies (Abdur Razzak et al., 2024; Chai et al., 2021; Han & Zhou, 2022; Mohsenpour et al., 2021; Mustafa et al., 2021; Oruganti et al., 2022).

First proposed in the 1950s, the application of microalgae in wastewater treatment represents a paradigm shift away from conventional linear, pollutant-centric approaches toward integrated resource-oriented solutions (Laizu et al., 2025; Ossai et al., 2026; Sutherland et al., 2020). Microalgae-based systems have since been extensively studied across a range of effluents, from domestic to agro-industrial sources and are increasingly recognized for their ability to reduce energy consumption (especially by minimizing aeration requirements), enhance nutrient removal, and generate high-value biomass (Figure 4) (Laizu et al., 2025; Mohsenpour et al., 2021; Oruganti et al., 2022).

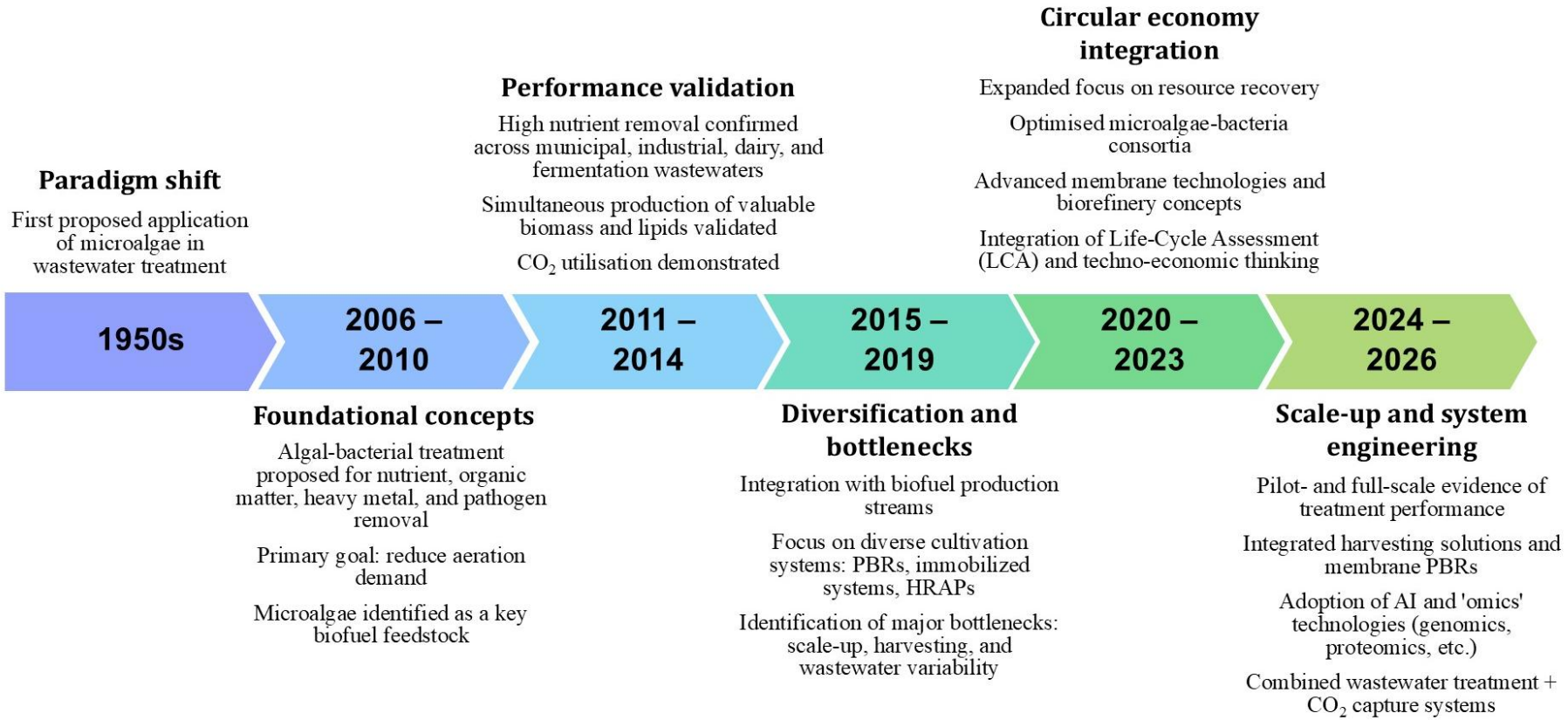

Figure 4: Evolution and future perspectives of microalgae-based wastewater treatment.

As Acién et al. (2016) note, the principal drivers of microalgal wastewater treatment technologies include greenhouse gas mitigation, improved energy balances, and nutrient recovery. However, their widespread adoption also hinges upon achieving positive economic returns where the valorisation of the biomass produced plays a crucial role in the viability of these systems (Acién et al., 2016; Sepúlveda-Muñoz et al., 2023).

The core of this approach is the metabolic versatility of microalgae, which enables efficient assimilation of nitrogen and phosphorus while simultaneously biofixing CO_2 through photosynthesis (González-Camejo et al., 2022; Mohsenpour et al., 2021; Mustafa et al., 2021). This dual functionality directly addresses two of the most pressing environmental challenges: eutrophication and climate change, particularly through applications such as sequestering carbon from industrial gas emissions, thereby positioning these systems at the interface of water treatment and climate mitigation (Abdur Razzak et al., 2024; Acién et al., 2016; Mustafa et al., 2021).

The resulting microalgal biomass, characterized by high concentrations of proteins, lipids, and carbohydrates, can be converted into a wide range of value-added products including biofertilizers, biostimulants and biopesticides, animal feed, biomaterials and biofuel (Abdur Razzak et al., 2024; Acién et al., 2016). Despite this biotechnological potential, commercial scalability remains limited by the disparity between technical readiness and economic feasibility, particularly regarding the high costs associated with algal harvesting and downstream processing (Acién et al., 2016; Mohsenpour et al., 2021; Oruganti et al., 2022). Furthermore, the microalgal cultivation in wastewater introduce significant biosafety challenges, the biomass may accumulate heavy metals, pathogenic microorganisms, and persistent organic pollutants, which prevents its application in sensitive sectors, such as food or pharmaceutical industries, and requires stringent regulatory frameworks (Acién et al., 2016; Mustafa et al., 2021; Ossai et al., 2026).

From a circular economy perspective, microalgae-based systems support several Sustainable Development Goals (SDGs), most notably SDG 6 (Clean Water and Sanitation) and SDG 12 (Responsible Consumption and Production) (El Wali et al., 2021; WHO & UN-Habitat, 2024). These systems respond to critical global pressures, including water scarcity (affecting an estimated 40% of the global population) and phosphorus depletion, while offering potential solutions for food security through nutrient recycling (Devos et al., 2023; El Wali et al., 2021; WHO & UN-Habitat, 2024).

In operational terms, microalgae-based treatment systems are often implemented with algal-bacterial consortia, wherein bacteria degrade organic matter into inorganic nutrients, which are then assimilated by microalgae for photosynthesis (Acién et al., 2016; Han & Zhou, 2022; Mohsenpour et al., 2021). This symbiotic relationship significantly reduces the need for mechanical aeration, while simultaneously enhancing BOD removal efficiency (Mustafa et al., 2021; Oruganti et al., 2022; Sutherland & Ralph, 2019). Moreover, the closed-loop metabolic relationship, where bacterial respiration releases CO_2 and mineralised nutrients, and algal growth regenerates oxygen, enabling efficient nitrogen and phosphorus uptake and contributing to carbon fixation (Acién et al., 2016; Mohsenpour et al., 2021; Oruganti et al., 2022).

Under optimal conditions, microalgae can exhibit higher CO_2 sequestration rates than terrestrial plants, reinforcing their utility in climate-resilient biotechnologies (Abdur Razzak et al., 2024; Mohsenpour et al., 2021; Mustafa et al., 2021). Their relative rapid growth, ability to assimilate both organic and inorganic carbon, and potential to yield a diversity of bio-based products position microalgae as keystone organisms in the development of sustainable bioprocesses (Abdur Razzak et al., 2024; Acién et al., 2016; Mohsenpour et al., 2021).

Although microalgae have been most commonly employed in tertiary treatment for nutrient polishing, achieving removal efficiencies up to 90% for nitrogen and 80% for phosphorus, they are increasingly explored for secondary treatment (Acién et al., 2016; Vargas et al., 2016). Nonetheless, technical barriers such as light limitation, bacterial competition, and the presence of inhibitory substances must be addressed to enable broader implementation (Acién et al., 2016; Han & Zhou, 2022; Mohsenpour et al., 2021).

Given the biological complexity and operational versatility of microalgae, to optimise the performance, reliability, and scalability requires a deeper understanding of both the specific mechanisms by which microalgae recover nitrogen and phosphorus, and the cultivation strategies, with special attention to column photobioreactors and their appropriate applications, topics addressed in the following subsections.

1.5.1. NITROGEN AND PHOSPHORUS REMOVAL MECHANISMS

The effective removal of nitrogen and phosphorus, key macronutrients driving eutrophication, is central to the performance of microalgae-based wastewater treatment systems (Arbib et al., 2013a; Li et al., 2023). These elements are not only essential for cellular

metabolism but also serve as indicators of treatment efficiency and compliance with environmental discharge standards (Acién et al., 2016; Arbib et al., 2013a; Mohsenpour et al., 2021). Microalgae offer a biologically driven platform for nutrient assimilation, complemented by microbial interactions that expand the range and efficiency of nutrient removal mechanisms (Figure 5) (Fallahi et al., 2021; Mohsenpour et al., 2021).

Figure 5: Schematic representation of the synergistic interactions in a microalgal-bacterial system. The diagram illustrates photosynthesis (green), aerobic growth (brown), nitrification (purple) and denitrification (blue) processes. Drawing from Biorender.

Nitrogen, a fundamental component of proteins, nucleic acids, and other cellular constituents, is primarily removed via microalgal assimilation and microbial nitrification-and denitrification pathways (Laizu et al., 2025; Mohsenpour et al., 2021; Torres-Franco et al., 2021). Microalgae preferentially assimilate ammonium (NH_4^+) due to its energetic advantage, incorporating it directly into biomass, however, this assimilation is limited by biomass productivity, which is strongly influenced by light availability (Acién et al., 2016; Chai et al., 2021; Nishi et al., 2022; Vargas-Estrada et al., 2021). Other oxidised forms, such as nitrate (NO_3^-) and nitrite (NO_2^-) can also be assimilated, although they require prior intracellular reduction, which increases metabolic demand with an associated decreased in biomass yields (Laizu et al., 2025; Mohsenpour et al., 2021; Rahimi et al., 2020).

This metabolic flexibility is reflected in the variable elemental composition of microalgal biomass, which depends on species, cultivation conditions, light intensity, temperature, and nutrient availability (Abdur Razzak et al., 2024; Han & Zhou, 2022; Oruganti et al., 2022). Nitrogen and phosphorus availability play a central role in determining the cellular C:N:P ratio. Under nitrogen-sufficient conditions, microalgae accumulate proteins

leading to a lower C:N ratio, whereas under nitrogen limitation, carbon is preferentially stored as lipids or carbohydrates, increasing the C:N ratio (González-Camejo et al., 2022; Laizu et al., 2025; Vargas-Estrada et al., 2021). Similarly, phosphorus concentration can trigger luxury uptake or result in phosphorus-depleted biomass (Mohsenpour et al., 2021). As a result, different stoichiometric representations coexist in the literature, ranging from the classic Redfield ratio for marine phytoplankton ($C_{106}H_{181}O_{45}N_{16}P$) (Oruganti et al., 2022) to nitrogen-richer formulations proposed for high load systems, such as $CH_{1.7}O_{0.4}N_{0.2}P_{0.0094}$ (González et al., 2008), and simplified elemental ratios represented microalgae biomass by CH_2ONP (Torres-Franco et al., 2021).

In an anoxic-aerobic configuration, the context of this thesis, microalgae and bacteria coexist in a synergistic and highly complex relationship where biological metabolisms occur simultaneously, including phototrophic growth of the photosynthetic biomass, aerobic and anoxic growth of heterotrophic biomass, mixotrophic and heterotrophic growth of microalgae and other process such as bicarbonate reactions, ammonification of soluble organic nitrogen, and hydrolysis of organic matter (Acién et al., 2016; Alcántara, Domínguez, et al., 2015; Torres-Franco et al., 2021).

The main metabolisms taking place in microalgal-bacterial wastewater treatment processes can be simplified as follows, highlighting the role of carbon dioxide as an electron acceptor in photosynthesis (Mohsenpour et al., 2021) and a carbon source for autotrophic growth during nitrification (Rahimi et al., 2020), alongside biomass production across all metabolic pathways:

Photosynthesis (microalgal):

$$CO_2 + H_2O + NH_4^+ + PO_4^{3-} \rightarrow \text{microalgal biomass} + O_2$$

Aerobic growth (heterotrophic bacteria):

$$\text{COD} + O_2 + NH_4^+ \rightarrow \text{bacterial biomass} + CO_2 + H_2O$$

Nitrification (bacterial):

$$NH_4^+ + O_2 + CO_2 \rightarrow \text{bacterial biomass} + NO_3^- + H^+ + H_2O$$

Denitrification (heterotrophic bacteria, anoxic):

$$NO_3^- + CH_3\text{COOH} \rightarrow \text{bacterial biomass} + HCO_3^- + H_2O + CO_2 + N_2$$

In domestic wastewater, which typically presents a low C:N ratio, the contribution of nitrification and denitrification becomes essential for achieving high nitrogen removal efficiencies (Mohsenpour et al., 2021; Oruganti et al., 2022). Nitrification is a two-step aerobic process in which ammonia-oxidising bacteria (AOB) convert NH_4^+ to NO_2^-, followed by the oxidation of NO_2^- to NO_3^- by nitrite-oxidising bacteria (NOB) (Chai et al., 2021; Rahimi et al., 2020). Denitrification then reduces NO_3^- to N_2 gas through a sequence of intermediate steps, NO_2^-, nitric oxide (NO) and nitrous oxide (N_2O), via heterotrophic microorganism under anoxic conditions (Chai et al., 2021; Rahimi et al., 2020). It is important to highlight that N_2O is biologically produced through incomplete hydroxylamine oxidation (NH_2OH), nitrite reduction and the incomplete heterotrophic denitrification. N_2O has a global warming potential 298 times higher than CO_2, raising environmental concerns about sustainability if not properly managed (Alcántara, Domínguez, et al., 2015; Li et al., 2023; Peng et al., 2023). Additionally, the nitrification pathway is often rate-limited due to the slow growth and environmental sensitivity of nitrifying bacteria, particularly in relation to temperature, pH and dissolved oxygen (DO) levels (Chai et al., 2021; Rahimi et al., 2020).

Phosphorus, though comprising less than 1% of algal dry biomass, plays a fundamental role in cellular energy metabolism, nucleic acid synthesis, and lipid structure (Acién et al., 2016; Laizu et al., 2025; Mohsenpour et al., 2021). Although the phosphorus removal mechanisms are not yet fully understood, the primary pathways include cellular assimilation, intracellular accumulation as polyphosphates, and chemical precipitation or adsorption (Laizu et al., 2025; Mohsenpour et al., 2021; Oruganti et al., 2022). Bacterial enzymatic hydrolysis of organic phosphorus in algal-bacterial consortia further enhances phosphorus bioavailability and removal efficiency (Acién et al., 2016; Mohsenpour et al., 2021; Oruganti et al., 2022).

Phosphorus uptake is strongly influenced by pH. The most bioavailable form, $H_2PO_4^-$, predominates at pH between 2.15 and 7.20 (Mohsenpour et al., 2021). Beyond 7.20, HPO_4^{2-} becomes dominant, while extreme pH values (<2.15 or >12.33), lead to forms such as H_3PO_4 or PO_4^{-3}, which are less accessible for biological uptake (Mohsenpour et al., 2021). Therefore, pH control is essential to maximize phosphorus uptake and avoid precipitation (Acién et al., 2016). Domestic wastewater, after secondary treatment, typically has a C:N:P ratio of approximately 100:25:12, optimal ratios for microalgal growth are closer to 100:14:2, supporting an effective N and P removal by assimilation (Acién et al., 2016; Oruganti et al., 2022). When phosphorus becomes limiting, external supplementation may be required to sustain nitrogen assimilation and overall biomass productivity, indicating that the

stoichiometric balance between these key nutrients presents a fundamental challenge for treatment optimization (Acién et al., 2016; Mohsenpour et al., 2021; Oruganti et al., 2022).

Ultimately, a comprehensive understanding of the mechanistic basis of nutrient removal in microalgae-based systems is essential for designing effective and resilient treatment processes. This mechanistic insight not only supports efficient wastewater treatment but also lays the groundwork for nutrient recovery, positioning these systems as pivotal technologies in the transition toward a circular economy. (Acién et al., 2016; Han & Zhou, 2022; Oruganti et al., 2022).

1.5.2. CULTIVATION STRATEGIES AND TREATMENT CONFIGURATIONS

The versatility of microalgal-bacterial systems enables their integration into various stages of wastewater treatment, offering a broad range of configurations adapted to influent characteristics and treatment objectives, with each application presenting distinct opportunities and constraints (Acién et al., 2016; Mohsenpour et al., 2021; Ren et al., 2024).

While primary effluents, rich in organic matter and nutrients, provide favourable conditions for microalgal growth, this application is challenged by factors such as limited light penetration associated with high turbidity, microbial competition, and the presence of potentially inhibitory compounds (Acién et al., 2016; Mohsenpour et al., 2021). Nevertheless, when microalgae are used as a secondary treatment stage, they can partially replace or supplement activated sludge processes (Mohsenpour et al., 2021). Compared to conventional systems, this approach reduces aeration energy demand, making it one of the most energy-efficient options available (Alcántara, Domínguez, et al., 2015; Peng et al., 2023). However, the overall energy demand of the treatment system can be reduced, although other processes, such as mixing, harvesting, and downstream still contribute to operational costs (Acién et al., 2016; Arbib et al., 2013a; Rahimi et al., 2020). The most favourable energy balance is achieved when microalgae are applied as secondary biological stage treating primary settled wastewater (Mohsenpour et al., 2021), where higher organic and nutrient loads support greater biomass productivity, an essential factor in systems designed to obtain by-products (González-Camejo et al., 2022; Mohsenpour et al., 2021).

In contrast, the use of microalgae as a tertiary treatment for nutrient polishing after conventional secondary treatment is the most commonly used and benefits from reduced organic loads and lower turbidity (Acién et al., 2016; González-Camejo et al., 2022).

However, nutrient supplementation may be required to sustain adequate biomass productivity (Acién et al., 2016; Mohsenpour et al., 2021). Biomass reuse depends on the quality, with potential applications including biofertilizer, animal feed, or biofuel production (Han & Zhou, 2022; Sepúlveda-Muñoz et al., 2023; Xu et al., 2024). Similarly, potential water reuse depends on effluent quality, including restricted/unrestricted agricultural irrigation or discharge into water bodies (Pratap et al., 2023; WHO & UN-Habitat, 2024).

Cultivation systems can be classified into suspended or immobilized configurations, each with distinct operational implications (Figure 6) (Oruganti et al., 2022). Immobilized cultivation systems can occur via natural adhesion forming biofilms or via active methods such as polymer entrapment, membrane confinement, or surface adsorption (Mohsenpour et al., 2021; Ren et al., 2024; Xu et al., 2024). Although these systems are less common at full scale, they offer advantages in terms of biomass harvesting efficiency and effluent clarity (Oruganti et al., 2022; Ren et al., 2024; Zhang et al., 2020). While this can simplify biomass harvesting and reduce energy consumption, immobilized systems remain limited to laboratory or pilot scales due to material costs and challenges in achieving high surface-area-to-volume ratios suitable for large-scale deployment (González et al., 2008; Mohsenpour et al., 2021; Ren et al., 2024).

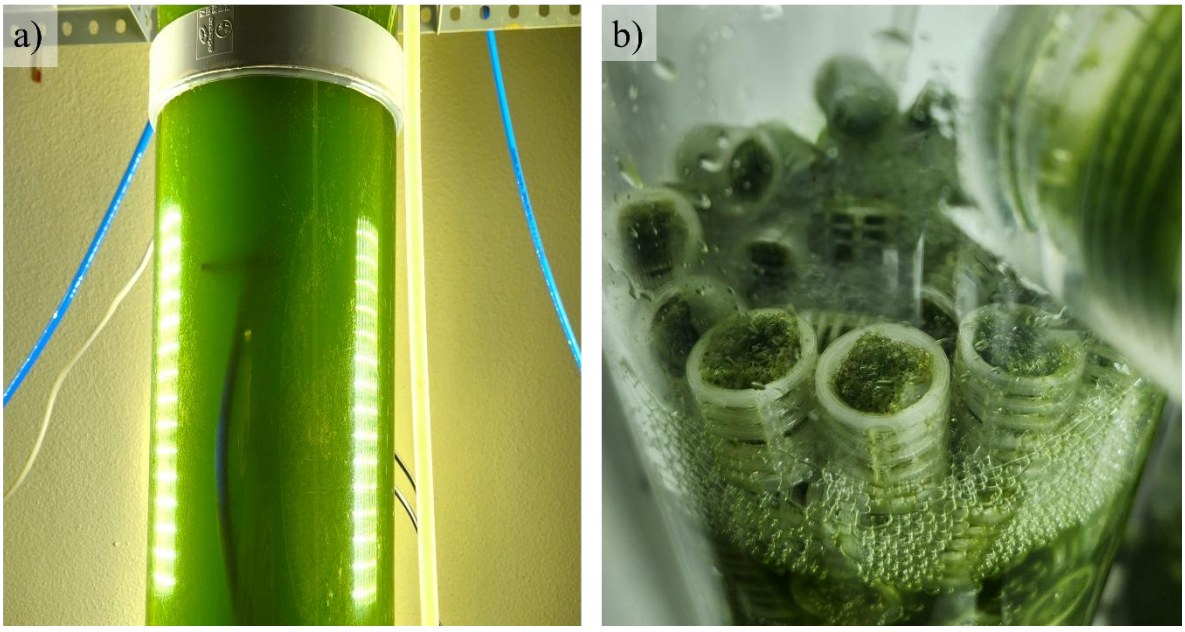

Figure 6: Photographs of microalgae cultivation systems: (a) suspended biomass configuration and (b) immobilised configuration.

Suspended cultures are the most widely applied in wastewater treatment, being operated in both open and closed photobioreactors (PBRs) (Figure 7) (Mohsenpour et al., 2021; Zhang et al., 2020). The distinction between these configurations is critical for operational management, since closed systems allow for better control of parameters such as temperature, pH, and dissolved oxygen, in addition to mitigating losses due to evaporation and risks of biological contamination (Abdur Razzak et al., 2024; Mohsenpour et al., 2021; Sepúlveda-Muñoz et al., 2023).

Figure 7: Photographs of closed microalgae cultivation systems installed at UNESP - Bauru: (a) column photobioreactors and (b) flat panel; and open system installed at the Institute of Sustainable Processes, University of Valladolid (c) high-rate algal ponds (HRAP).

Open reactors, such as HRAPs, are simple and require low construction and operational costs but have disadvantages such as limited process control and high impact of environmental variables, vulnerability to contamination, poor biomass settleability, and inefficiencies related to low surface-area-to-volume ratios (low light penetration) (Abdur Razzak et al., 2024; Arbib et al., 2013a; Mohsenpour et al., 2021; Sepúlveda-Muñoz et al., 2023). In open cultivation systems, environmental losses such as ammonia volatilisation (at pH 9 to 11) and phosphorus precipitation can significantly affect nutrient balance and

performance metrics, complicating treatment assessment (Acién et al., 2016; González et al., 2008; Ren et al., 2024). These challenges underscore the need for integrated monitoring and control strategies to optimise both biological uptake and abiotic removal pathways (Acién et al., 2016).

Closed systems provide superior control over fundamental operational parameters, including light intensity, pH, temperature, gas exchange and mixing (Mohsenpour et al., 2021; Sepúlveda-Muñoz et al., 2023; Solimeno et al., 2017). These systems are typically configured as bubble-column, tubular, flat-panel or thin-layer reactors, each designed to minimize the light path and optimize photosynthetic efficiency (Acién et al., 2016; Arbib et al., 2013a; Laizu et al., 2025). Their main advantages include enhanced biomass productivity, lower contamination risk, and high process reproducibility (Abdur Razzak et al., 2024; Arbib et al., 2013a). However, their widespread implementation remains limited by substantial energy demands, particularly for mixing, material requirements, and capital costs (Acién et al., 2016; Mohsenpour et al., 2021).

Advanced configurations, such as hybrid anaerobic–aerobic bioreactors, alternating redox systems, and other designs are being investigated to improve treatment performance, although the complexity of process control remains a significant technical barrier (Acién et al., 2016; Ren et al., 2024). These systems enable the mineralization of organic compounds, methane recovery, and nutrient uptake, while reducing dependence on intensive mechanical aeration through photosynthetic oxygenation (Alcántara, Domínguez, et al., 2015; Devos et al., 2023; Sepúlveda-Muñoz et al., 2023). Alternating redox conditions in such reactors can also facilitate enhanced nitrogen removal through nitrification and denitrification sequences (Meng et al., 2024; Tang et al., 2025). However, despite their potential, these systems present challenges related to process complexity, microbial management, and real-time control (Meng et al., 2024; Ren et al., 2024; Zhang et al., 2020).

Despite all these promising configurations, several critical operational bottlenecks continue to limit the scale-up and economic viability of microalgal bacterial wastewater treatment systems (Acién et al., 2016). These include:

- Dependency on environmental conditions, particularly solar radiation and temperature, compromising consistency and reliability, and resulting in seasonal fluctuations in performance (Acién et al., 2016; Mohsenpour et al., 2021; Rahimi et al., 2020),

- Outdoor systems such as lagoons-type frequently present lower photosynthetic efficiency, a limitation that restricts biomass productivity and imposes an extensive area demand (Acién et al., 2016; Meng et al., 2024),
- Higher HRTs compared to conventional technologies, resulting in the need for reactors with significantly larger volumes and larger areas (Acién et al., 2016; Oruganti et al., 2022),
- Although photosynthetic oxygenation reduces aeration costs, the energy consumption for mixing, harvesting, and CO_2 injection remains high, especially in closed PBRs, representing an obstacle to implementation (Mohsenpour et al., 2021; Ren et al., 2024),
- Microalgae biomass has poor natural sedimentation due to their small cell size, density similar to water, and negative surface charge, which often results in low harvesting efficiency, and consequently in concentration of suspended solids in final effluent above regulatory discharge limits (Arbib et al., 2013a; González et al., 2008; Zhang et al., 2020).

To maintain optimal biomass productivity, it is essential to control both biotic factors, including pathogen presence and competition with other microalgae, and abiotic factors such as light intensity, nutrient concentrations, pH, and temperature (Acién et al., 2016; Oruganti et al., 2022). Light saturation and photoinhibition pose a delicate balance: while increased irradiance boosts productivity up to a species-specific limit, excess light can damage photosystems and suppress growth, particularly under elevated temperatures (Abdur Razzak et al., 2024; Mohsenpour et al., 2021; Oruganti et al., 2022). Furthermore, carbon limitation observed in domestic wastewater may require external supplementation, such as CO_2, or organic carbon sources (e.g., acetate, glycerol) to sustain growth and enhance nutrient removal, which in turn affects economic feasibility (Acién et al., 2016; Mohsenpour et al., 2021; Oruganti et al., 2022)

To overcome the operational bottlenecks explained above, especially the need for reduced land footprint and the necessity to comply with stringent legislation regarding effluent standards and biomass quality, the transition to closed systems is the most robust technological solution, offering a high-density cell platform with better control of ecological niches (Laizu et al., 2025; Sepúlveda-Muñoz et al., 2023). This operational advantage allows for the stable integration of microalgal-bacterial processes within a single-stage configuration, where

combining aerobic and anoxic/anaerobic microenvironments emerges as a viable alternative. (Abdur Razzak et al., 2024; Laizu et al., 2025; Sepúlveda-Muñoz et al., 2023).

Among closed configurations, column PBR stands out as particularly suitable for wastewater treatment. PBRs offer a high surface-to-volume ratio, efficient light distribution, enabling a better control of dissolved oxygen, a critical parameter for preventing photosynthetic inhibition and ensuring the stability of overall system performance (Arbib et al., 2013a; Laizu et al., 2025; Sepúlveda-Muñoz et al., 2023; Zhang et al., 2020). They are particularly indicated when biomass productivity and nutrient recovery must be maximised, or when stringent contamination control is required (Arbib et al., 2013a). Furthermore, their design provides operational resilience under adverse climatic conditions, such as low temperatures or variable irradiance (Arbib et al., 2013a; Laizu et al., 2025). The integration of TPBRs into combined anaerobic–aerobic systems facilitate a synergistic metabolic environment that enhances overall nutrient removal and resource recovery.

While research continues to refine system configurations, reduce operational costs, and enhance performance, it is evident that no single design can universally address all wastewater types and treatment goals. Adapting system configurations to influent characteristics, resource availability, and reuse objectives is critical to developing resilient, scalable, and circular microalgae-based treatment solutions.

2.

Experimental set-up, design and analytical methods

2.1. SINGLE-STAGE COLUMN PHOTOBIOREACTOR: INFLUENCE OF OPERATIONAL PARAMETERS

2.1.1. OBJECTIVE OF THE STUDY

A single-stage column photobioreactor (PBR) with an algal-bacterial consortium treating synthetic wastewater was operated under continuous flow conditions to evaluate the performance of a simplified and more cost-effective alternative to conventional two-stage anoxic-aerobic systems. Despite the potential of this configuration, two key knowledge gaps can be identified: the role of algal-bacterial symbiosis in nutrient removal within single-stage column PBR is still largely unknown, and the optimization of operational parameters requires further investigation. The system was assessed under varying HRT, biomass concentrations in the PBR, and two different illuminated surface-to-volume ratios. The purpose of this study is then to investigate the performance of a single-stage PBR under controlled laboratory conditions, to evaluate in a first time the effect of HRT, surface-to-volume ratio and biomass concentration on treatment efficiency and biomass productivity.

2.1.2. SINGLE-STAGE PHOTOBIOREACTOR DESIGN

The single-stage PBR was constructed from a transparent methacrylate vertical tube with an internal diameter of 15 cm and a liquid height of 124.5 cm, corresponding to a working volume of 22 L (Figure 8). To evaluate different metabolic pathways, the PBR was spatially divided into two functional zones: an upper illuminated zone, where the incidence of light can support phototrophic activity, and a lower light-shielded zone where the absence of light was intended to support anoxic conditions. The light-shielded zone was created by enclosing the bottom 41.5 cm (representing one-third of the total liquid height) with a black cardboard shield, while the illuminated zone corresponded to the remaining 83 cm (two-thirds of the liquid height). The illuminated zone provided a surface area of 0.39 m^2, resulting in a surface-to-volume ratio (S/V) of 17.8 m^2 m^{-3}. When the PBR operated without the black shield (i.e., with the entire liquid height illuminated), the S/V increased to 26.7 m^2 m^{-3}, with the former light-shielded zone representing an additional surface area of 0.20 m^2 (total surface area of 0.59 m^2).

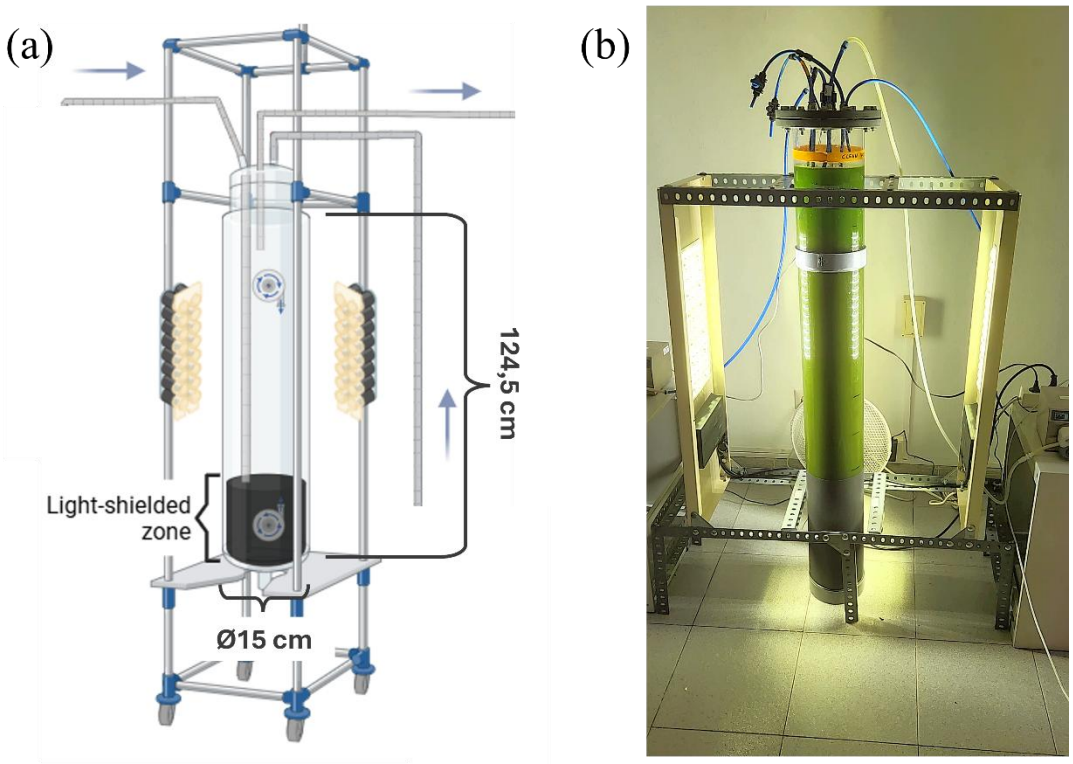

Figure 8: (a) Schematic diagram of the single-stage PBR showing the illuminated and light-shielded zones, and (b) photograph of the PBR during continuous operation. Drawing from Biorender.

To ensure continuous agitation of the cultivation broth, one pump was installed at the bottom (Eden 159, Eden WaterParadise, Spain) and a second pump was installed in the upper third part of the PBR (CompactON 300, Eheim, Spain). Illumination was provided by two LED PCBs panels (Philips S.A., Poland) arranged vertically on opposite sides of the PBR. The external light source was operated under 24-hour photoperiod. This continuous illumination was chosen to establish consistent and reproducible baseline conditions, eliminating the variability introduced by light-dark cycles as an additional factor of variability.

The reactor was equipped with a removable lid featuring multiple ports, including an inlet for wastewater feed, an outlet for the next step in the treatment (settler), an inlet for biomass recirculation, a liquid sampling port, and a gas sampling port. This modular design allowed for convenient adjustments to the influent flow rate, enabling the variation of the HRT during the experimental periods, sampling, and maintenance throughout the experimental period.

2.1.3. PHYSICAL-CHEMICAL AND BIOLOGICAL ANALYSES

2.1.3.1. TOTAL SUSPENDED SOLIDS (TSS) AND VOLATILE SUSPENDED SOLIDS (VSS)

TSS and VSS concentrations were measured according to Standard Methods (APHA, 2017). For TSS determination, a measured volume of homogenised sample was filtered through a pre-dried and pre-weighed (M_{filter}) glass fiber filter (1.5 µm pore size) and placed in an oven at 103 to 105°C for 24 hours. After drying, the filter was cooled to room temperature in a desiccator and weighed (M_{dry}). For VSS determination, the same filter from the TSS analysis was placed in a muffle furnace and ignited at 550°C for 15 minutes. After ignition, the filter was cooled to room temperature in a desiccator and weighed ($M_{ignited}$). The weight lost on ignition represents the volatile suspended solids fraction. The TSS and VSS concentration (g L^{-1}) was determined by Equations 1 and 2:

$$TSS\ (mg\ L^{-1}) = \frac{M_{dry} - M_{filter}}{V_{sample}} \quad (1)$$

$$VSS\ (mg\ L^{-1}) = \frac{M_{ignited} - M_{filter}}{V_{sample}} \quad (2)$$

2.1.3.2. DISSOLVED NUTRIENTS AND CARBON

Samples were filtered through 0.45 µm membrane filters prior to analysis. For total organic carbon (TOC), inorganic carbon (IC) and total nitrogen (TN) concentrations, the filtered samples were transferred into vials, placed in the autosampler, and then determined using a Shimadzu TOC-VCSH analyser (Japan) equipped with a TNM-1 chemiluminescence module.

$N\text{-}NH_4^+$ was determined by the Nessler method using a Shimadzu UV-2550 spectrophotometer (Japan) at 425 nm. A 10 mL aliquot of filtered sample was placed in a test tubes, 12 µL of EDTA solution was added, and the tube was agitated. After waiting for 3 minutes, 0.4 mL of Nessler reagent was added, and the tube was agitated again. After 10 minutes of reaction time, the absorbance was measured and the remaining drainage was disposed of in a mercury waste tank.

For $N\text{-}NO_2^-$, $N\text{-}NO_3^-$ and orthophosphate ($P\text{-}PO_4^{3-}$), the sample were filtered through 0.22 µm membrane filters prior to analysis and quantified by high-performance liquid chromatography with ion conductivity detection (HPLC-IC) using a Waters 432 conductivity detector (USA).

2.1.3.3. MICROALGAE IDENTIFICATION AND QUANTIFICATION AND ELEMENTAL COMPOSITION OF BIOMASS

The identification and quantification of the microalgae consortium was conducted by microscopy examination using an OLYMPUS IX70 microscope (USA). Samples were fixed with Lugol solution (5% v/v) and formaldehyde solution (10% v/v). The fixed samples were stored at -20°C until analysis.

The determination of carbon (C), hydrogen (H), nitrogen (N) and oxygen (O) content of the biomass was carried out from freeze-dried biomass using an elemental analyser EA Flash 2000 (Thermo Fisher Scientific, USA).

2.1.3.4. NITROUS OXIDE (N_2O)

N_2O was determined using a gas chromatograph (Bruker Scion 436, Palo Alto, USA) equipped with an electron capture detector (ECD) and a HS-Q packed column, according to the procedure described by Frutos et al., (2015). Gas samples (100 µL) were collected from the headspace of the PBR using a gas-tight syringe inserted through a septum port located at the top of the reactor. Sampling was performed in duplicate at each collection time.

2.1.4. CALCULATIONS

The biomass productivity (BP) (g m^{-3} d^{-1}) set via harvesting from the settler was determined according to Equation 3 (González-Camejo et al., 2022):

$$BP = \frac{(Q_{wastage} \times TSS) + (Q_{out} TSS_{out})}{V_{PBR}} \quad (3)$$

Where $Q_{wastage}$ is the wastage flowrate withdrawn from the bottom of the settler (L d^{-1}); Q_{out} is the effluent flowrate from the outlet of the settler (L d^{-1}); TSS is the biomass

concentration of the $Q_{wastage}$ (g L^{-1}); TSS_{out} is the biomass concentration of the effluent and V_{PBR} is the volume of the PBR (m^3).

The nutrient removal efficiency (NRE) was calculated according to Equation 4:

$$NRE_i = \frac{C_{SWW} - C_{out}}{C_{SWW}} \times 100 \quad (4)$$

Where NRE_i represents the removal efficiency (%) of the parameter *i* (TOC, IC, TN, $N\text{-}NH_4^+$ and $P\text{-}PO_4^{3}$), C_{SWW} is the concentration of the parameter *i* in the SWW and C_{out} is the concentration of the parameter *i* in the effluent of the settler. Mass balance calculation was conducted for TOC, IC, TN, $N\text{-}NH_4^+$ and $P\text{-}PO_4^{3-}$, in each operational stage.

The nitrogen mass balance was calculated according to Equation 5 (Toledo-Cervantes et al., 2019):

$$Q_{in} \cdot TN_{in} = \left(V_{PBR} \cdot BP \cdot \frac{\%N}{100}\right) + (Q_{out} \cdot TN_{out}) + (N_{loss}) \quad (5)$$

where Q_{in} is the flow rate of the inlet SWW (L d^{-1}); TN_{in} is the total nitrogen concentration in the inlet SWW (g L^{-1}); V_{PBR} is the reactor volume (m^3); BP is the biomass productivity (g m^{-3} d^{-1}); $\%N$ is the nitrogen content in the biomass (%); Q_{out} is the flow rate of the effluent (L d^{-1}); TN_{out} is the total nitrogen concentration in the effluent (g L^{-1}) and N_{loss} represents the unaccounted nitrogen in the mass balance, calculated as the closing term. The N_{loss} was calculated as the difference between the TN input and the sum of TN in the effluent and the N recovered in the biomass.

2.2. SINGLE-STAGE COLUMN PHOTOBIOREACTOR: UNCOVERING NITROGEN REMOVAL

2.2.1. OBJECTIVE OF THE STUDY

In Chapter 3, the operational conditions of a single-stage column PBR treating synthetic wastewater were tested, demonstrating high removal efficiencies for organic carbon, nitrogen and phosphate. However, the specific contributions of microalgal assimilation and bacterial nitrification-denitrification to nitrogen removal remained unclear, as both pathways

occurred simultaneously. Moreover, the complex synergy between microalgae and bacteria in photobioreactors critically influences nutrient removal efficiency, but the competition between assimilation and nitrification has not been fully elucidated. The purpose of this study is then to investigate the interplay between nutrient and carbon removal pathways in a single-stage microalgal-bacterial photobioreactor treating domestic wastewater by selectively inhibiting nitrification with allylthiourea (ATU), in order to evaluate the effect of bacterial activity suppression and the contribution of microalgal assimilation to total nitrogen removal rates, and the shifts in microbial population structure, carbon fate mechanisms, and phosphate removal dynamics, thereby demonstrating that, under those operational conditions for single-stage PBR, nitrogen removal is mainly dominated by microalgae assimilation complemented by bacterial nitrification-denitrification to achieve complete nitrogen removal.

2.2.2. SINGLE-STAGE PHOTOBIOREACTOR DESIGN

The same single-stage column PBR described in Section 2.1.2 was subsequently used for a second experiment, carried out immediately after the first. In this second experiment, the black cardboard shield was removed, resulting in a fully illuminated configuration, as illustrated in Figure 9.

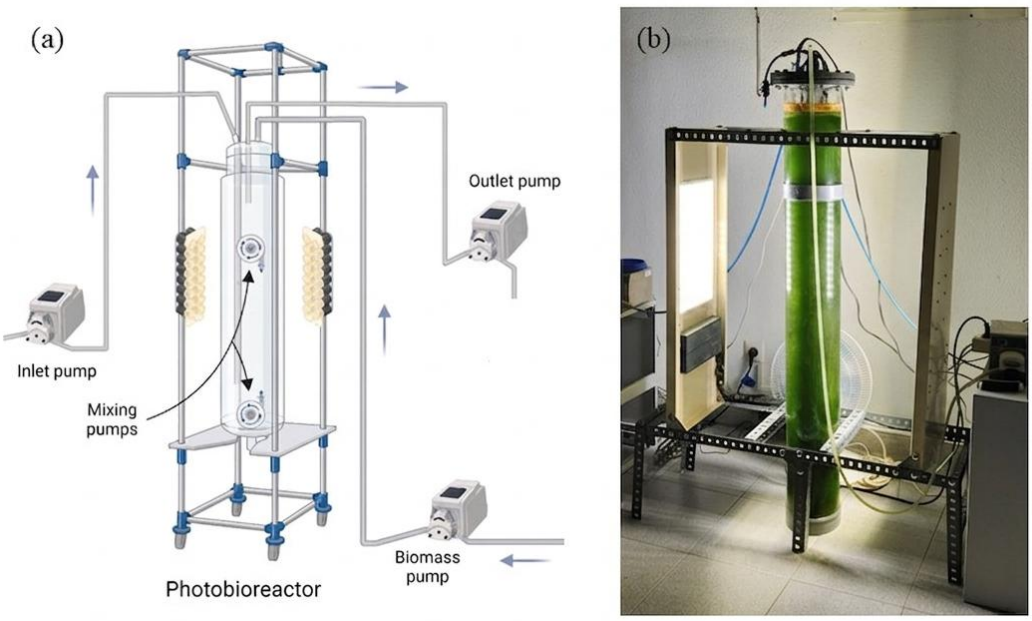

Figure 9: (a) Schematic diagram of the single-stage PBR and (b) photograph of the PBR during continuous operation. Drawing from Biorender.

2.2.3. MICROBIAL COMMUNITY, MICROSCOPIC, AND PHYSIOLOGICAL ANALYSES

In addition to the physical-chemical analyses described in Section 2.1.3, the microbial community structure was evaluated through 16S rRNA gene high-throughput sequencing. Total genomic DNA quality was evaluated according to sample quality control procedures. The target region of the 16S rRNA gene was amplified using specific primers (e.g., 515F-806R for V4) containing unique barcodes. PCR reactions were performed using 15 μL of Phusion® High-Fidelity PCR Master Mix (New England Biolabs), 0.2 μM of forward and reverse primers, and approximately 10 ng of template DNA. PCR products were purified using magnetic bead purification, quantified, and pooled in equimolar ratios. Sequencing libraries were generated, indexed, and validated for concentration (Qubit and real-time PCR) and size distribution (Agilent Bioanalyzer). Quantified libraries were sequenced on an Illumina platform by Novogene (Europe). Paired-end raw reads were assigned to samples based on unique barcodes and trimmed. Clean tags were assembled using FLASH (v1.2.11) and quality-filtered using fastp (v0.23.1). Chimera sequences were detected and removed using VSEARCH (v2.16.0) against the SILVA reference database. Amplicon Sequence Variants (ASVs) and taxonomic assignments were generated using DADA2 within the QIIME 2 framework against the SILVA database (v138.1). Alpha and beta diversity analyses (including PCoA/NMDS based on UniFrac distances) were performed using QIIME 2 and R software. Microalgae identification and cell biometry were conducted by microscopic examination (OLYMPUS IX70, USA) on samples fixed with 5% acidic Lugol's solution and stored at 4 °C, according to the Utermöhl method (1958). Additionally, the physiological status of the photosynthetic microorganisms was assessed by measuring the quantum yield (Q_Y) using an AquaPen AP 110-C PAM fluorometer (Photon Systems Instruments, Czech Republic). Prior to measurement, samples were adapted to a dark environment for 15 minutes.

2.2.4. CALCULATIONS

The concentration of free ammonia [NH_3] (mg N L^{-1}) was estimated from the Anthonisen equation as represented in Equation 6 (González-Camejo, Montero, et al., 2020):

$$[\mathrm{NH_3}] = \frac{[NH_4{}^+]}{1+10^{-\mathrm{pH}+0.09018+\frac{2729.92}{\mathrm{T}+273}}} \quad (6)$$

where $[NH_4^+]$ is the concentration of ammonium in the PBR; pH is the pH value of the cultivation broth in the PBR and T is the liquid temperature (°C).

The carbon mass balance was calculated according to Equation 7:

$$Q_{in} \times ([TOC_{in}] + [IC_{in}]) = \left(V_{PBR} \times BP \cdot \frac{\%C}{100}\right) + Q_{out} \cdot ([TOC_{out}] + [IC_{out}]) + \\ + C_{Loss} \quad (7)$$

where $[TOC_{in}]$ is the total organic carbon concentration in the inlet SWW (L d^{-1}); $[IC_{in}]$ is the inorganic carbon concentration in the inlet SWW (g L^{-1}); $\%C$ is the carbon content in the biomass; $[TOC_{out}]$ is the total organic carbon concentration in the effluent (g L^{-1}); $[IC_{out}]$ is the inorganic carbon concentration in the effluent (g L^{-1}) and C_{Loss} represents the unaccounted carbon in the mass balance.

2.3. COLUMN PHOTOBIOREACTOR WITH SUPPORT MEDIA

2.3.1. OBJECTIVE OF THE STUDY

The purpose of the study in Chapter 5 is to evaluate the influence of varying the quantity of surface area provided by support media for attached biomass on the performance of column photobioreactors treating real domestic wastewater. The study was developed under controlled laboratory conditions, using biological duplicates, to investigate the effect of increasing attached biomass on treated effluent quality, specifically focusing on nitrogen and phosphorus removal, and to improve biomass separation processes, thereby exploring practical applications for enhancing photobioreactor efficiency.

2.3.2. COLUMN PHOTOBIOREACTOR DESIGN

The column PBRs were constructed using acrylic tubes 5 mm thick, 104 mm in internal diameter and 1000 mm in height. Each PBR was equipped with a ¾" threaded inlet 10 cm from the base and for ¾" threaded outlet spaced 20 cm apart, the first of which was

equipped with a sampling tap. The PBRs were closed using acrylic lids that contain two ½" threaded holes for fixing the air diffusers, made of plastic with 10 µm pores, used to generate rising bubbles (Figure 10).

Figure 10: Column photobioreactors with and without support media.

2.3.3. BIOBOB®: THE SUPPORT MEDIA

The support media originally developed by BIOPROJ, a Brazilian company, named Biobob®, is an advanced patented carrier for cell immobilisation designed for fixed biofilm processes in wastewater treatment. The Biobob® was developed specifically for bacterial immobilisation, offering high active surface area for biomass attachment, low hydrodynamic resistance even after colonisation, and applicability in moving bed, integrated fixed-film, and fixed bed reactors systems, enabling compact system designs with reduced capital and operational costs.

However, the use of this support media for mixed cultures of microalgae and bacteria has been poorly investigated. Moreover, the original Biobob® dimensions were not suitable for the laboratory-scale PBRs used in this study. Therefore, a smaller version proportional to the reactor size was developed and named mini-Biobob (Roveroto et al., 2021). Manufactured

using a 3D printer with transparent plastic material, the mini-Biobob measures 13 mm in diameter and 18 mm in height, featuring openings on the sides, as well as on the top and bottom, while maintaining its original cylindrical shape (Figure 11). The support was filled with the same polyurethane foam as the original Biobob®, with 50% porosity and a density of 28 kg m^{-3}.

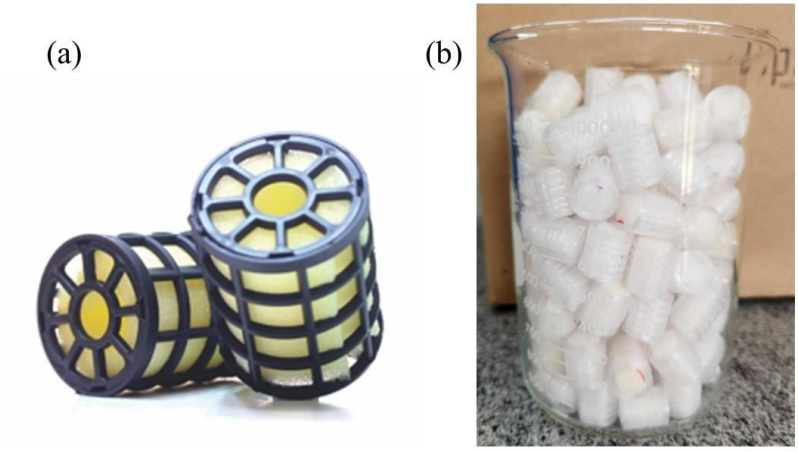

Figure 11: Support media: (a) original Biobob® and (b) mini-Biobob.

2.3.4. PHYSICAL-CHEMICAL ANALYSES

2.3.4.1. ALKALINITY MEASUREMENT

Alkalinity was determined by potentiometric titration following Section 2320 B of Standard Methods (APHA, 2017). A 50 mL sample (V_{sample}) was measured in a graduated cylinder, and the initial pH was recorded. The sample was titrated under magnetic stirring with a standard sulfuric acid solution (H_2SO_4) of known normality ($N_{H_sSO_4}$). The volume of acid required to reach pH 4.3 was recorded as $V_{pH\,4.3}$. Alkalinity (mg $CaCO_3$ L^{-1}) was calculated as follows (Equation 8):

$$Total\ alkalinity\ (mg\ CaCO_3 L^{-1}) = \frac{V_{pH\,4.3} N_{H_2SO_4}\ 50\,000}{V_{sample}} \quad (8)$$

2.3.4.2. CHEMICAL OXYGEN DEMAND (COD)

Dissolved COD was determined using the closed reflux colorimetric method described in Section 5220 D of Standard Methods (APHA, 2017). Samples were filtered through 0.45 µm membrane filters prior to analysis. An appropriate sample volume was added to borosilicate tubes containing the digestion solution with potassium dichromate ($K_2Cr_2O_7$) and silver sulfate (Ag_2SO_4) in concentrated H_2SO_4. The tubes were tightly closed and placed in the digester at 150°C for 120 minutes. After cooling slowly to room temperature, the sample absorbances were measured at 420 nm using a spectrophotometer (DR6000 UV-VIS, HACH). At this wavelength, the decrease in dichromate ion ($Cr_2O_7^{2-}$) concentration is proportional to the COD concentration

2.3.4.3. DRY WEIGHT (DW) TOTAL SUSPENDED SOLIDS (TSS)

Dry weight were determined following Section 8111 G of Standard Methods (APHA, 2017). For raw effluent, a 50 mL aliquot was used; for reactor samples, a 25 mL aliquot was used. Each volume was measured in a graduated cylinder, which was rinsed with deionised water to ensure complete solids transfer. Samples were transferred to pre-weighed crucibles and evaporated to dryness on a steam bath. The evaporated sample was dried for 1 h in an oven at 103 to 105°C. The crucible was cooled in a desiccator to room temperature and weighed. The drying, cooling, and weighing cycle was repeated until the weight change was less than 0.5 mg.

Total suspended solids were determined following Section 2540 D of Standard Methods (APHA, 2017). A measured volume of homogenised sample was filtered through a pre-dried (103 to 105°C for 1 h) and weighed glass fiber membrane (GF-5, Macherey-Nagel, Düren, Germany) named M_{dry}. The filter was washed with three successive 10 mL portions of deionised water, dried at 103 to 105°C for h, cooled in a desiccator, and weighed, named M_{filter}. The TSS concentration (mg L^{-1}) was determined by Equation 9:

$$TSS\ (mg\ L^{-1}) = \frac{M_{filter} - M_{dry}}{V_{sample}} \quad (9)$$

2.3.4.4. TOTAL NITROGEN (TN), TOTAL KJELDAHL NITROGEN (TKN) AND NITRATE (NO_3^--N)

Samples were filtered through 0.45 µm membrane filters prior to analysis. TN, NO_3^--N, and TKN were quantified using the tube NANOCOLOR® test total Kjeldahl nitrogen TKN 16 (Nanocolor, Macherey-Nagel, Düren, Germany) which contains pre-dispensed reagents, following the instructions of manufacturer. Absorbance measurements were performed a Nanocolor™ UV/VIS II spectrophotometer (Macherey-Nagel, Germany).

For TN determination, the sample pH was adjusted to 5 to 9 before analysis. A 2.0 mL aliquot of sample were added with 2.0 mL of digestion reagent (R1) in a digestion tube, capped, shaken, and heated at 100°C for 60 minutes. After digestion, the tube was cooled to room temperature, one NANOFIX reagent was added, and the tube was shaken. A 0.5 mL of this digested solution was transferred to another tube and mixed with 0.5 mL of R2 reagent. After 10 minutes, the absorbance was measured at 345 nm.

For NO_3^--N determination, the sample pH was adjusted to 1 to 13. A 0.25 mL aliquot of the sample was mixed with 0.25 mL of R2 reagent in a reagent tube. After 10 minutes, the absorbance was measured at 345 nm. The TKN concentration was then calculated as the difference between TN and NO_3^--N.

2.3.4.5. TOTAL PHOSPHORUS

Total phosphorus was quantified by the colorimetric method utilising ascorbic acid, following Section 4500-P of Standard Methods (APHA, 2017). Samples were filtered through 0.45 µm membrane filters prior to analysis. For sample digestion, one drop of phenolphthalein indicator was added to 50 mL of sample. If a pink colour developed, H_2SO_4 (5N) was added dropwise until the colour disappeared. Then, 1 mL of H_2SO_4 (5N) and 0.4 g of ammonium persulfate ($(NH_4)_2S_2O_8$) were added. The flask was placed on a preheated hot plate and boiled gently for 40 minutes. After cooling, one drop of phenolphthalein indicator was added again, and the solution was neutralised with NaOH (5N) to a faint pink colour. The volume was then brought to 100 mL with deionised water.

The mixed reagent was prepared in following order: 50 mL of H_2SO_4 (5N), 5 mL of potassium antimonyl tartrate solution, 15 mL of ammonium molybdate solution, and 30 mL of ascorbic acid solution. All reagents were allowed to reach room temperature before mixing.

For colorimetric determination, 8 mL of the mixed reagent was added to 50 mL of the neutralised, digested sample and mixed well. After 11 minutes, the absorbance of each sample was measured using a DR6000 UV-VIS spectrophotometer (HACH) at 880 nm.

2.4. STATISTICS, DATA VISUALISATION AND AI DECLARATION

Results are expressed as mean ± standard deviation of the monitored parameters under steady-state operation, for single-stage PBR configuration. The PBR with support media did not achieve steady state and was analysed during the stable operational period. Normality was assessed using the Shapiro-Wilk test. Statistical comparisons were performed using Student's T-test for parametric data, and Brunner-Munzel and Mann-Whitney tests for non-parametric data. All analyses were performed in the Jamovi software (version 2.3.28).

Schematic figures were created using BioRender.com (Toronto, Canada) and Canva (Sydney, Australia). For the visual enhancement and aesthetic refinement of the figures and images presented in this study, the Gemini (Google) artificial intelligence model was utilised. This tool was employed exclusively for lighting optimisation in photographs and for improving the layout of elements within figures, ensuring that the conceptual content and original data remained unaltered. During the preparation of this work, the author used DeepSeek for language refinement and grammar correction, and LeadSpace and Scopus-AI for literature review. The author is solely responsible for the scientific content, data interpretation, and final conclusions.

3.

Influence of the HRT, biomass concentration and illuminated S/V ratio on the performance of domestic wastewater treatment in a single-stage algal-bacterial column photobioreactor [1]

[1] This Chapter has been published in a modified version as:
dos Santos, T. L., Vargas-Estrada, L., Blanco, S., da Silva, G. H. R., & Muñoz, R. (2025). Influence of operational parameters on the performance of domestic wastewater treatment in a single-stage algal-bacterial column photobioreactor. *Algal Research*, 92, 104417. https://doi.org/10.1016/j.algal.2025.104417

ABSTRACT

This study evaluated the performance of a single-stage photobioreactor (PBR), under varying hydraulic retention times (HRT) (4, 3 and 2 days), biomass concentrations (2.7 and 1.6 g TSS L^{-1}) and illuminated surface/volume ratios (17.8 and 26.7 m^2 m^{-3}) in a continuous system operated for 192 days. The system achieved removal efficiencies of Total Organic Carbon of 94-96%, Total Nitrogen of 92-97% and phosphate of 91-100% regardless of the operational conditions. $N\text{-}NH_4^+$ removal was primarily driven by assimilation into algal-bacterial biomass. Nitrate and nitrite accumulation in the cultivation broth was not observed and N_2O generation was negligible. Increased light availability boosted biomass productivity up to 335.7 ± 77.8 g m^{-3} d^{-1}. The reduction in biomass concentrations from 2.7 to 1.6 g L^{-1} of TSS decreased microalgal concentration and diversity, particularly affecting filamentous bacteria. These results demonstrate that a single-stage PBR can achieve performance comparable to conventional two stages anoxic-aerobic photobioreactors, while being more cost-effective and sustainable, highlighting its potential for advanced wastewater treatment and resource recovery.

Keywords: Biomass productivity, Hydraulic retention time, Light availability, Microalgal-bacterial symbiosis, Solid retention time.

3.1. INTRODUCTION

As anthropogenic activities drive global biogeochemical cycles beyond sustainable thresholds, domestic wastewater has emerged as a critical challenge for water security due to the complex mixture of organic matter, nutrients (e.g., nitrogen and phosphorus), pathogens, heavy metals and emerging pollutants including pharmaceuticals, personal care products, surfactants, pesticides, plasticizers, and others (Mohsenpour et al., 2021; Han & Zhou, 2022; Oruganti et al., 2022; Wali et al., 2021; Yan et al., 2022; Li et al., 2023). Conventional technologies treating domestic wastewaters such as activated sludge systems are often limited by high energy consumption associated with mechanical aeration and may achieve incomplete nutrient removal (e.g., 90–95% nitrogen and 20–40% phosphorus removal without tertiary treatment) (Alcántara, Posadas, et al., 2015a; Foladori et al., 2020; Mohsenpour et al., 2021). These limitations are linked to the multi-stage configuration typically required for advanced nutrient removal (e.g., sequential processes like nitrification, denitrification, and phosphorus precipitation) (Han & Zhou, 2022; Kwon et al., 2019; Posadas et al., 2017).

In contrast, algae-bacteria technologies have emerged as a promising alternative, leveraging symbiotic microbial relationships for more sustainable wastewater treatment, to reduce aeration needs, enhance nutrient recover, and produce valuable biomass (Karemore et al., 2015; Mohsenpour et al., 2021; Torres-Franco et al., 2021; Vargas-Estrada et al., 2021). However, their net energy balance can be compromised by the energy requirements for mixing, and particularly by the energy-intensive harvesting of biomass (Alcántara, Posadas, et al., 2015b; Posadas et al., 2017).

Despite these challenges, microalgae-bacteria consortia remain a promising platform for wastewater treatment. In this symbiotic system, microorganisms play complementary roles for simultaneous carbon and nitrogen removal (Alcántara, Posadas, et al., 2015b). The process is based on bacterial oxidation of organic carbon and the conversion of nitrogen compounds, producing CO_2. This CO_2 is then utilized by photoautotrophic microalgae, which in return provide O_2 through photosynthesis. This synergy can eliminate the need for external aeration and chemical precipitation of phosphorus (Kwon et al., 2019; Rada-Ariza et al., 2019; Zhong et al., 2024). Additionally, the process facilitates phosphorus recovery primarily through assimilation into the microbial biomass, and generates a valuable biomass that can be used as a feedstock for bioproducts manufacture a soil amendment or biostimulant, restoring the

nutrient cycle and improving crop productivity (Arbib et al., 2013a; Mohsenpour et al., 2021; Oruganti et al., 2022).

Typically, studies assessing the performance of algal-bacterial consortia for wastewater treatment have been carried out in open photobioreactor such as high-rate algal ponds (HRAP), which can suffer from low photosynthetic efficiencies and nutrient removal (Karemore et al., 2015; Andrade et al., 2016; Mohsenpour et al., 2021). In contrast, closed photobioreactors represent a suitable configuration to enhance the efficiency of microalgae-bacteria based wastewater treatment systems due to their larger illuminated surface area to volume ratio, better control of operational parameters, and higher biomass productivity (Arbib et al., 2013a; Karemore et al., 2015; Posadas et al., 2017; Deprá et al., 2019). This superior potential has been evidenced by Arbib et al. (Arbib et al., 2013b), who performed a direct comparison between a HRAP and an airlift tubular photobioreactor (TPBR) treating urban wastewater. The TPBR achieved significantly higher nutrient removal efficiencies (89% TN and 86% TP removal) compared to the HRAP (65% TN and 58% TP removal). This enhanced performance was concomitant with a substantially higher biomass areal productivity, which reached 21.8 g SS m^{-2} d^{-1} in the TPBR, compared to 8.3 g SS m^{-2} d^{-1} in the HRAP (Arbib et al., 2013b). Nevertheless, closed PBRs still face challenges in optimizing operational parameters to maximize both microalgae growth and nutrient removal efficiency (Arbib et al., 2013a; Andrade et al., 2016).

The HRT and SRT critically influence the balance between biomass activity and productivity (González-Camejo et al., 2022; Meng et al., 2024). Selecting appropriate values is essential for maintaining cells in their exponential growth phase, which optimizes both biomass productivity and carbon/nutrient removal efficiency (Posadas et al., 2017). The choice of these values is a key operational decision that must be tailored to the specific system, taking into account ambient conditions, nutrient availability, and reactor design (González-Camejo et al., 2022). Notably, Meng et al. (Meng et al., 2024) studied the influence of the SRT in the simultaneous nitrification-denitrification and phosphorous removal in a sequencing batch reactor. The authors demonstrated that a 15-day SRT achieved over 98% of phosphorus and 85% of nitrogen removal, primarily through nitrification-denitrification, while shorter SRT (5-10 days) favoured assimilation as the dominant process. This finding supports the approach of our study, as it confirms that manipulating the SRT is a viable strategy to shift the dominant nitrogen removal pathway towards assimilation.

Moreover, the light intensity can affects algal photosynthesis, bacterial nitrification, and biological community structure (Oruganti et al., 2022; Shinichi Akizuki et al., 2020; Zhi et al., 2023). While high light intensities (>450 μmol m^{-2} s^{-1}) can induce photoinhibition in both microalgae and nitrifying bacteria, this effect can be relevant for single-stage systems, where controlled nitrite oxidizing bacteria (NOB) inhibition creates a carbon-efficient shortcut for nitrogen removal via nitrite, an effect that can be balanced by operating at high biomass concentrations (Kwon et al., 2019; Shinichi Akizuki et al., 2020; Oruganti et al., 2022; Meng et al., 2024). In this context, the literature reports photobioreactors operation under a wide range of biomass concentration, ranging from 0.1 to 8 g TSS L^{-1}. Unfortunately, high biomass concentrations (>2 g TSS L^{-1}) should be avoided to prevent detrimental self-shading effects (Posadas et al., 2017; Foladori et al., 2020). On the other hand, biomass productivity ranging between 295.6 and 343.5 g m^{-3} d^{-1} have been achieved under different production strategies in an outdoor TPBR treating synthetic wastewater (Andrade et al., 2016). Nonetheless, gaps remain regarding in understanding the interplay of these key parameters on the overall performance of single-stage algal-bacterial photobioreactor. A systematic study investigating their combined effect is lacking.

In this context, this study aims to bridge this gap by evaluating the effect of the HRT, biomass concentration and illuminated surface area to volume ratio on the performance of carbon, nitrogen and phosphorous removal in a single-stage algal-bacterial column photobioreactor during domestic wastewater treatment. In addition, the impact of these operational parameters on the microalgae population structure was assessed. The experimental design herein proposed was specifically intended to fill the above mentioned research gap by testing a matrix of these key parameters to map their individual and combined effects on system performance, thereby identifying the most promising conditions for efficient nutrient removal via assimilation.

3.2. MATERIALS AND METHODS

3.2.1. INOCULUM

The inoculum consisted of a mixture of concentrated microalgae-bacteria consortium and fresh aerobic activated sludge (AS). The AS was collected from the activated sludge

secondary settler of Valladolid wastewater treatment plant (WWTP), with a total suspended solids (TSS) concentration of 4.2 g L^{-1}.

The algal-bacterial consortium was obtained from an indoor 180 L HRAP treating real centrate from the same WWTP as described elsewhere (Hoyos et al., 2024).

This consortium was predominantly composed of filamentous bacteria (80% of the community) and 20% of *Mychonastes homosphaera* morphotype and was concentrated by centrifugation (4000 rpm, 15 minutes), removing the supernatant, and mixing the resulting biomass pellet with the AS broth. The mixture was then resuspended in synthetic wastewater (SWW) to reach a final volume of 22 L, achieving an initial total suspended solids (TSS) concentration of 1.8 g L^{-1}.

3.2.2. SYNTHETIC WASTEWATER COMPOSITION

The SWW was prepared to minimize fluctuations in composition and to maintain stable operating conditions. The SWW was prepared based on the BG 11 medium adapted from Ferro et al., (2019) using tap water. The composition of the SWW was (per L): 0.625 g glucose, 0.7 g $NaHCO_3$, 0.16 g peptone, 0.11 g meat extract, 0.15 g NH_4Cl, 0.04 g K_2HPO_4, 0.075 g $MgSO_4.7H_2O$, 0.036 g $CaCl_2.2H_2O$, 0.02 g Na_2CO_3 and 1 mL of micronutrients solution composed of (per L): 6.0 g citric acid, 6.0 g ferric ammonium citrate, 1.0 g $EDTA.Na_2$, 2.86 g H_3BO_3, 1.81 g $MnCl_2.4H_2O$, 0.39 g $Na_2MoO_4.2H_2O$, 0.08 g $CuSO_4.5H_2O$, 0.05 g $Co(NO_3)_2.6H_2O$, 0.22 g $ZnSO_4.7H_2O$.

The resulting SWW had a pH of 8.1 ± 0.3, 368.3 ± 28.5 mg L^{-1} of total organic carbon (TOC), 135.2 ± 12.1 mg L^{-1} of inorganic carbon (IC), 72.6 ± 5.2 mg L^{-1} of total nitrogen (TN), and 18.5 ± 1.6 mg L^{-1} of phosphorus ($P\text{-}PO_4^{3-}$), which corresponded to a C:N:P mass ratio of 20:4:1. Theoretical concentrations of other elements were estimated as follows: potassium (K) of 17.96 mg L^{-1}, calcium (Ca) 9.81 mg L^{-1}, zinc (Zn) 0.05 mg L^{-1}, magnesium (Mg) 7.40 mg L^{-1}, sulphur (S) 9.79 mg L^{-1}, and iron (Fe) 0.75 mg L^{-1}

3.2.3. EXPERIMENTAL SET-UP

The SWW was stored at 4°C in a refrigerated reservoir and continuously pumped into the PBR by a peristaltic pump (SK-HandyPump-1). The effluent was withdrawn from the PBR (described in Section 2.1.2) by an identical peristaltic pump and delivered to a 1 L conical

settler (Figure 12). Inside the settler, clarified supernatant overflowed from the top by gravity and was collected in a plastic container, while the settled biomass was recirculated from the bottom back to the PBR using a peristaltic pump (Dosiper C1R, Clinter) at a flow rate of 0.75 L d^{-1}. Excess biomass was withdrawn daily from the settler bottom to control the solid retention time (SRT). The experimental period was extended to 192 days.

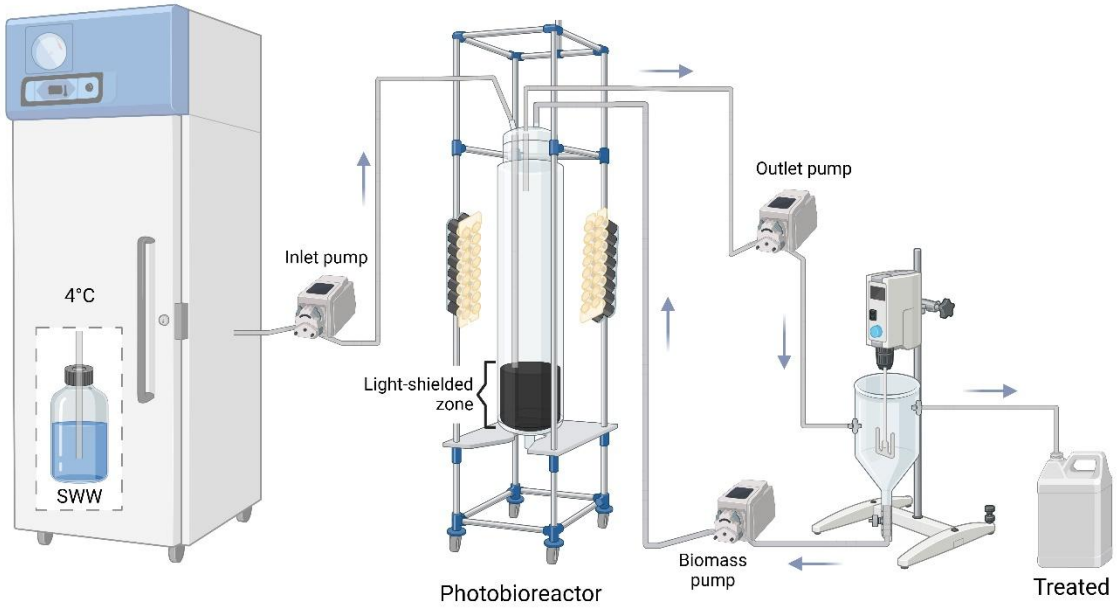

Figure 12: Schematic diagram of the experimental set-up.

The PBR was continuously illuminated with an average light intensity of 431 ± 18 µmol m^{-2} s^{-1}. The available illuminated surface area varied throughout the experiment: 0.39 m² with the black cardboard shield (Stages I to IV), and 0.59 m² without the shield (Stage V).

The average light intensity inside the PBR was calculated using a light attenuation model (Solimeno et al., 2017). Covering the one-third of the PBR surface with the black cardboard shield reduced total light flux entering the reactor from 21 µmol s^{-1} (Stage V) to 8-12 µmol s^{-1} (Stage I-IV), as detailed in Table 2.

3.2.4. OPERATIONAL CONDITIONS AND SAMPLING PROCEDURES

The experiment was divided into five operational stages. The initial 45-day period was devoted to system stabilization until steady state conditions were achieved. The HRT was selected based on (Alcántara, Domínguez, et al., 2015). During Stage I, the system was operated for 36 days at an HRT of 4 days. In Stage II, the HRT was reduced to 3 days, which was maintained for 31 days. During Stage III (21 days of operation), the HRT was further reduced to 2 days. An initial SRT of 10 days was chosen based on previous literature studies to ensure community stability (Zhi et al., 2023). In Stage IV (HRT = 2 days), the biomass concentration in the PBR was maintained below 2 gTSS L^{-1} by centrifuging a certain volume of the culture, withdrawing the biomass pellet, and returning the supernatant to the PBR. This operational shift reduced SRT from 10 to 3 days. Stage IV was operated for 41 days. Finally, the black cardboard shield was removed in Stage V and the operating conditions were kept similar to Stage IV, for 18 days. The operational conditions set in this experiment are summarized in Table 2.

Table 2: Operational conditions and process parameters during the evaluation of the performance of the PBR.

	Stage I	**Stage II**	**Stage III**	**Stage IV**	**Stage V**
Period (d)	36	31	21	41	18
HRT (d)	4	3	2	2	2
SRT (d)	11 ± 2	10 ± 2	10 ± 1	3 ± 1	3 ± 1
Illuminated area S (m^2)	0.39	0.39	0.39	0.39	0.59
Surface light intensity ($\mu mol\ m^2\ s^{-1}$)			431 ± 18		
S/V ($m^2\ m^{-3}$)	17.8	17.8	17.8	17.8	26.7
Average internal light flux ($\mu mol\ s^{-1}$)	8	7	8	12	21

The pH, dissolved oxygen (DO), and temperature were daily monitored at 11:00 am. Twice a week, liquid samples of 100 mL were withdrawn from the SWW, the PBR and the

effluent of the settler to measure the concentration of IC, TOC, TN, N-NH_4^+, N-NO_2^-, N-NO_3^-, and P-PO_4^{3-}. The concentration of TSS and volatile suspended solids (VSS) was determined in the PBR, bottom of settler and effluent of the settler. The concentration of N_2O in the headspace of the PBR was measured in duplicate by collecting 100 µL of gas samples twice a week. Additionally, samples from the culture broth of the PBR were collected at the end of each operational stage to determine the structure of population of microalgae.

3.2.5. ANALYTICAL PROCEDURES

The pH was measured with a SensION™ + PH3 pHmeter (HACH, The Netherlands). The temperature inside the PBR was monitored with a multiparameter analyser C-3020 (Consort, Belgium) and DO was monitored using an OXI 3310 oximeter (WTW, Germany). The photosynthetic active radiation (PAR) at the PBR walls was measured with a LI-250A light meter (LI-COR Biosciences, Germany). TSS, VSS, TOC, IC and TN, N-NH_4^+, N–NO_2^-, N–NO_3^-, P-PO_4^{3-}, N_2O, the content of C, H, N, S and O in the microalgae biomass, the structure of the microalgae consortium were analysed according to description in Section 2.1.3.

3.3. RESULTS AND DISCUSSION

3.3.1. EVOLUTION OF ENVIRONMENTAL PARAMETERS DURING PHOTOBIOREACTOR PERFORMANCE

Temperature, DO, and pH were periodically monitored throughout the experiment. Throughout Stage I to III the pH remained stable and averaged 7.4 ± 0.3 (Figure 13). Interestingly, the decrease in biomass concentration in Stage IV enhanced microalgae photosynthetic activity, and the pH increased up to 7.8 ± 0.4 (p<0.05). This increasing pH trend continued in Stage V up to an average pH of 8.6 ± 0.6. No external control was required to maintain the pH in the algal-bacterial broth, demonstrating that under the tested conditions, the pH stability and subsequent increase suggest a net dominance of CO_2-consuming processes, such as photosynthesis, over acidifying processes like nitrification.

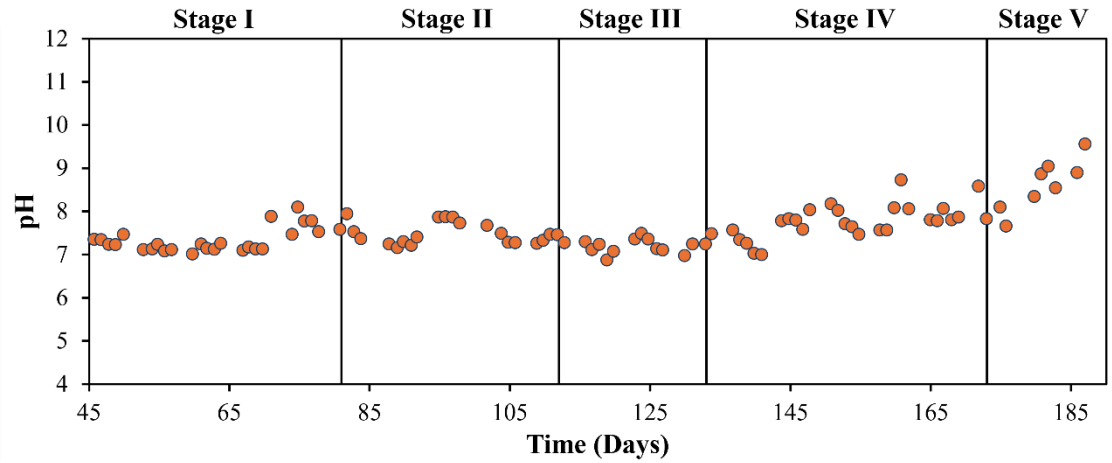

Figure 13: Time course of the pH in the algal-bacterial broth during PBR operation.

The temperature of the cultivation broth remained stable (30 ± 1°C) throughout all stages (Figure 14a). On the other hand, DO levels increased progressively across operational stages, likely due to enhanced photosynthetic activity in spite of the increasing oxygen demand when decreasing the HRT. Thus, DO concentrations remained <3 mg O L^{-1} for the first 14 days of Stage I, likely due to the low biomass concentration and low photosynthetic activity of a microalgal-bacterial consortium acclimating to the environmental and operational conditions in the photobioreactor. The subsequent rise in DO, reaching values >12 mg O_2 L^{-1} in Stage V (Figure 14b), is a consequence of the enhanced photosynthetic activity associated with the increased in IC removal (Figure 15), which was driven by the higher light intensity provided. The oxygen production from this intensified photosynthesis far exceeded the residual oxygen demand for nitrification, leading to the oxygen accumulation observed.

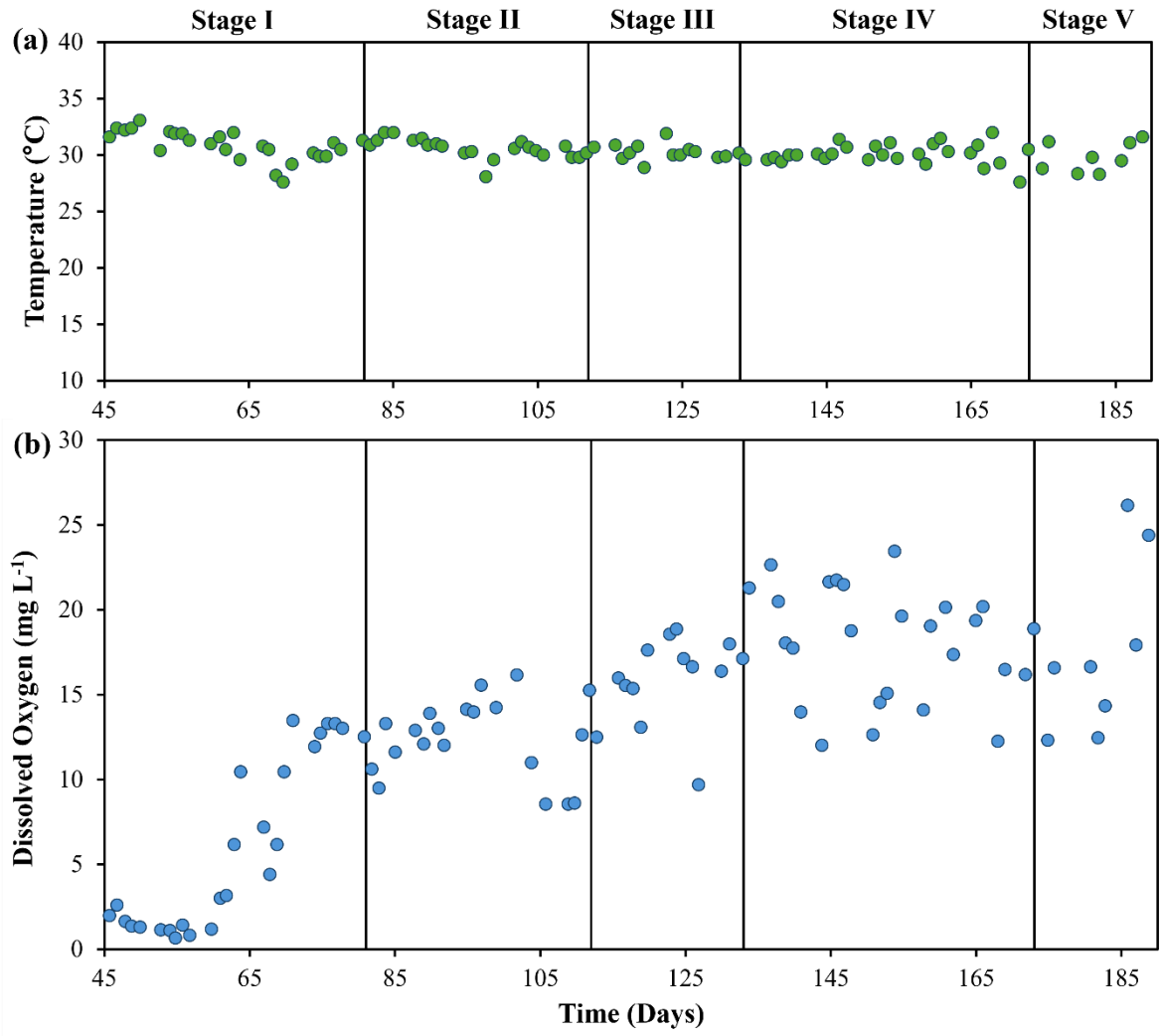

Figure 14: Time course of the (a) temperature and (b) dissolved oxygen concentration in the algal-bacterial broth during PBR operation.

3.3.2. CARBON AND PHOSPHORUS REMOVAL

The PBR herein evaluated demonstrated a highly efficient organic carbon removal, consistently achieving TOC removal efficiencies above 94 ± 1% across all operational stages at TOC loading rates ranging from 85 to 199 g TOC m^{-3} d^{-1} (Figure 15). This performance is comparable to other single-stage algal bacterial systems treating municipal wastewater. For instance, Aparicio et al., (2024) reported COD removal efficiencies higher than 86% in a membrane-assisted HRAP treating urban wastewater, while Arango et al., (2025) achieved 92-98% COD removal in 50 L raceways PBRs. Similarly, He et al., (2013) reported TOC removal efficiencies of 65-98% in a tubular PBR treating primary-treated municipal wastewater, while Posadas et al., (2013) achieved 90% TOC removal in a biofilm reactor

treating domestic wastewater. On the other hand, the anoxic-aerobic configurations of Alcántara et al., (2015) and Torres-Franco et al., (2021) also achieved high TOC removal (85-96%). Therefore, this study confirmed that single-stage configuration photobioreactors can achieve comparable organic matter removals than more complex two-stage systems.

This study demonstrated a strong correlation between microalgal activity and IC removal, as evidenced by the concurrent increase in both parameters following operational changes. The reduction of HRT in Stages I to III, which enhanced biomass productivity by 15%, resulted in the IC removal rate increased from 4.6 to 16.7 mg IC L^{-1} d^{-1}. This suggests that the photosynthetic activity was the primary driver of inorganic carbon assimilation. The reduction in biomass concentration in the PBR during Stage IV to 1.5 ± 0.4 g VSS L^{-1}, improved light penetration, subsequently increasing the average IC removal efficiency from 24 ± 3% in Stage III up to 30 ± 7%. This tendency was reinforced in Stage V, where the increased illuminated surface-to-volume ratio from 17.8 to 26.7 m^2 m^{-3} in Stage V boosted light supply from 168 to 253 μmol s^{-1}. This increase, combined with the TOC was nearly completely removed (>94% efficiency), create ideal conditions for photoautotrophy. Following the depletion of organic carbon source, a 750% increase in IC removal rate compared to Stage I was observed, reaching 38.9 mg IC L^{-1} d^{-1}, which far exceeded the relative increased in light availability, highlights a significant metabolic shift within the system in response to the changing carbon availability. It is important to note that this IC consumption was not solely due to microalgae; other processes like nitrification also contributed to the overall removal.

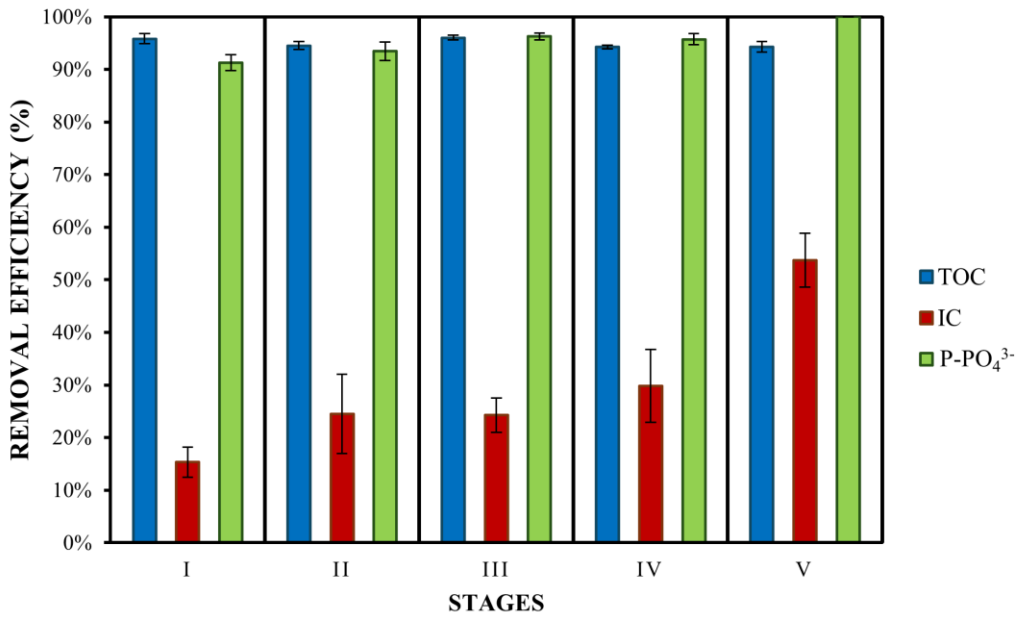

Figure 15: Steady state TOC, IC and $P\text{-}PO_4^{3-}$ removal efficiencies during PBR operation.

Steady state $P\text{-}PO_4^{3-}$ removal efficiencies reached 96 ± 1% in Stages III and IV, and increased up to 100% in Stage V (Figure 15). In this context, the SWW herein used exhibited a N:P molar ratio of 26:1, which is higher than the optimal ratio of 11:1 recommended by Karemore et al., (2015) for promoting algal cell growth. While phosphorous deficiency can hinder the growth of nitrifying bacteria, it does not significantly affect microalgae due to their ability to perform luxury uptake (González-Camejo et al., 2022). Additionally, since pH values remained below 10 and these conditions do not support phosphate precipitation, it can be inferred that the high phosphorous removal efficiency observed in this study was primarily driven by phosphorous assimilation into biomass, aligning with the recent findings of Torres-Franco et al., (2021).

3.3.3. NITROGEN REMOVAL

The TN removal efficiency increased from 92 ± 6% in Stage I to 98 ± 1% in Stage V (Figure 16). TN removal was directly linked to assimilation into new biomass (Posadas et al., 2017). This process primarily depends on light availability and IC supply during photosynthetic growth, although heterotrophic metabolism can also contribute to biomass formation (Posadas et al., 2017). The N content in microalgae typically ranges from 6.6% to

9.3% (Posadas et al., 2017) and in this study, varied from 7.4 ± 0.4% to 8.7 ± 0.3%, with the highest value observed in Stage III.

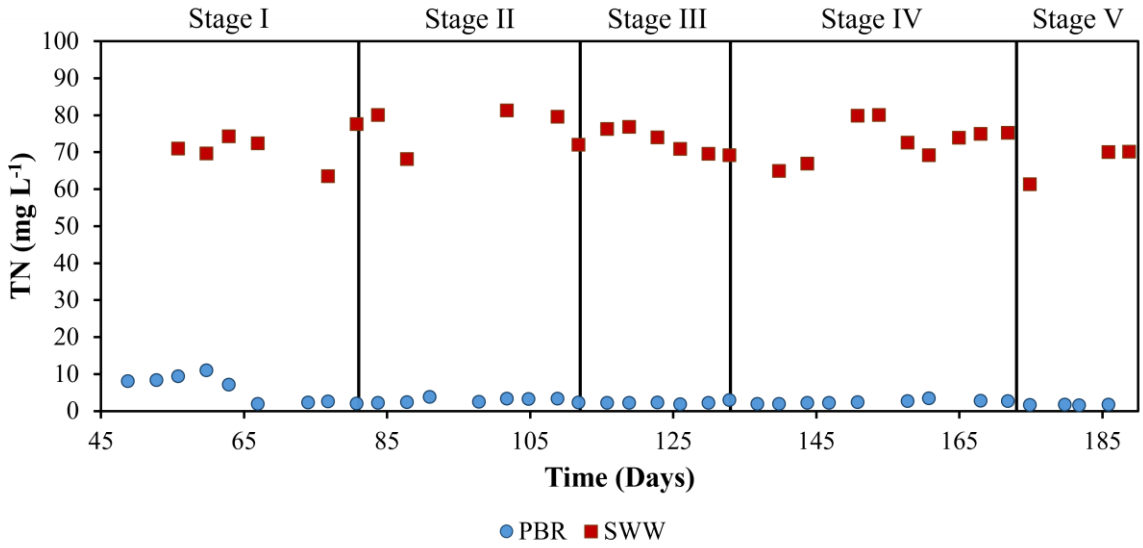

Figure 16: Time course of Total nitrogen (TN) in the cultivation of the PBR (blue circles) and in SWW (red squares) during the different operational stages.

This effective TN removal was the result of an active NH_4^+ uptake, which consistently exceeded 98% across all stages (Figure 17), mainly driven by the low energy requirements for ammonium microalgae assimilation (González-Camejo et al., 2022). The biomass composition remained consistent across all stages, with an empirical composition of $CH_{1.8}O_{0.5}N_{0.2}$. This consistency supports the assumption of a theoretical biomass composition of $CH_{1.7}O_{0.4}N_{0.2}P_{0.0094}$ (González et al., 2008), and suggests that, in this case, the changes in operational conditions did not significantly impact the biomass composition.

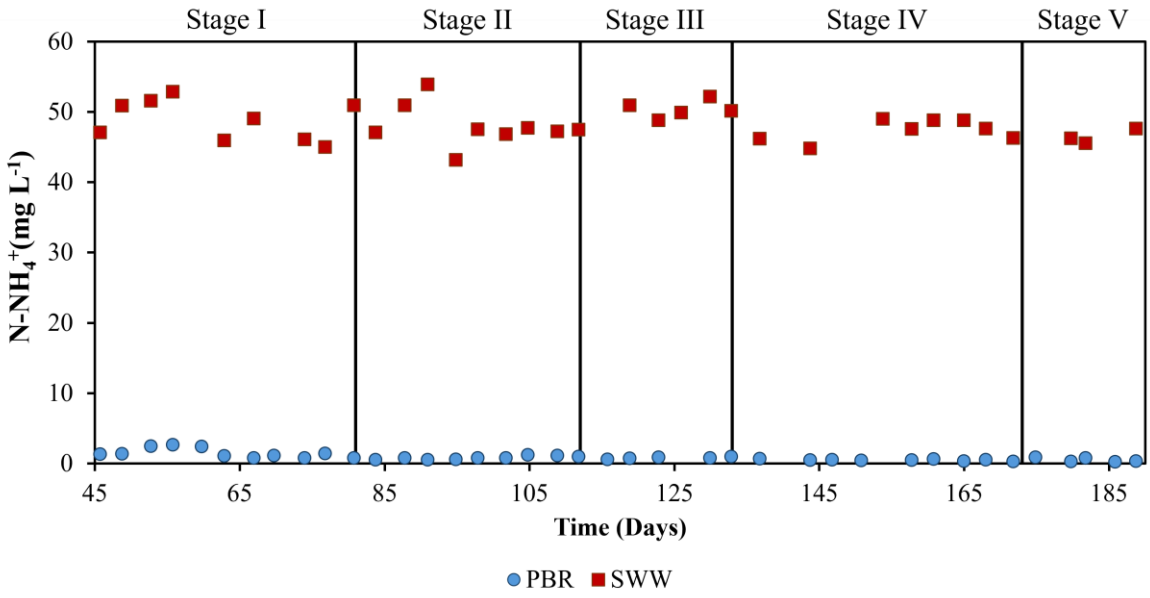

Figure 17: Time course of N-NH_4^+ in the cultivation of the PBR (blue circles) and in SWW (red squares) during the different operational stages.

The ratio of total carbon removed to ammonium removed (mg $TOC_{removed}$/mg N-$NH_4^+{}_{removed}$) averaged 7.3 ± 0.3 throughout the study, while the carbon to nitrogen ratio in the biomass (mg $C_{biomass}$/mg $N_{biomass}$) obtained from the elemental analysis was in average 6.1 ± 0.4. These results suggest that the primary mechanism of N-NH_4^+ removal was assimilation into algal-bacterial biomass, which was consistent with the findings of Alcántara et al., (2015).

The adoption of the González et al., (2008) stoichiometry, originally determined from swine manure, for domestic wastewater treatment is consistent with a resource recovery paradigm. This formulation assumes a high-protein biomass (approximately 12% N on total biomass mass), representing an upper-performance scenario where N is actively assimilated. However, domestic wastewater is often limited in inorganic carbon relative to microalgal demands (Acién et al., 2016). Although the lower C:N ratio, typical from domestic wastewater, the consistent C:N removal ratio and biomass C:N obtained in this study suggest that the algal-bacterial consortium compensated for carbon limitation, maintaining assimilation as the dominant N removal pathway.

Interestingly, the step reduction in HRT conducted from Stage I to III did not significantly affect NH_4^+ concentration in the PBR (p>0.05), consistent with findings by Buha et al., (2017) operating two identical aerobic–anoxic sequencing bioreactors at high N-NH_4^+ concentrations.

It is important to highlight that the concentrations of $N\text{-}NO_2^-$ and $N\text{-}NO_3^-$ in the SWW fluctuated across the five operational stages due to variations in the characteristics of the tap water used for SWW preparation (Figure 18). The reduction in the HRT from Stages I to III increased $N\text{-}NO_2^-$ concentration in PBR from 0.3 ± 0.1 mg L^{-1} to 0.6 ± 0.1 mg L^{-1}. Despite this increase, concentrations remained significantly lower than the 5 mg L^{-1} reported in an algal-bacterial PBR treating SWW at an 8-days HRT (Zhong et al., 2024). During Stage III, nitrogen mass balance demonstrated that N_{loss} peak at 40% of total nitrogen removal, representing its highest contribution throughout the stages. Nonetheless, at this particular stage, the PBR exhibited the highest microalgal density (9.28×10^{10} ind L^{-1}; Figure 21) with filamentous bacteria comprising 59% of the total microbial population, confirming the fact that biomass assimilation was still the primary nitrogen removal.

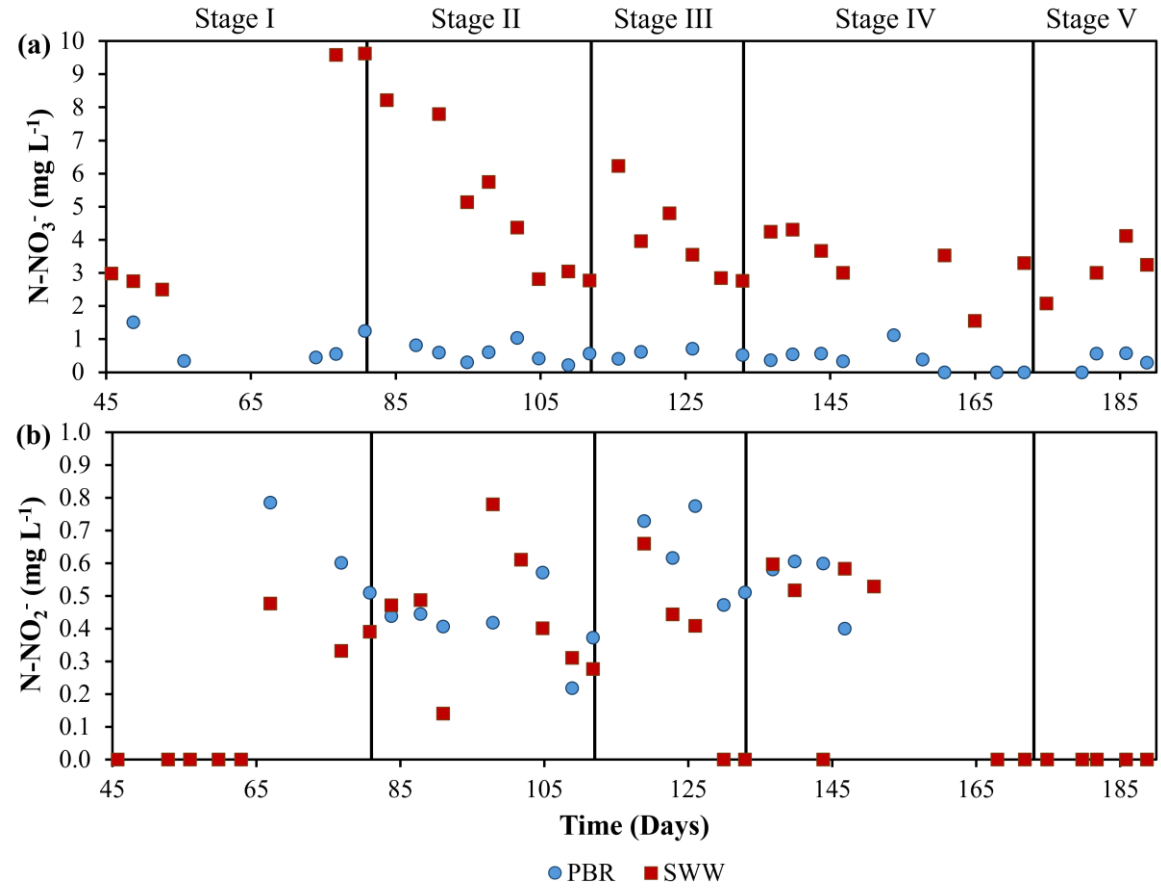

Figure 18: Time course of the different nitrogen species a) $N\text{-}NO_3^-$; and b) $N\text{-}NO_2^-$ in the cultivation of the PBR (blue circles) and in SWW (red squares) during the different operational stages.

On the other side, the reduction of SRT, in our particular study, from 10 days (Stages I to III) to 3 days (Stages IV and V), associated to the decrease in biomass concentration from 2.7 ± 0.2 to 1.6 ± 0.2 g TSS L^{-1}, prevented the nitrate and nitrite accumulation. This can be attributed to the effective light penetration and potential inhibition of NOB under the prevailing conditions, preventing nitrite accumulation despite the relatively short SRT. Notably, $N\text{-}NO_2^-$ was undetectable in Stage V, suggesting that either complete nitrite oxidation by NOB or nitrite denitrification might have occurred (Buha et al., 2017). Despite the high DO levels, the mass balance calculation for Stage V indicated a nitrogen loss of 25% of the total nitrogen removal, with nitrogen assimilation dominating (0.55 g N d^{-1}), likely due to the enhanced microalgae and nitrifying bacterial activities. These findings align with the consistently high $N\text{-}NO_3^-$ removal efficiencies of 87 ± 1% across all stages (Figure 18a), driven by microalgal activity. The high nitrate removal be attributed to the nitrate uptake rate exceeding the ammonia nitrification rate (González-Camejo et al., 2019).

Although the complex relationship between microalgae and bacterial consortia influences nutrient removal, nitrification is typically favoured by longer SRT, which allow the enrichment of nitrifying bacteria, while denitrification is primarily driven by the prevalence of anoxic conditions, achievable under various SRT and HRT conditions (Aparicio et al., 2024; Arango et al., 2025). Whilst excessively short SRTs (e.g., <2 days) can lead to NO_2^- accumulation due to a higher ammonia oxidizing bacteria (AOB) activity compared to the activity of microalgae and NOB, which can negatively impact microalgal performance (González-Camejo et al., 2022). The results obtained in this study indicated that the selected operational conditions effectively supported system stability, by preventing the accumulation of nitrogenous intermediates and promoting efficient removal.

Moreover, the increased illuminated area did not influence the nitrogen species assimilation as $N\text{-}NO_2^-$ remained undetectable in Stage V, despite the high sensitivity of NOB to excessive light intensity provided to the PBR, which exceeded the reported limit of tolerance of NOB >450 µmol m^{-2} s^{-1} (Shinichi Akizuki et al., 2020). Indeed, a prolonged light exposure can damage nucleic acids and chromophores in AOB and NOB, with NOB being more sensitive and AOB exhibiting a faster recovery and developing greater photoresistance (Kwon et al., 2019). Additionally, NOB are typically more light-sensitive than AOB, which can lead to partial nitrification and nitrite accumulation due to inhibition of the second nitrification step (González-Camejo et al., 2022). However, the $N\text{-}NO_3^-$ and $N\text{-}NO_2^-$ remained consistent in the PBR across all stages.

Finally, N_2O emissions were monitored throughout all experimental stages, with measured concentrations of 2.11 mg N L^{-1} in the headspace of the PBR, representing 0.1% of the influent TN. These emissions were significantly lower than the typical 1.6% of influent TN mass load used for environmental impact assessments of wastewater treatment (de Haas & Andrews, 2022), confirming its negligible impact on both greenhouse gas emissions and nitrogen mass balance of the system. It is important to highlight that N_2O emissions were only detected in stages I-III, when the system was operated under an illuminated S/V ratio of 17.8 m^2 m^{-3} and the microalgae concentration within the reactor was >2 g TSS L^{-1}, which could have significantly promoted self-shading effect and anoxic zones inside the cultivation broth. Interestingly, when the biomass concentration within the reactor was set below 2 g TSS L^{-1}, N_2O emissions were not detectable. Thereby, the lower biomass concentration likely reduced the self-shading effect within the reactor, resulting in negligible N_2O emissions from the microalgae-bacteria consortium. It has been recently demonstrated that microalgae can produce N_2O under dark conditions and low DO levels (Jo et al., 2024; Li et al., 2023). However, the operational conditions imposed in this work (i.e. continuous illumination), along with the high photosynthetic microalgae activity recorded (DO >5 mg L^{-1}), suggest that N_2O emissions were likely attributed to bacterial activity. N_2O is an intermediate and byproduct of denitrification and nitrification processes, respectively (Jo et al., 2024), and is mainly produced from nitrite. Thereby, the presence of NO_2^- in the reactor during Stages I to III can be attributed to the activity of aerobic AOB, and since no NO_3^- accumulation within the reactor was observed, it could be suggested that simultaneous denitrification-nitrification was being carried out in the PBR.

3.3.4. BIOMASS PRODUCTIVITY AND MICROALGAE POPULATIONS

Despite the HRT reduction in Stages I to III, biomass productivity increased from 218.4 ± 22.6 to 250.6 ± 37.9 g m^{-3} d^{-1}. Upon implementation of a more intensive biomass withdrawal strategy in Stages IV and V, which reduced the SRT to 3 days, biomass productivity increased up to 522.4 ± 126.9 g m^{-3} d^{-1} in Stage IV. This improvement can be attributed to diminished self-shading effects, enhanced nutrients availability for microalgae growth and increased biomass withdrawal rate, which maintained PBR concentration below 2 g TSS L^{-1}.

Increasing the S/V ratio to 26.7 m^2 m^{-3} in Stage V reduced biomass productivity to 339.7 ± 70.1 g m^{-3} d^{-1}, although statistical analysis indicated no significant difference between Stages IV and V. This result reveals that the biomass productivity was limited by microalgae physiological aspects resulting from the continuous illumination. Typically, during saturated illumination the photosynthetic rate reaches its maximum value and does not increase with increasing illumination (Esteves et al., 2024). Hence, the absence of a dark cycle, where microalgae could have recovered and improve their cell division in addition to the resulting oxygen supersaturation (>12 mg O_2 L^{-1} in Stage V, Figure 14b) could have imposed an additional constraint, potentially inhibiting sensitive microbial populations within the consortium. In this context, the high dissolved oxygen concentrations prevailing during most of the experimental period might have induced the formation of reactive oxygen species (ROS) with potential to damage the photosynthetic system (Esteves et al., 2024).

In outdoor systems, biomass production is fundamentally limited by the natural photoperiod. For instance, the optimized strategy in the outdoor tubular PBR studied by Andrade et al., (2016) achieved a daily productivity of 257.8 g m^{-3} d^{-1}, a value constrained by the hours of daylight. Therefore, while optimizing the S/V ratio remains crucial for light capture, this study demonstrates that its effectiveness is ultimately bounded by the physiological limits of the consortium.

Moreover, biomass concentration exhibited an inverse correlation with DO (de Godos et al., 2014). Thus, the reduction of average biomass concentrations from 2.7 ± 0.2 g VSS L^{-1} in Stage III to 1.5 ± 0.3 g VSS L^{-1} in Stage V (Figure 19) resulting from increased biomass harvesting rates, were associated with higher DO levels (Figure 14b). This increased DO concentration in addition to the high light intensity, could have induced the ROS formation, limiting microalgae growth.

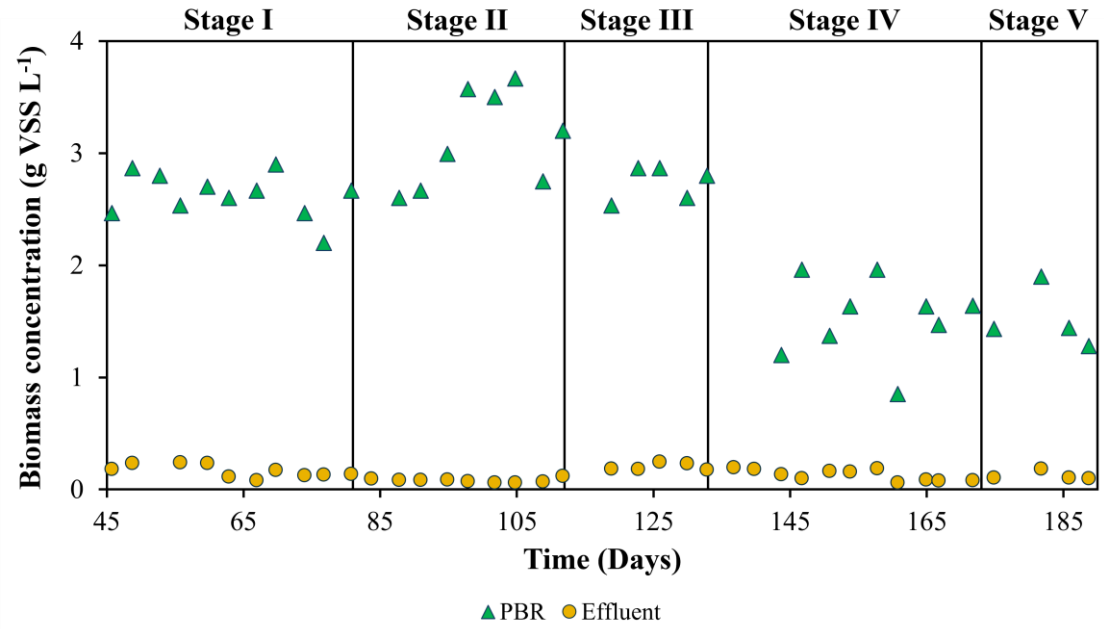

Figure 19: Time course of the biomass concentration in g VSS L^{-1} in the PBR and effluent through the study.

The effluent TSS concentrations average 0.14 ± 0.06 g L^{-1} throughout the study, corresponding to a biomass removal efficiency of 94 ± 3% in the settler. Despite this high efficiency, this biomass concentration consistently exceeded the maximum TSS discharge limit established by the European Union Legislation (35 mg L^{-1}) (EU, 2024). Similar results were reported by Toledo-Cervantes et al., (2016) in a pilot HRAP with biomass recirculation based on biomass productivity control, where TSS concentration of 70 ± 50 mg L^{-1} also exceeded regulatory limits, demonstrating that increased biomass wastage rates could reduce TSS concentrations, while potentially enhancing photosynthetic efficiency. However, the limited sedimentation capacity of many microalgae species frequently leads to effluent with TSS levels that exceed the allowable discharge thresholds for natural water bodies (Alcántara, Domínguez, et al., 2015).

Microscopic analysis of the microalgal-bacterial community, based on morphological identification, was conducted under stable operational performance, as each experimental stage was maintained for a period equivalent to at least 8 HRT prior to data collection, ensuring system stability. Under these conditions, the most frequently observed morphotypes in the PBR during the experimental stages belonged to three phyla and different classes: Chlorophyta (Green Algae), the class Chlorophyceae (including *Scenedesmus* morphotype, *Scenedesmus quadricauda* morphotype, and *Tetradesmus obliquus* morphotype) and the class

Trebouxiophyceae (*Mychonastes homosphaera* morphotype and *Chloroidium ellipsoideum* morphotype); Bacillariophyta (Diatoms), the class Bacillariophyceae (*Nitzschia palea* morphotype); and Cyanobacteria (including *Pseudanabaena* morphotype and filamentous bacteria) (Figure 20).

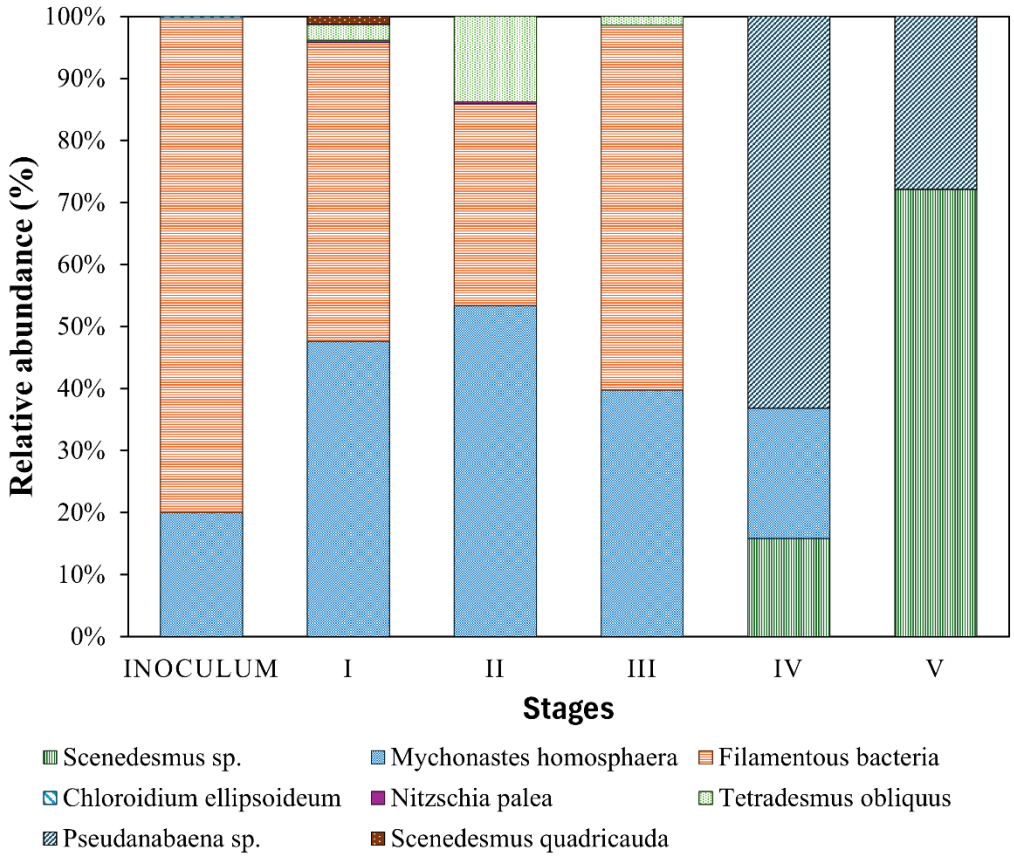

Figure 20: Time course of the relative abundances (%) per species of the main phyla of microalgae in the PBR during the operational stages.

The initial high relative abundance of filamentous bacteria over microalgae (*Mychonastes homosphaera* morphotype) in the inoculum likely contributed to the low dissolved oxygen (DO <5 mg L^{-1}) observed during the first 14 days of operation (Figure 14b). In Stage I, the decline in filamentous bacteria (48% of total population), alongside an increase in the relative abundance of *Mychonastes homosphaera* morphotype (48%), resulted in a reduced cell density but increased biovolume (Figure 21), reflecting the replacement of numerous small bacterial cells with fewer, larger microalgal cells. The colonial morphology of emergent species (*Tetradesmus obliquus* morphotype with 3% and *Scenedesmus quadricauda* morphotype with 1%) further enhanced the biovolume of the prevailing

microbial community. The reduction of HRT in Stage II an increase in the relative abundance of *Mychonastes homosphaera* morphotype (53%) and *Tetradesmus obliquus* morphotype (14%) was observed, driving a 32% biovolume increase and peak TSS (3.2 ± 0.4 g L^{-1} on average), concomitant with a 11% reduction in cell density versus Stage I. The disappearance of *Scenedesmus quadricauda* morphotype suggests potential competitive exclusion for nutrients (increased of IC and $P\text{-}PO_4^{3-}$; Figure 15 and TN; Figure 16) under these conditions. Stage III (HRT = 2d) was characterized by a 127% increase in cell density, primarily composed of filamentous bacteria morphotype (59%). The observed microbial shift suggests that the reduction in HRT created selective pressure that favoured the proliferation of these bacterial morphotypes. This shift occurred alongside a reduced relative biovolume (6 μm^3 $cell^{-1}$), reflecting the substitution of larger microalgae (*Mychonastes homosphaera* morphotype: 40%; *Tetradesmus obliquus* morphotype: 1%) by smaller and numerous bacterial cells. The highest N_{loss} observed in this stage, coupled with the increased relative abundance of bacterial morphotypes, suggests a period of intensified bacterial activity.

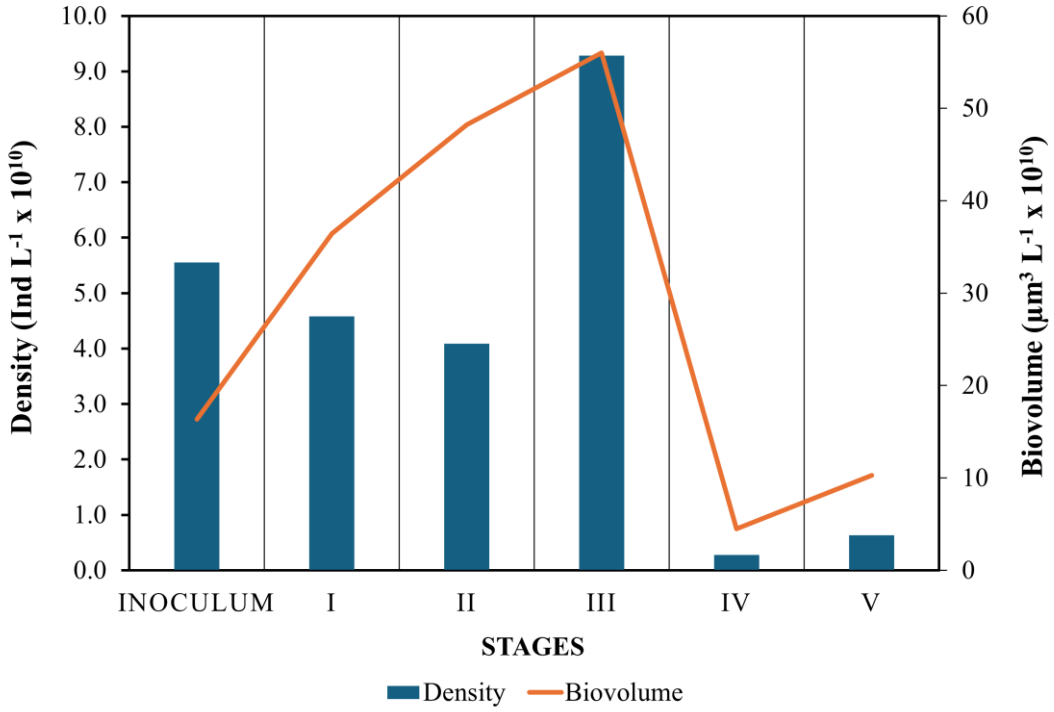

Figure 21: Time course of total microalgae densities and total microalgae biovolume, as estimated by microscopic analysis in the PBR during the operational stages.

The biomass withdrawal strategy in Stage IV reduced microalgae concentration and density to their lowest recorded levels. Notably, *Pseudanabaena* morphotype showed the highest relative abundance (63%) alongside *Mychonastes homosphaera* morphotype (21%) and *Scenedesmus* sp. (16%) morphotype. However, the period of enhanced light availability in Stage V was accompanied by a 126% increase in cell density and a 129% increase in biovolume, achieving the highest relative cell volume (16.2 μm^3 $cell^{-1}$) observed in the study. In stage V, *Scenedesmus* morphotype became the most prevalent (72%), while *Pseudanabaena* morphotype abundance declined to 28% and *Mychonastes homosphaera* morphotype was undetectable.

The enhanced S/V ratio in Stage V particularly favoured *Scenedesmus* morphotype potentially due to its reported tolerance to high light intensities compared to *Pseudanabaena* morphotype (Posadas et al., 2017). Interestingly, the reduced SRT in Stages IV and V was associated with decreased microalgal richness and diversity, particularly affecting filamentous bacteria. This observation aligns with previous studies showing that an extended SRT supports a broader range of growth parameters and microbial diversity (Mansfeldt et al., 2019; Zhi et al., 2023).

3.4. CONCLUSION

This study demonstrated that a single-stage algal-bacterial photobioreactor achieved high removal efficiencies for ammonium (up to 99%), total nitrogen (92-97%), total organic carbon (up to 95%) and phosphate (100% in Stage V), alongside a biomass productivity of 336 ± 79 g m^{-3} d^{-1} by balancing the HRT, SRT, and light availability. The system maintained high bioremediation efficiency, comparable to more complex multi-stage systems, even at short HRTs (2 days), highlighting the potential of single-stage PBRs as an alternative for wastewater treatment, characterized by its operational simplicity inherent to a compact, single-tank design, high nutrient removal efficiency, and biomass production with biotechnological potential. Future research should focus on exploring the treatment of different effluents with varying C:N:P ratios to increase its applicability and scalability and to demonstrate the occurrence of simultaneous nitrification-denitrification in the algal-bacterial broth.

4.

Uncovering nitrogen removal in algal-bacterial processes for domestic wastewater treatment[2]

[2] This Chapter has been published in a modified version as:
Santos, T. L. dos, Vargas-Estrada, L., Blanco, S., Silva, G. H. R. da, & Muñoz, R. (2026). Uncovering nitrogen removal in algal-bacterial processes for domestic wastewater treatment. *Journal of Water Process Engineering*, *86*, 109975. https://doi.org/10.1016/j.jwpe.2026.109975

ABSTRACT

The synergy between microalgae and bacteria in photobioreactors is complex, with the competition between assimilation and nitrification critically influencing nutrient removal efficiency. This study investigated the interplay between nutrient and carbon removal pathways in a single-stage microalgal-bacterial photobioreactor treating domestic wastewater by selectively inhibiting nitrification with allylthiourea (ATU). The inhibition successfully suppressed bacterial activity, reducing the NH_4^+ removal rate by 20% and increasing the contribution of microalgal assimilation to total nitrogen removal from 59% to 68%. Moreover, ATU addition induced a change in microbial population structure, as suggested by the decline in relative abundance of Proteobacteria and Bacteroidota phyla, which ultimately mediated a shift in the share of carbon fate mechanisms. The total organic carbon removal efficiency decreased from 94 ± 1% to 88 ± 1%, while the carbon assimilation efficiency into biomass was increased from 65% to 80%. Thus, mixotrophic microalgae like *Scenedesmus* sp. became the dominant genus, alongside the cyanobacterium *Nodosilinea*. Phosphate removal remained consistently high (97-98%) and unaffected by ATU addition, indicating its decoupling from nitrification. The results demonstrated that nitrogen removal was mainly dominated by microalgae assimilation complemented by bacterial pathway, consistent with nitrification-denitrification to achieve complete nitrogen removal.

Keywords: Algal–bacterial interactions; nitrogen assimilation, single-stage PBR, biomass productivity.

4.1. INTRODUCTION

The treatment and disposal of domestic wastewater represent a significant global challenge, driven by the increasing volumes generated, its potential contribution to greenhouse gas emissions and eutrophication, and urgent need for water reuse (Fallahi et al., 2021; Rahimi et al., 2020; Yan et al., 2022). Conventional nutrient removal in wastewater treatment plants (WWTPs) is often energy intensive and inefficient in terms of resource recovery, particularly for domestic wastewaters with low C:N ratios and phosphorus concentrations (Fallahi et al., 2021; Mohsenpour et al., 2021; Tang et al., 2025).

Nitrogen transformation in biological wastewater treatment systems involves multiple pathways, including ammonification, nitrification, denitrification, assimilatory and dissimilatory nitrate reduction to ammonium, anammox, and nitrite-nitrate interconversion (Liu et al., 2023; Rahimi et al., 2020). Of these, the nitrification-denitrification pathway is the most widely adopted for engineered biological nitrogen removal (Fallahi et al., 2021; Liu et al., 2023; Rahimi et al., 2020; Yan et al., 2022). However, this multi-step process is energy-intensive due to the aeration demand for nitrification and the external carbon source requirements for heterotrophic denitrification (Rahimi et al., 2020; Yan et al., 2022). In addition, an incomplete hydroxylamine oxidation (NH_2OH), nitrite reduction or an incomplete heterotrophic denitrification, can biologically produce N_2O, a potent greenhouse gas with a global warming potential 298 times greater than CO_2, posing a significant sustainability challenge for conventional biological processes (Alcántara, Domínguez, et al., 2015; Alcántara, Posadas, et al., 2015a; Peng et al., 2023).

As a sustainable alternative to activated sludge processes, microalgal-bacterial consortia offer several advantages, as the photosynthetically produced oxygen from the assimilation of inorganic carbon by microalgae can sustain the activity of ammonia-oxidising bacteria (AOB) and nitrite-oxidising bacteria (NOB) for nitrification. Hence, a simultaneous nitrogen and phosphorus removal, with potential for resource recovery as algal-bacterial biomass, can be carried out while addressing critical challenges of water scarcity (Al-Jabri et al., 2021; González-Camejo et al., 2022; Karya et al., 2013; Rahimi et al., 2020; Shinichi Akizuki et al., 2020; Vargas-Estrada et al., 2021; Wali et al., 2021; Zhang et al., 2020).

In these systems, a fundamental competitive dynamic occurs: microalgae and AOB primarily utilize ammonium (NH_4^+) as their nitrogen source and nitrogen/electron donor source, respectively (Fallahi et al., 2021; Krustok et al., 2016). On one hand, the excess of

oxygen produced by microalgae is used by AOB to oxidise NH_4^+ to NO_2^-, which is further oxidised to NO_3^- by NOB. These processes maintain minimal NH_4^+ concentrations in the cultivation broth and prevent microalgae inhibition while maintaining NO_3^- for microalgae assimilation (González-Camejo et al., 2022). Even if microalgae can assimilate nitrate, this pathway is typically less efficient than NH_4^+ uptake (Nishi et al., 2022). Hence, competition for ammonia governs the overall nitrogen removal efficiency and process stability (Fallahi et al., 2021; González-Camejo, Montero, et al., 2020; Krustok et al., 2016). Despite microalgae and nitrifiers can symbiotically coexist, their relationship involves complex interactions and specific operational parameters. Typically, nitrification is carried out by Proteobacteria and Bacteroidetes, with *Nitrosomonas* and *Nitrospira* typically identified as the key AOB and NOB species. Nonetheless their sensitivity to high light intensities could limit their presence in microalgae cultures (Rahimi et al., 2020). In addition, the high DO concentrations resulting from photosynthetic microalgae metabolism can hinder the heterotrophic nitrate denitrification, which is a strictly anaerobic process. The dynamics and dominance of these pathways, which intersect with carbon removal mechanisms, remain poorly characterized, particularly in single-stage photobioreactors.

A particularly relevant mechanism in single-stage photobioreactors, especially when devoted to the treatment of wastewaters with a low C:N ratio, is the simultaneous nitrification-denitrification (SND). This biological mechanism involves aerobic autotrophic nitrifiers and aerobic denitrifiers, which possess the capacity to perform denitrification under oxygen-saturated conditions. On the other hand, SND can be also conducted by aerobic autotrophic nitrifiers and anaerobic heterotrophic denitrifiers when oxygen diffusion limitations create anoxic microniches, allowing the coexistence of both microbial groups (Rahimi et al., 2020). To elucidate the occurrence of these interactions, allylthiourea (ATU), a well-established inhibitor of the key AOB enzyme ammonia monooxygenase (AMO), can be added to the algal-bacterial cultivation broth as an experimental tool to selectively inhibit nitrification and elucidate the mechanisms involving competition for nitrogen between microalgae and bacteria. Indeed, ATU chelates copper at its active site in AMO at specific concentrations, transiently inhibiting AOB activity without significantly affecting microalgal activity (Ginestet et al., 1998; González-Camejo et al., 2022) and allowing to elucidate the occurrence of denitrification.

Therefore, the main objective of this study was to elucidate the respective contributions of nitrogen assimilation by microalgae and bacteria, and nitrification-

denitrification by bacteria, by selectively inhibiting nitrification, providing critical insights for optimizing algal-bacterial wastewater treatment.

4.2. MATERIALS AND METHODS

4.2.1. SYNTHETIC WASTEWATER COMPOSITION

The SWW was prepared according to Section 3.2.2 (BG 11 medium modified). The SWW had a pH of 8.1 ± 0.2 and concentrations of total organic carbon (TOC) of 360.2 ± 21.1 mg L^{-1}, inorganic carbon (IC) of 109.7 ± 5.1 mg L^{-1}, total nitrogen (TN) of 70.5 ± 7.8 mg L^{-1} and total phosphorus (TP) of 15.0 ± 2.6 mg L^{-1}. The SWW was supplemented with 0.05 g L^{-1} of allyl-thiourea ($C_4H_8N_2S$) to inhibit nitrification, resulting in an inlet TN concentration of 85.9 ± 5.6 mg L^{-1}.

4.2.2. INOCULUM

This initial consortium was subsequently subjected to a 192-days optimization experiment (described in Chapter 3), during which the consortium was acclimated to the SWW and to the PBR operational and environmental conditions. This long-term operational served to select a robust algal-bacterial community adapted to the target operational parameters. At the end of this process, the photosynthetic population structure of the adapted consortium was composed of *Scenedesmus* sp. (77%) and *Pseudanabaena* sp. (23%).

4.2.3. EXPERIMENTAL SET-UP

The experimental system (Figure 22) consisted of an indoor column PBR as described in Section 2.2.2. The synthetic wastewater (SWW) was stored at 4 °C in a refrigerated reservoir and pumped into the PBR by a peristaltic pump (SK-HandyPump-1) at a flow rate of 22 L d^{-1}. The PBR effluent was directed to the bottom of the conical settler, where the clarified supernatant overflowed from the top and was discharged as treated effluent. The settled biomass was recirculated from the bottom of the settler back to the PBR at 0.75 L d^{-1} using a second peristaltic pump. The system was operated under continuous illumination to

eliminate the variability introduced by light-dark cycles and an average photosynthetic active radiation (PAR) of 316.6 ± 9.9 µmol m^{-2} s^{-1}.

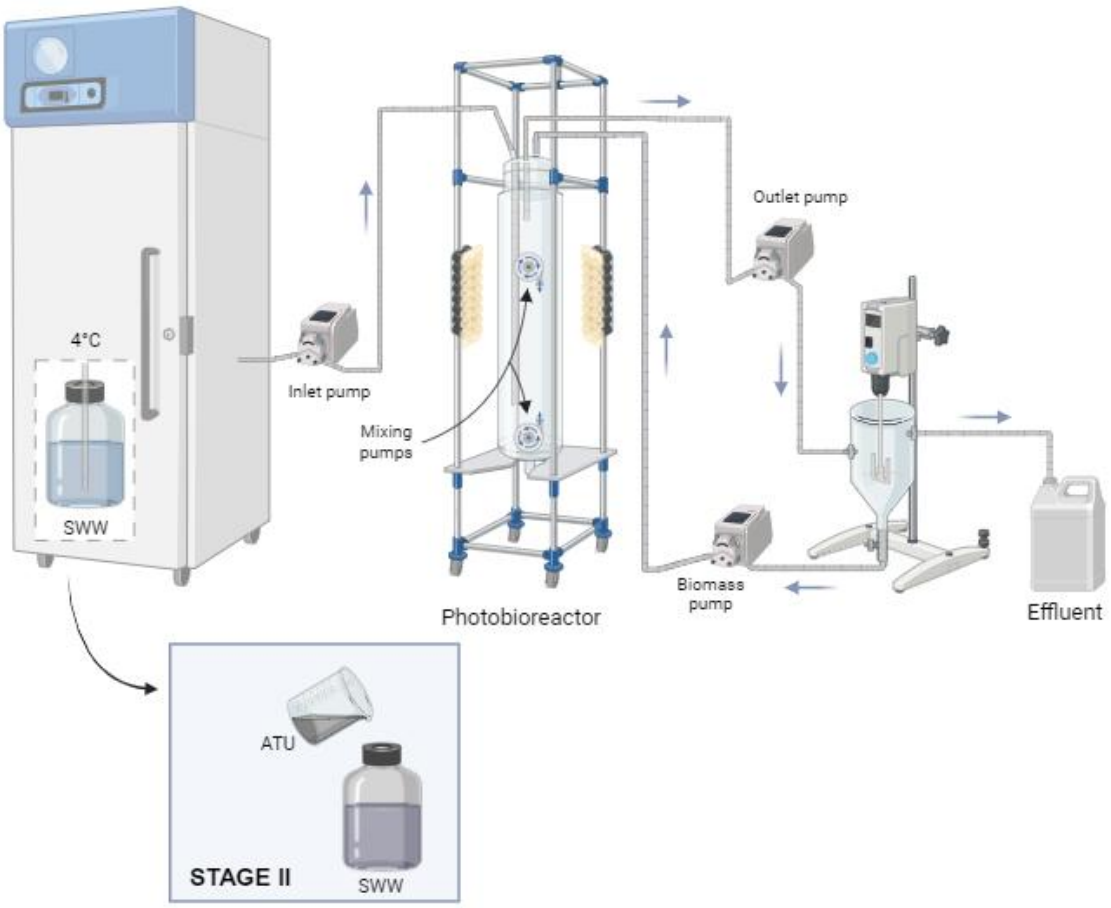

Figure 22: Schematic diagram of the experimental set-up.

Biomass concentration in the PBR was maintained below 2 g TSS L^{-1} by continuous withdrawal from the bottom of the settler. The volume withdrawn was centrifuged (4000 rpm, 20 min), the biomass pellet was discarded, whilst the supernatant was recycled to the PBR to preserve the mass balance. This operational strategy resulted in a solid retention time (SRT) of 3 ±1 days. These operational conditions favoured the dominance of bacteria with high specific growth rates, thereby promoting partial nitrification without significant nitrite accumulation (González-Camejo et al., 2022).

The 38-day experiment was divided in two sequential operational stages: an initial 23 days stage when the system was only feed with SWW, followed by a 15 days stage when ATU was added to the SWW at a concentration 0.05 g L^{-1} to inhibit nitrification. A hydraulic retention time (HRT) of 1 day was maintained throughout both operational stages.

4.2.4. SAMPLING AND ANALYTICAL PROCEDURES

Process parameters including pH (SensION™ + PH3 pHmeter, HACH, Spain), temperature (multiparameter analyser C-3020, Consort, Belgium) and dissolved oxygen (DO, OXI 3310 oximeter, WTW, Germany) were daily monitored at 11:00 a.m. PAR was measured weekly using a LI-250A light meter (LI-COR Biosciences, Germany).

Liquid samples of 100 mL were collected twice a week from the SWW, PBR, settled biomass and effluent for solids and dissolved nutrient quantification. Following ATU addition, the sampling frequency was changed to one sample per day. TSS, VSS, TOC, IC and TN, N-NH_4^+, N–NO_2^-, N–NO_3^-, P-PO_4^{3-}, N_2O, the content of C, H, N, S and O in the microalgae biomass, the structure of the microalgae consortium were analysed according to description in Section 2.1.3. The microbial community analysis and physiological status of the photosynthetic microorganisms, measured by Q_Y, was realized according to description in Section 2.2.3.

4.3. RESULTS AND DISCUSSION

4.3.1. MICROBIAL COMMUNITY DYNAMICS

The selective inhibition of AOB with ATU triggered a profound ecological restructuring of the photobioreactor consortium, which reshaped both eukaryotic and prokaryotic communities. This shift in microbial structure was characterized by the suppression of nitrifying and heterotrophic bacteria, which consequently favoured photosynthetic organisms adapted to exploit the newly available ammonium.

A succession on phototrophic microorganisms was observed throughout the operational stages. Initially dominated by *Scenedesmus* sp. (77%), the predominant photosynthetic microorganisms shifted to *Pseudanabaena* sp. (89%) at the end of the Stage I (Figure 23). This shift can be attributed to the reduction in HRT to 1 day, which imposed a washout pressure that likely favoured the filamentous morphology of *Pseudanabaena*. The subsequent addition of ATU leaded to NH_4^+ accumulation, favoured *Scenedesmus* sp. and *Nodosilinea* sp. to re-establish as the dominant genera (collectively 96% relative abundance), which became the primary driver of NH_4^+ assimilation. The suppression of *Pseudanabaena* (99% reduction) aligns with ecological principles of nutrient competition and demonstrates its

competitive inferiority against specialized ammonium assimilators under the experimental conditions. The competitive advantage of *Scenedesmus* under these conditions aligns with previous report (Krustok et al., 2016) and could be explained by its metabolic flexibility for both photoautotrophic and mixotrophic growth, while *Nodosilinea* benefited from its exclusive dependence on NH_4^+ due to the lack of nitrate reductase (L. Yi et al., 2024). Together, these patterns illustrate how a single operational perturbation can restructure microbial community composition by altering a key environmental filter (NH_4^+ availability), driving succession towards populations with complementary metabolic strategies for ammonium assimilation.

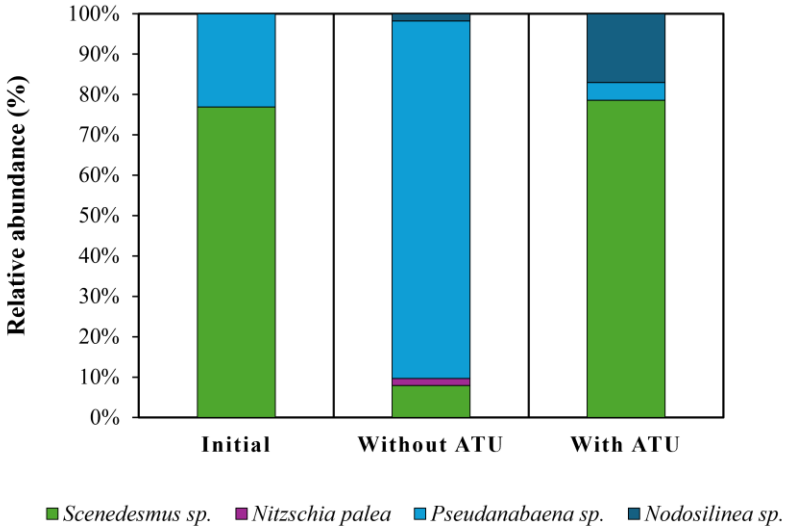

Figure 23: Time course of the relative abundances (%) of the main microalga species.

This taxonomic reorganization was further supported by examining cell density and biovolume changes (Figure 24). The pronounced decrease in total biovolume following ATU addition was primarily driven by the collapse of *Pseudanabaena* sp., which experienced a 97% reduction in biovolume (from 1.1×10^{11} to 4.2×10^{9} $\mu m^3 L^{-1}$) and a 99% reduction in cell density. In contrast, *Scenedesmus* sp. maintained stable population density and biovolume, while *Nodosilinea* sp. showed only modest growth.

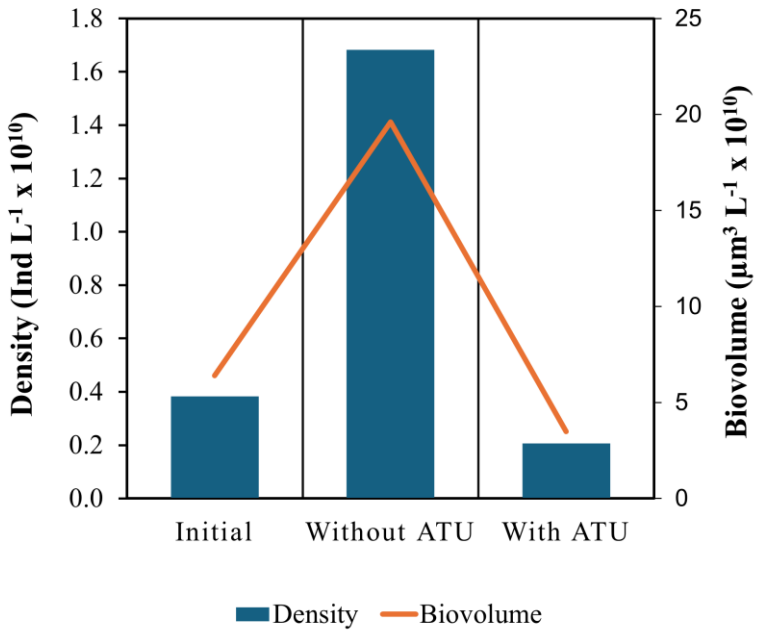

Figure 24: Time course of total microalgae densities (blue bars) and total microalgae biovolume (orange line).

Experimental evidences confirms that ATU selectively inhibits nitrifying bacteria while preserving microalgal functionality. Rossi et al., (2018) demonstrated that microalgal photosynthetic activity was maintained after ATU supplementation in respirometric assays. Similarly, Krustok et al., (2016) reported sustained algal growth and even higher chlorophyll *a* concentration in reactors with ATU. Consistent with these findings, a stable photosynthetic performance was observed throughout this ecological shift as shown by Q_Y values consistently exceeding 0.65 in both operational stages. Indeed, the marginal Q_Y reduction from 0.69 ± 0.01 to 0.66 ± 0.02 following ATU addition suggests a minimal impact on photochemical efficiency, further confirming the well-established tolerance of microalgae to ATU (Rossi et al., 2018; Sánchez-Zurano et al., 2020) (Figure 25).

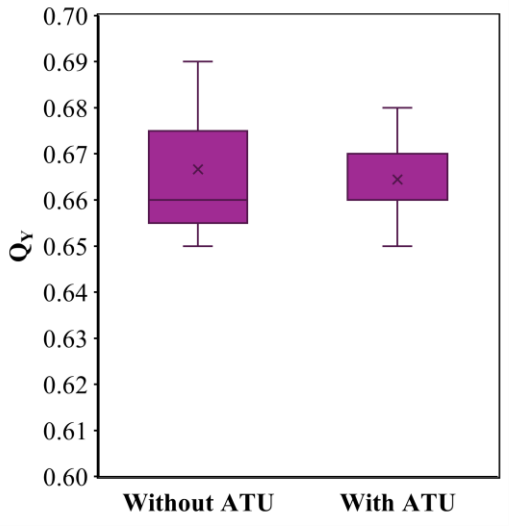

Figure 25: Distribution of photosynthetic quantum yield (Q_Y) in the PBR. The 'x' symbol denotes the median value, boxes represent the interquartile range and whiskers show the data range.

The prokaryotic community revealed a parallel restructuring at the phylum level (Figure 26a). The ATU addition shifted the composition from Cyanobacteria (43%), Proteobacteria (27%) and Bacteroidota (12%) to one dominated by Cyanobacteria (60%), Firmicutes (19%) and a reduced proportion of Proteobacteria (8%). This was characterized by the expansion of *Nodosilinea* (from 1% to 46% of cyanobacteria), likely favoured by the altered nutrient regime, considering its growth is positively influenced by NH_4^+ and its ability of grow in low phosphate concentration (Yadav et al., 2021), outcompeting *Pseudanabaena* (41% to 12% of cyanobacteria, Figure 26b).

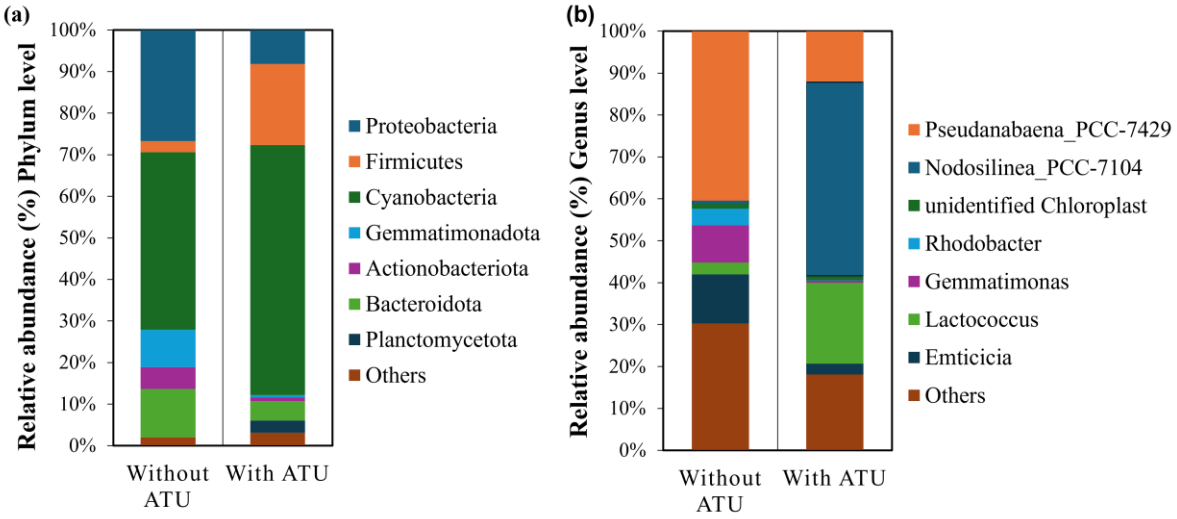

Figure 26: Time course of a) the relative abundance per phyla of bacteria and b) the relative abundance per genus of bacteria.

Interestingly, some members of both Proteobacteria and Bacteroidota have been identified as heterotrophic nitrifying bacteria (Lapébie et al., 2019; Wang et al., 2024a), which have the ability to produce hydroxylamine, nitrite and nitrate by nitrification using organic carbon for their growth. Declines in the abundance of Bacteriodota (12% to 5%), which important in carbon and nitrogen cycling during wastewater treatment (Liu et al., 2023), Gemmatimonadota (9% to 1%) and Actinobacteriota (5% to 1%), further underscore the widespread impact of ATU on heterotrophic bacteria involved in nitrogen and carbon transformation. In contrast, Planctomycetota emerged, reaching a 3% relative abundance.

Phylogenetic restructuring was further elucidated by examining abundance shifts at the family level (Figure. 27). The heatmap highlights the specific taxonomic drivers of phylum-level changes. Most notably, the rise of the cyanobacterial family *Nodosilineaceae* indicates its role as the dominant taxon after nitrification inhibition. Conversely, the decline in the abundance of families within the Proteobacteria phylum, such as *Rhodobacteraceae* and *Rhizobiaceae*, visually confirmed the functional reduction of this group, which includes known nitrifying and metabolically versatile heterotrophs crucial for processes like organic carbon degradation (Morillas-España et al., 2021).

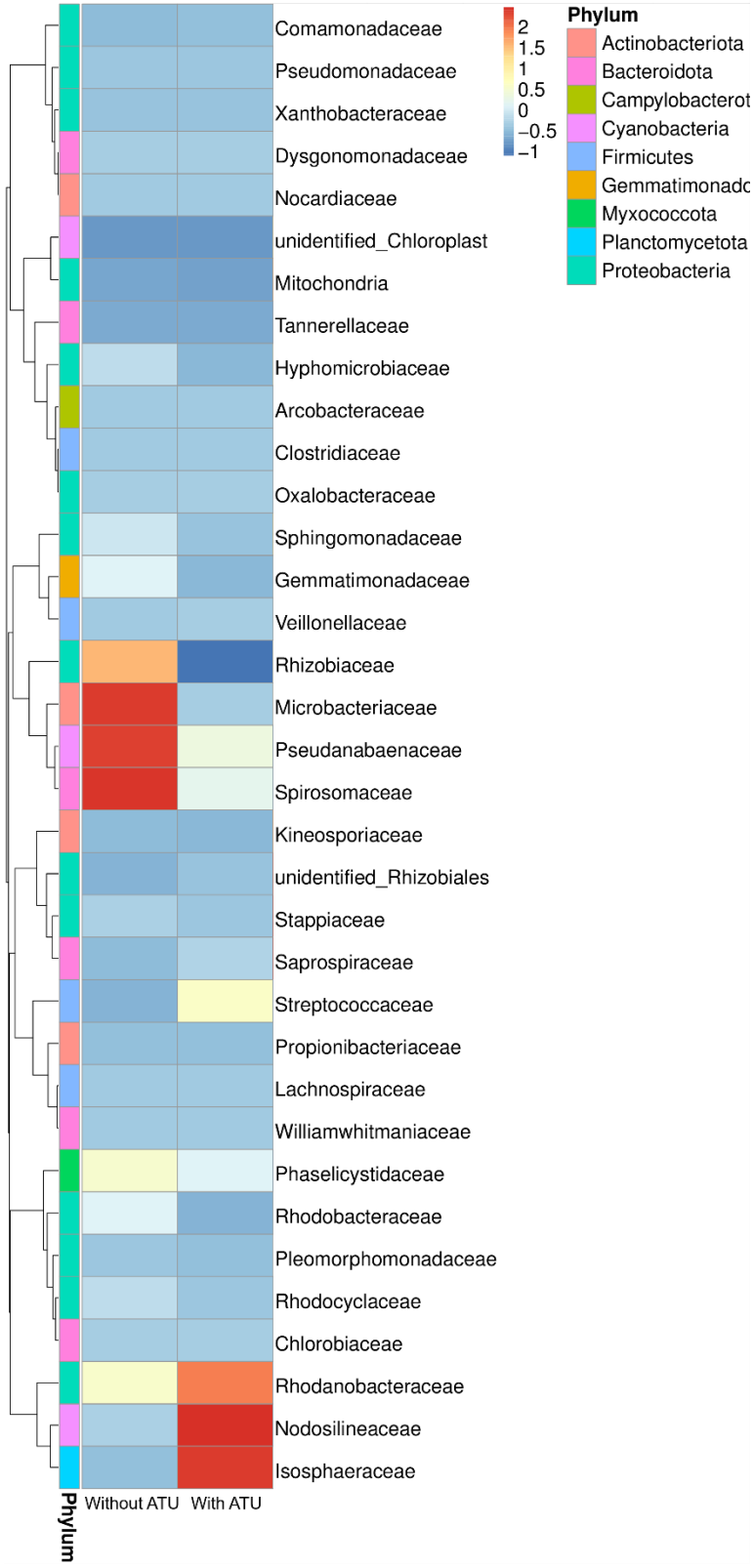

Figure 27: Taxonomic abundance cluster heatmap at family level.

This community turnover was quantified by Amplicon Sequence Variants (ASVs) analysis (Figure 28), which revealed low overlap (38 shared ASVs). The high proportion of

unique ASVs to each condition, 81.4% before *versus* 84.9% after ATU addition indicates a high degree of dissimilarity and a substantial shift in the microbial community structure induced by nitrification inhibition.

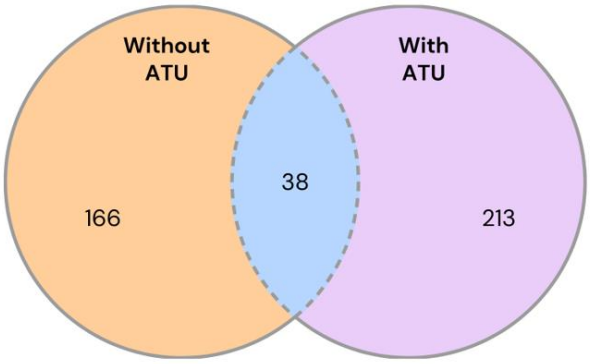

Figure 28: Venn diagram based on feature sequences.

Alpha diversity indices (Table 3) confirmed the distinct compositional contrast, showing that the community exhibited a higher overall diversity before ATU addition, as indicated by greater Shannon and Simpson indices. This suggests a well-balanced distribution of taxa abundance. After ATU addition, reduced diversity indices were recorded likely due to the selective environment, while exhibiting a higher taxonomic richness.

Table 3: Alpha-diversity information of all samples

	Without ATU	**With ATU**
Chao1	208.138	259.591
Dominance	0.194	0.240
Goods coverage	0.999	0.999
Observed features	204	251
Pielou e	0.463	0.419
Shannon	3.552	3.337
Simpson	0.806	0.760

Finally, it must be stressed that the prevailing PBR operational conditions may have already been selected for a light-tolerant community. Thus, high light intensities can inhibit some nitrifying bacteria (Vargas et al., 2016). Therefore, the baseline community prior to ATU addition likely represented a consortium already adapted to photic conditions, with ATU application exerting a strong selective pressure that reshaped community dynamics. The emergence of *Scenedesmus* sp. and *Nodosilinea* sp. highlights the dominance of photosynthetic microorganisms capable nitrogen removal via assimilatory mechanisms.

4.3.2. EFFECT OF ATU ADDITION ON NITROGEN REMOVAL

The selective inhibition of nitrifying bacteria with ATU was used to infer the contributions of microalgal assimilation and bacterial nitrification and potential denitrification to nitrogen removal. This approach revealed a system where assimilation was the predominant pathway, a trait that was reinforced following the inhibition of competing bacterial processes.

The introduction of ATU into the SWW increased TN concentration from 72.5 ± 6.2 to 87.6 ± 3.7 mg L^{-1}, potentially providing an additional nitrogen source. In this context, the TN removal efficiency in the PBR decreased from 96.7 ± 1.4% to 83.7 ± 1.8% following nitrification inhibition (Figure 29).

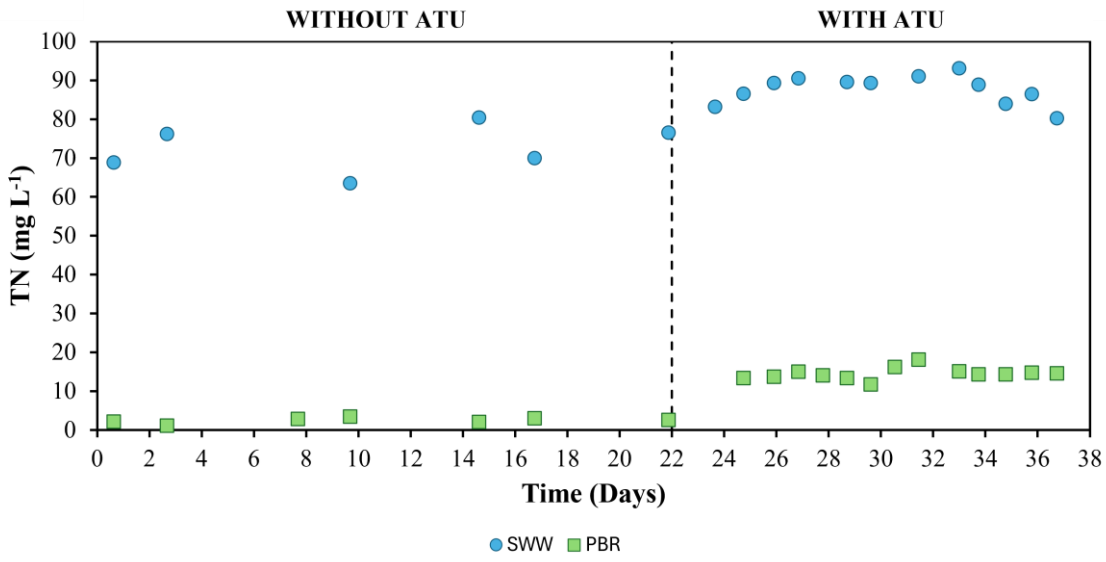

Figure 29: Time course of Total nitrogen (TN).

Despite this reduction in nitrogen removal, the post-inhibition removal efficiency aligns with the performance of algal-bacterial PBRs primarily relying on nitrogen assimilation, reported as 68-79% (Alcántara, Domínguez, et al., 2015) and 80 ± 6% in enclosed tubular and 92 ± 5% to open PBRs (Posadas et al., 2014). The relative contribution of assimilation *versus* nitrification in algal-bacterial systems is highly variable and influenced by operational parameters and community structure (Fallahi et al., 2021). It is important to highlight that while assimilation enables nutrient recovery, its dependence on biomass harvesting and stoichiometric limits constrains the ultimate removal capacity, a role partially played by the nitrification pathway in uninhibited systems. The successful suppression of nitrification was confirmed by the accumulation of NH_4^+ in the PBR, which increased from 0.5 ± 0.1 to 8.9 ± 0.8 mg L^{-1} concomitantly with a reduction in ammonium removal rate from 44.6 to 36.3 mg L^{-1} d^{-1} (Figure 30).

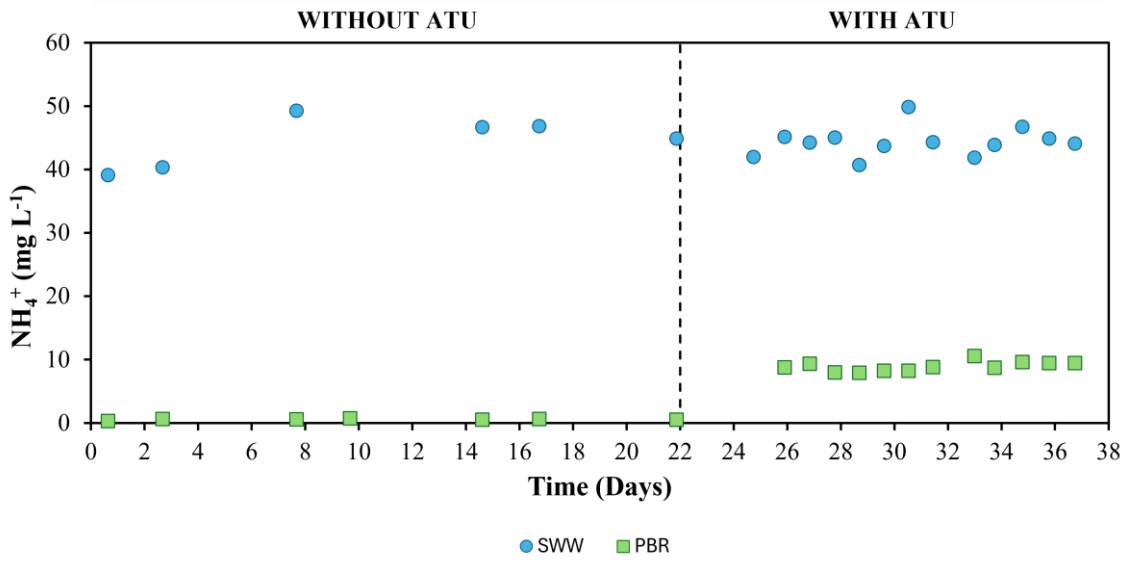

Figure 30: Time course of ammonium (N-NH_4^+).

The transient accumulation of NO_2^-, which emerged the fourth HRT cycle following ATU addition (Figure 31) is an indicator of inhibited NOB activity. Thus, the NO_2^- concentration in the SWW from day 27 until the end of Stage II was 0.65 ±0.37 mg L^{-1}, and averaged 0.48 ± 0.30 mg L^{-1} in the PBR, which is consistent with minimal NOB activity during this stage. While NO_2^- accumulation can theoretically arise from other pathways (e.g., partial denitrification), this alternative is unlikely in our system given the consistently high dissolved oxygen levels (10.1 ±1.0 mg O_2 L^{-1}). Therefore, the observed NO_2^- accumulation

likely resulted from a combination of low SRT (3 days), inhibitory NH_3 levels and the action of ATU (González-Camejo, Montero, et al., 2020).

The calculated free ammonia (NH_3) concentration increased from 0.01 ± 0.01 to 0.22 ± 0.09 mg N L^{-1} as a result of ATU addition. While this concentration remained below the reported inhibitory threshold for microalgae such as *Neochloris oleoabundans* and *Dunaliella tertiolecta* (2.3 and 3.3 mg NH_3 L^{-1}, respectively (Chai et al., 2021)), it approached levels documented to be toxic for NOB, which can be inhibited at concentrations ranging from 0.1 to 3 mg N L^{-1} (González-Camejo et al., 2022). The transient NO_2^- accumulation observed shortly after ATU addition serves as indirect evidence of nitrifying activity prior to ATU addition.

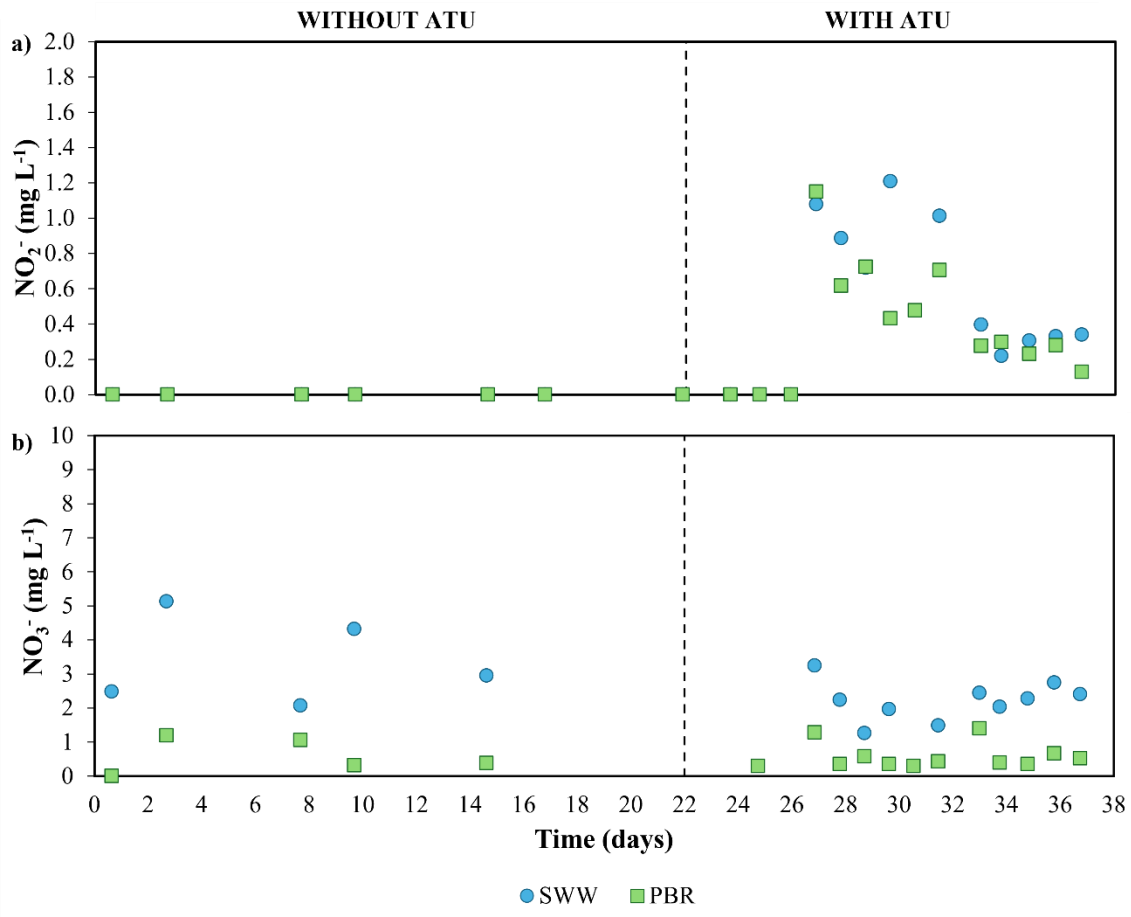

Figure 31: Time course of a) Nitrite (N-NO_2^-); and b) Nitrate (N-NO_3^-).

On the other hand, the nitrogen mass balance (Figure 32) revealed that microalgal assimilation was already the dominant removal mechanism before ATU addition, representing a contribution of 59%. Following inhibition, the newly established consortium (dominated by

Scenedesmus) increased the relative contribution of nitrogen assimilation to 67%. This result underscore the significant role of the nitrifying community in the uninhibited system, while simultaneously confirming microalgal-bacterial assimilation as the primary removal route under these conditions. This preference is mechanistically explained by microalgae preferentially assimilating NH_4^+ over NO_3^- for biomass synthesis (Krustok et al., 2016), a process facilitated by the absence of the energy-intensive nitrate reduction step required when nitrate is the nitrogen source (Chai et al., 2021; Nishi et al., 2022).

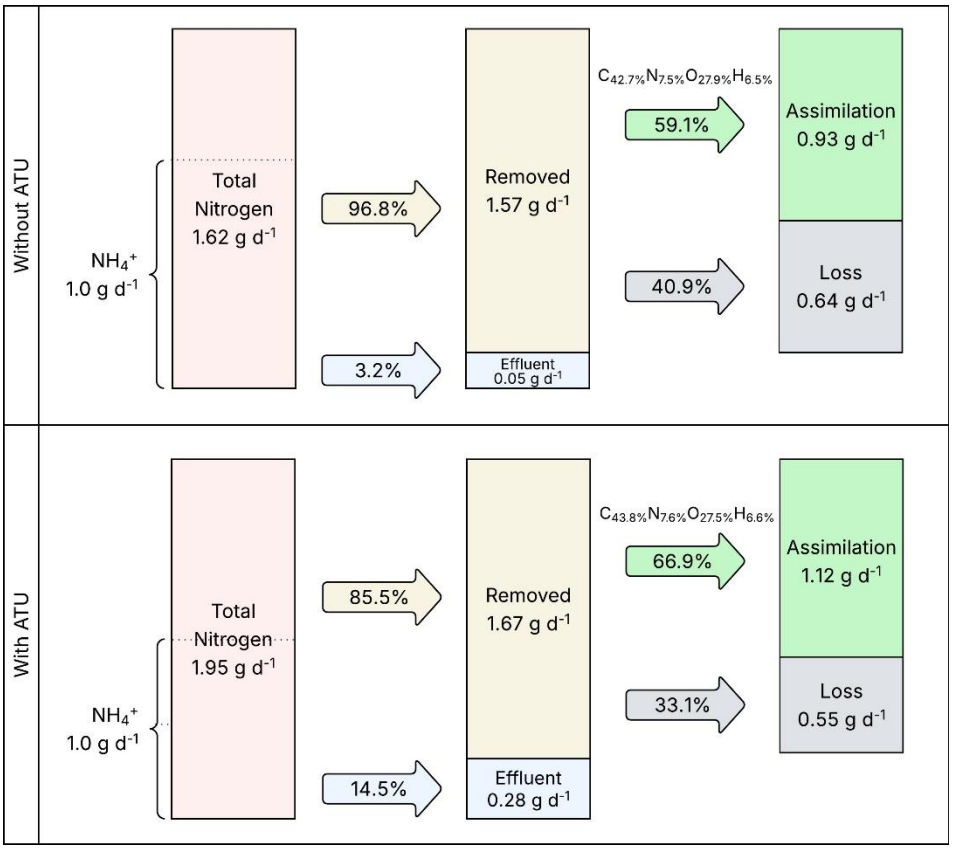

Figure 32: Schematic mass balance of nitrogen during both operational conditions. Assimilation refers to the N content in microalgal biomass.

The functional shift recorded is associated with the observed restructuring of the prokaryotic community. The addition of ATU led to a reduction in the relative abundance of key bacterial phyla, including Proteobacteria and Bacteroidota (Figure 26a), that represent functionally versatile heterotrophic populations responsible of carbon and nitrogen cycling (Lapébie et al., 2019; Wang et al., 2024a). Bacteroidota are considered primary degraders of polysaccharides (Lapébie et al., 2019), while Proteobacteria, primarily made up of gram-negative heterotrophic bacteria (Wang et al., 2024b) capable of utilizing NH_4^+-N and NO_2-N

in their metabolism, can have an important role during denitrification (Yue et al., 2024). Many organisms within these groups are capable of conducting heterotrophic nitrification and removing nitrogen via aerobic denitrification, generally less efficient than conventional anaerobic denitrification (Baskaran et al., 2020).

The pronounced reduction of Proteobacteria and Bacteroidota activity following ATU addition was reflected in the reduced N_{loss} observed in the system, from 0.64 to 0.55 g d^{-1}, as the competing ammonia oxidation pathway was suppressed. However, the remaining N_{loss} of 33% (estimated based on the TN removed) after inhibition suggests the involvement of alternative pathways. This could be attributed to the combined effect of the aforementioned abiotic and heterotrophic processes, and the activity of resilient or emerging microbial groups. Notably this persistence is potentially linked to the increased abundance of the cyanobacterium *Nodosilinea*, which may perform aerobic nitrification and nitrate reduction (Phyu et al., 2025) or facilitate other nitrogen loss processes. Thus, the post-inhibition N_{loss} likely represents a combination of multiple concurrent biological and physical processes, facilitated by a restructured microbial community.

Importantly, the reduction in TN removal following ATU addition cannot be attributed solely to substrate limitation, as nitrate was consistently present in the influent and nitrite accumulated transiently. Instead, it likely resulted from a combination of factors: the direct loss of nitrification as a removal pathway, the indirect suppression of heterotrophic bacterial groups associated with denitrification and organic carbon turnover, and the incomplete compensation by enhanced algal assimilation.

This finding contrasts with studies by Krustok et al., (2016) and Karya et al., (2013), where nitrification was identified as the dominant route for NH_4^+ removal. The discrepancy can be attributed to key operational differences, most notably the significantly higher light intensity (316.6 µmol m^{-2} s^{-1}) and continuous photoperiod (24h) in our work, compared to 100 µmol m^{-2} s^{-1} under a 16:8h light:dark cycle (Krustok et al., 2016) and 63 µmol m^{-2} s^{-1} used by these authors (Karya et al., 2013). These conditions strongly favour photosynthetic activity and assimilatory uptake by microalgae over bacterial nitrification. Furthermore, the different operational HRT, SRT and C:N:P ratios among studies likely selected for a microbial community dominated by organisms with high assimilatory capacity, as evidenced by the dominance of *Scenedesmus* sp. This view is supported by Bankston et al., (2020), who found algal assimilation to be nearly twice as higher as nitrification on treatment of poultry litter slurry anaerobic digestate. These data confirm that the nitrification process can directly

compete with and limit microalgae growth, a phenomenon previously suggested in lab-scale and pilot-scale studies (González-Camejo et al., 2019). The demonstrated dominance of nitrogen assimilation shows that microbial community function, and consequently nutrient removal pathways, can be strategically controlled by tailoring the operational environment to enhance nitrogen recovery efficiency.

In this study, N_2O emissions remained negligible (77.0 ± 19.7 ppm_v in the PBR headspace; equivalent to 1.1 mg N L^{-1}), representing less than 0.1% of total nitrogen losses. This low production correlates with the operational conditions featuring high DO levels, negligible NO_2^- accumulation and the suppression of the nitrification pathway (during Stage II). These findings align with Kim et al., (2010), who demonstrated that N_2O emission during nitrification largely depend on AOB activity. The complete mechanisms of N_2O formation remain debated, however, it is established that production occurs through both autotrophic nitrification (via AOB activity) and incomplete heterotrophic denitrification, with enhanced emissions under conditions of low DO, elevated NO_2^- concentrations, and low C/N ratios (Ni et al., 2011).

4.3.3. EFFECT OF ATU ADDITION ON CARBON AND PHOSPHORUS REMOVAL

The addition of ATU induced a shift in carbon cycling in the algal-bacterial PBR dynamics. The decrease in TOC removal efficiency from 94 ± 1 to 88 ± 1% (Figure 33) suggests a partial suppression of heterotrophic activity responsible for organic carbon mineralization. Furthermore, the observed decrease in TOC removal efficiency suggests a secondary effect of suppression of heterotrophic activity, while the maintained overall biomass productivity and quantum yield (Q_Y) confirm that the core photosynthetic function was preserved, as supported by previous literature (Krustok et al., 2016). This may be a secondary consequence of nitrification inhibition. While primary action of ATU is inhibiting the ammonia monooxygenase (AMO), a potential broader effect can also chelate the copper cofactor in multiple microbial enzymes, potentially inhibiting the metabolic activity of heterotrophs (M. Yi et al., 2020). The observed reduction in the relative abundance of key heterotrophic phyla, specifically Firmicutes and Bacteroidota, which typically remove TN by consuming TOC under anoxic conditions (Yue et al., 2024), likely impaired organic carbon mineralization, leaving a fraction of TOC bioavailable in the PBR.

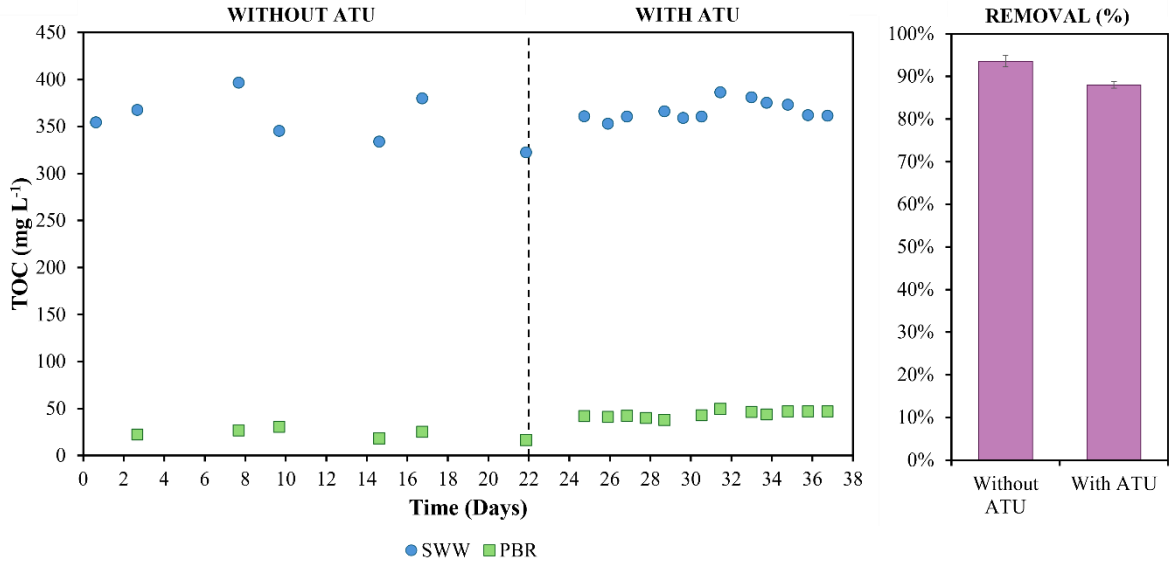

Figure 33: Time course of TOC concentrations in the PBR. The corresponding removal efficiency (%) is shown as magenta columns.

This primary disruption of nitrogen transformations and heterotrophic metabolism cascaded into a reconfiguration of carbon processing. The carbon mass balance (Figure 34) revealed an important metabolic shift. The efficiency of carbon assimilation into biomass increased from 65% to 80% following ATU addition. This suggests that the inhibition of heterotrophic bacteria may have reduced competition for organic carbon, thereby increasing its availability for other metabolisms, such as the mixotrophic microalga *Scenedesmus*. The sustained TOC removal during the period of *Scenedesmus* dominance is consistent with its effectively assimilating both the increased NH_4^+ and available organic carbon. This correlation suggests a possible role for *Scenedesmus* in organic carbon uptake under these conditions. Given the potential of heterotrophic bacteria from the Rhodobacteraceae family consuming organic carbon, the observed decline in the group, along with Proteobacteria, and the rise of Firmicutes, provides a taxonomic explanation for the observed restructuration of carbon metabolism pathways in the consortium. Furthermore, the alteration of nitrogen availability following ATU inhibition induced a shift in the microbial community structure, favouring the dominance of versatile microalgae like *Scenedesmus* sp., while the bloom of cyanobacteria highlights the functional redundancy for nutrient assimilation within the consortium.

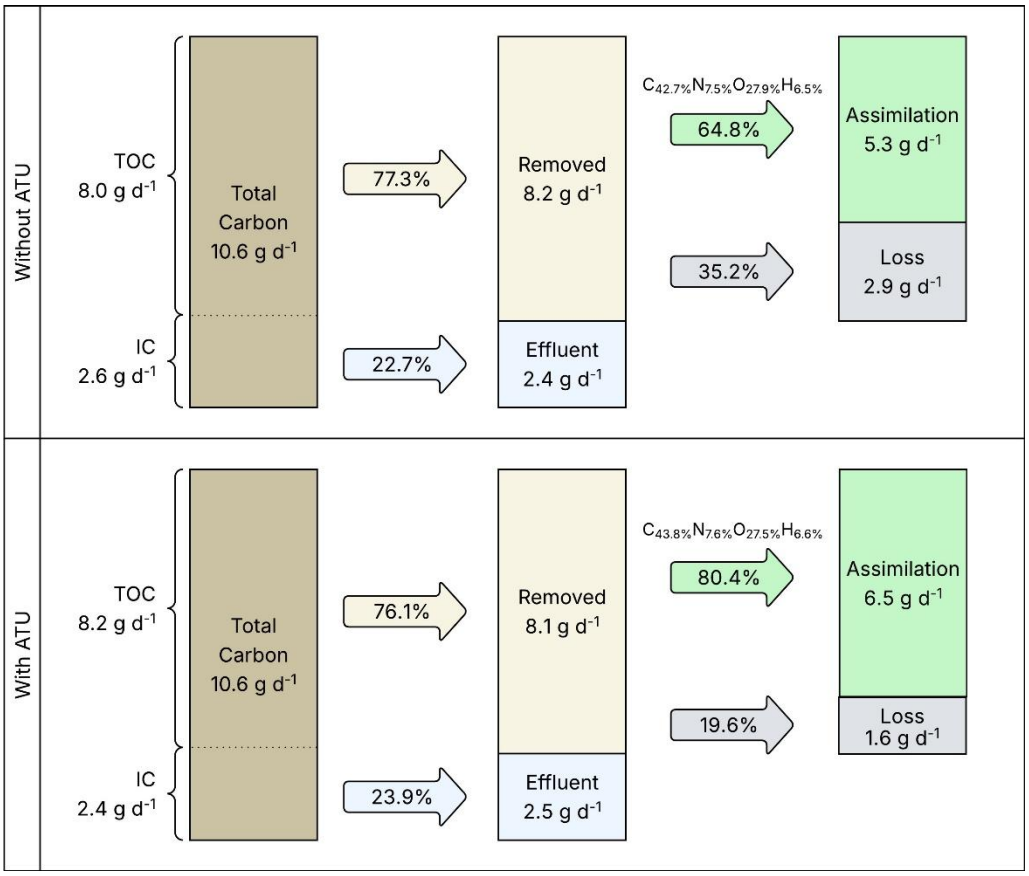

Figure 34: Schematic mass balance of carbon during both operational conditions. Assimilation refers to the C content in microalgal biomass.

The carbon mass balance further supports this mechanism. While the total carbon concentration in the effluent remained virtually constant (113.3 ± 10.1 mg L^{-1}; p >0.05), the C_{Loss} decreased from 35% to 20%, indicating a suppression of heterotrophic activity and the redirection of carbon to algal assimilation. The increase in the organic carbon required per unit of ammonium removed, from 7.6 to 9.0 mg_{TOC} $mg_{N\text{-}NH4+}{}^{-1}$, reflects this transition from a community predominantly dominated by heterotrophic bacteria to one dominated by mixotrophic algae with a different carbon-to-nitrogen utilization ratio. Furthermore, the consistent IC removal efficiency, averaged 23 ± 7% along both operational stages (Figure 35), reinforces that photosynthetic assimilation by microalgae was the primary mechanism for IC removal.

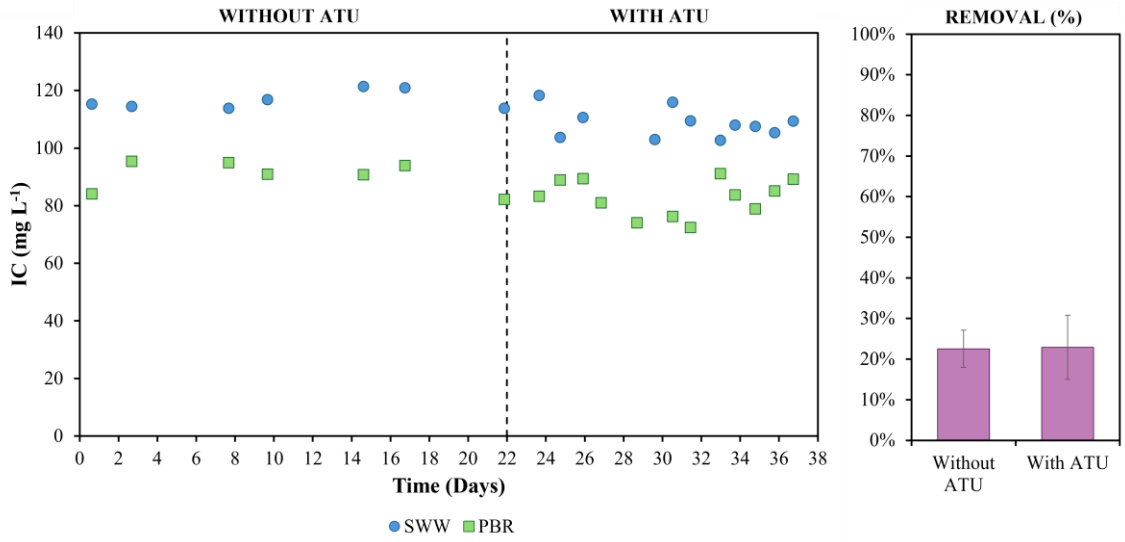

Figure 35: Time course of IC concentrations in the PBR. The corresponding removal efficiency (%) is shown as magenta columns.

On the other hand, the PBR supported consistently high P-PO_4^{3-} removal efficiencies of 98 ± 4% without ATU and of 97 ± 7% with ATU (Figure 36), with no statistically significant difference between stages (p >0.05).This indicates that nitrification activity exerted a negligible impact on phosphate removal, consistent with the findings of Krustok et al., (2016) at low P concentrations. Despite microalgae are able to assimilate N under P-limited conditions (Krustok et al., 2016), nitrifying bacteria growth can be significantly affected (González-Camejo et al., 2022). Notably, the N:P ratios (5:1 without ATU and 6:1 with ATU) are in agreement with the optimal 5:1-8:1 range needed to sustain high removal efficiencies by *Scenedesmus* sp. (Xin et al., 2010), suggesting that the nutrient balance was theoretically favourable for a concurrent N and P removal. Furthermore, given that the pH remained below 8 (Figure 37), a range where no significant phosphate precipitation occurs, it can be inferred that the high phosphorus removal efficiency was primarily driven by assimilation into biomass.

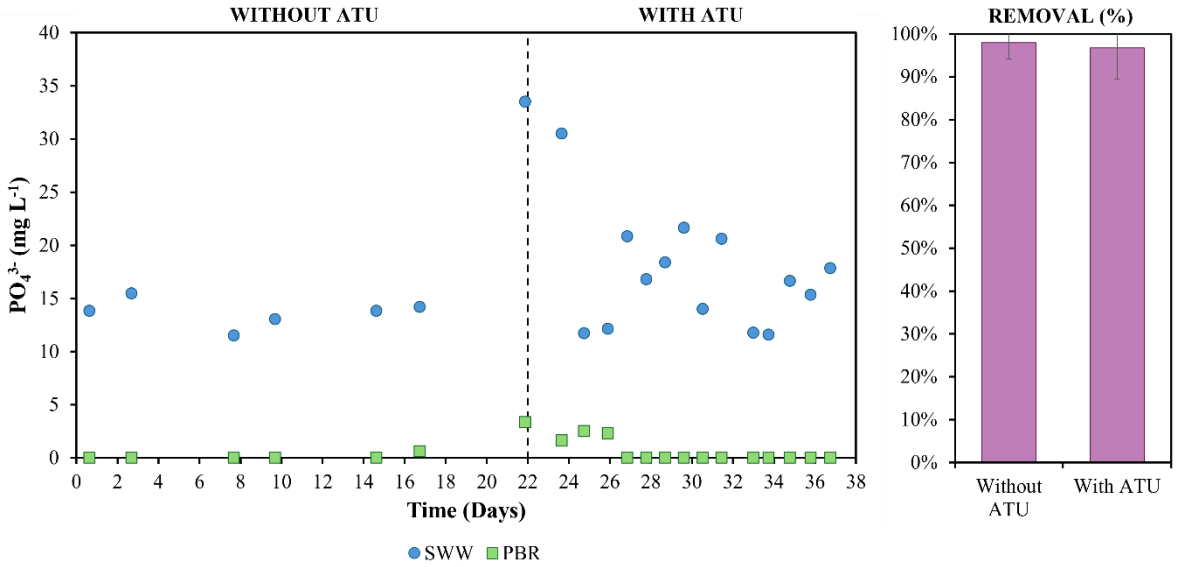

Figure 36: Time course of P-PO_4^{3-} concentrations in the PBR. The corresponding removal efficiency (%) is shown as magenta columns.

4.3.4. EFFECT OF ATU ADDITION ON PHOTOBIOREACTOR PERFORMANCE AND BIOMASS PRODUCTIVITY

The PBR maintained stable bioremediation performance throughout the experimental period, demonstrating system resilience to the imposed metabolic inhibition (Figure 37). The pH remained constant at 7.4 ± 0.2 without external control and was unaffected by ATU-based nitrification inhibition.

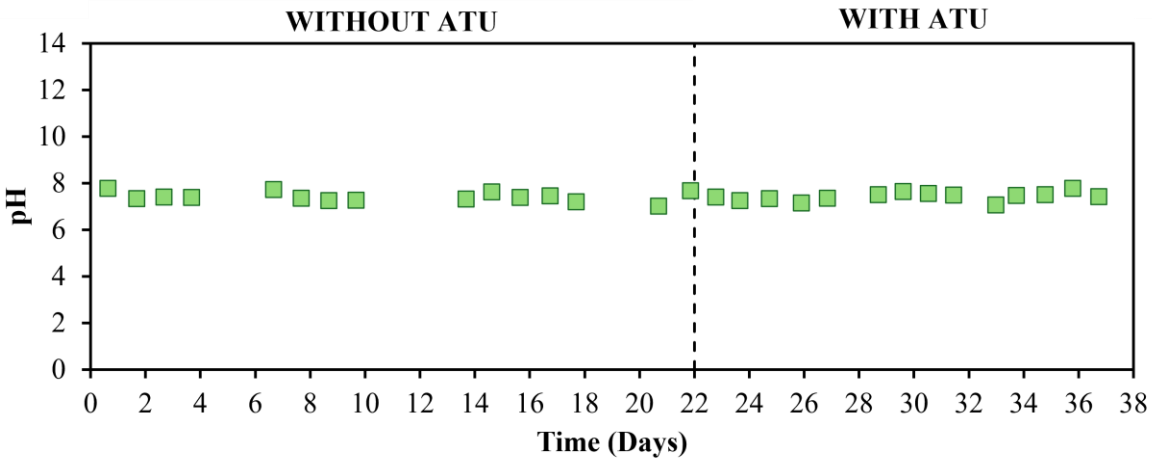

Figure 37: Time course of pH in the algal-bacterial broth during PBR operation.

Similarly, the DO concentration remained stable at 10.4 ± 2.1 mg L^{-1} across both operational stages (Figure 38). The high stability of DO following ATU addition can be attributed to the high turbulence in the algal cultivation broth mediated by the two submerged pumps, which allow stripping out the excess of DO not consumed by nitrifiers in Stage II.

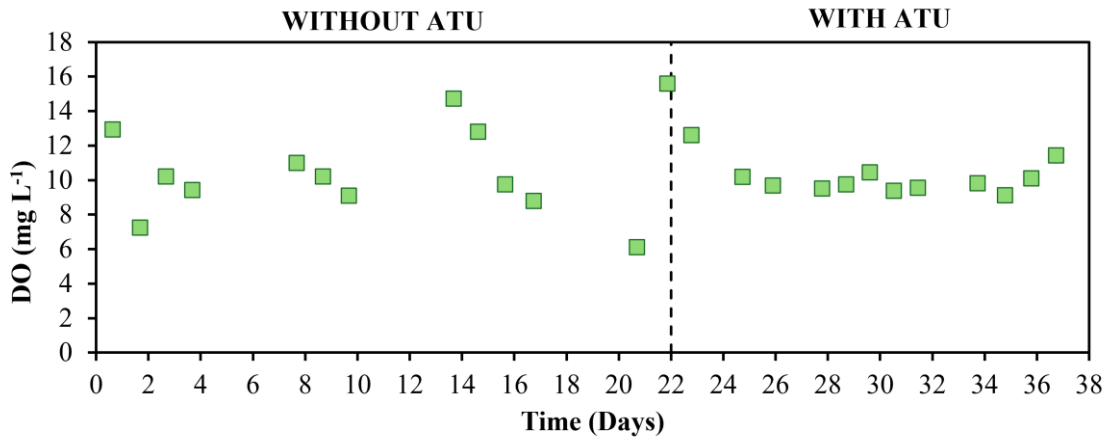

Figure 38: Time course of dissolved oxygen (DO) in the algal-bacterial broth during PBR operation.

Temperature averaged 30.3 ± 1.7°C (Figure 39), which could potentially favour AOB growth over microalgae (González-Camejo, Montero, et al., 2020). However, as both experimental stages experienced the same averaged temperature, the comparative assessment of nitrification inhibition remains valid. The constant light irradiance may have provided partial compensation by inhibiting nitrifying bacteria (González-Camejo, Montero, et al., 2020), though this effect was consistent across both stages.

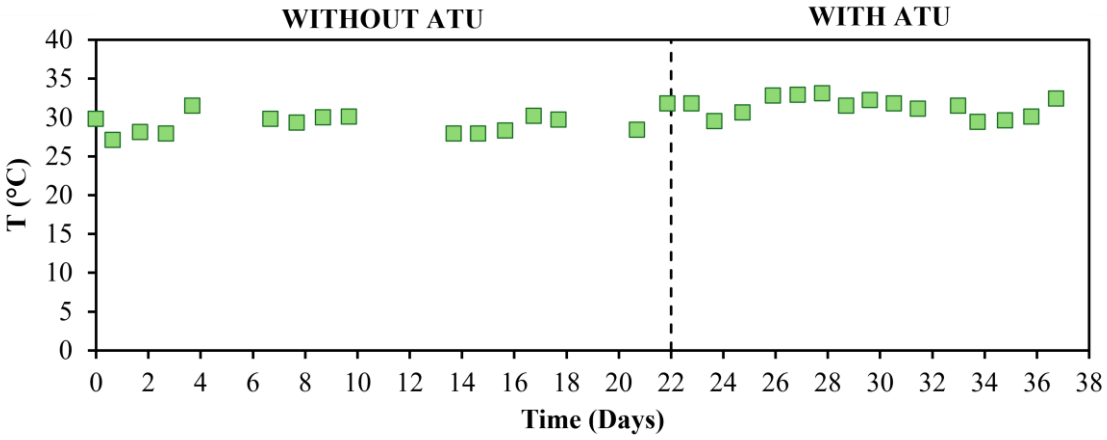

Figure 39: Time course of temperature in the algal-bacterial broth during PBR operation.

The operational strategy of maintaining the biomass concentration below 2 gTSS L^{-1} in the PBR was successful, as reflected in the stable VSS profiles, where median values remained similar between operational stages (Figure 40a). This strategy is known to favour bacterial communities that exhibit faster growth rates compared to microalgae (González-Camejo, Aparicio, et al., 2020). Despite the significant ecological shift, the selective inhibition of nitrifiers by ATU did not lead to a statistically significant effect on the overall biomass productivity (p >0.05), which increased from 563 ± 118 to 672 ± 163 g m^{-3} d^{-1} (Figure 40b). This stability in productivity was accompanied by a consistent elemental composition of the biomass, with nitrogen and carbon contents remaining at 7.5 ± 0.1% and 42.7 ± 0.7% in Stage II compared to 7.6 ± 0.1% and 43.8 ± 0.5% in Stage I, respectively.

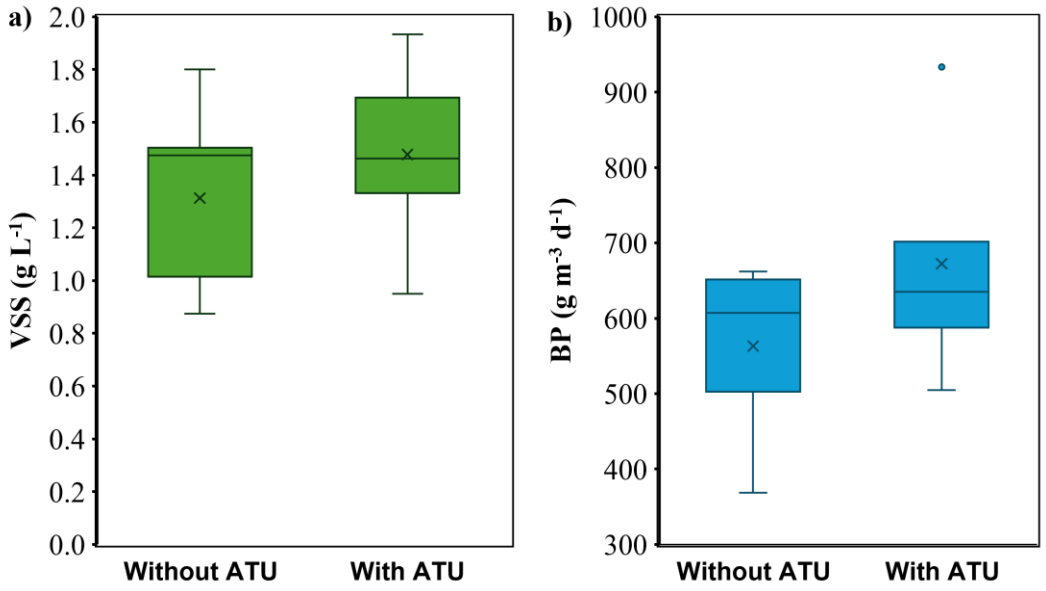

Figure 40: Distribution of a) volatile suspended solids and b) biomass productivity in the PBR with and without ATU treatment. The 'x' symbol denotes the median value, boxes represent the interquartile range, whiskers show the data range, and dots are individual measurements.

The alteration of metabolic dynamics by ATU points towards an inhibition beyond nitrifiers. This is evidenced by a decrease in the specific ammonium removal rate from 79.1 to 52.9 mg NH_4^+ g^{-1} $_{biomass}$, indicating that a less efficient metabolism occurred simultaneously with an overall decreased in total TOC removal. This finding suggests that the resulting community is not only less efficient in its nitrogen metabolism but also less effective at consuming the available organic carbon substrate, reinforcing the hypothesis of an inhibitory effect of ATU on heterotrophic biomass.

4.4. CONCLUSION

This study demonstrates that nitrogen removal in a single-stage algal-bacteria PBR was governed by concurrent action of assimilation and nitrification. The reduction in total nitrogen removal upon nitrification inhibition suggests that this pathway likely weakened a subsequent denitrification process. The strategic nitrification inhibition with ATU was pivotal in decoupling these processes, confirming microalgal assimilation as the dominant mechanism under the tested condition and revealing the critical role of bacterial community structure. The maintenance of nitrogen removal performance after ATU addition indicated that other microorganisms beyond strict nitrifiers contributed to nitrogen removal, suggesting a degree of functional redundancy within the consortium, where heterotrophic bacteria and other autotrophs likely played a complementary role. Furthermore, the increase in NH_4^+ availability following inhibition induced a shift in the microbial community structure, favouring versatile microalgae like *Scenedesmus* sp., while the bloom of cyanobacteria highlights the functional redundancy for nutrient assimilation within the consortium.

A key advantage of the dominant nitrogen assimilatory mechanisms is the efficient direction of nitrogen into biomass, yielding a product with high nutrient content better suited for valorisation purposes. Furthermore, this process entailed consistently low N_2O emissions regardless of the operational stage, underscoring its secondary environmental benefit. Ultimately, the findings confirm that the balance between nitrogen assimilation and oxidation is adjustable, highlighting the flexibility of microalgae-bacteria consortia for advancing circular wastewater treatment models focused on nutrient recovery. While ATU supplementation was used as a proof-of-concept tool, practical application would rely on sustainable operational controls to reduce nitrification and favour the process towards nutrient recovery. To further refine this strategy and completely uncover the mechanisms, future research should employ advanced tools such as isotopic tracers to partition nutrient fluxes. Complementary techniques, including photosynthetic pigment analysis or 18S rRNA gene quantification should be used to precisely elucidate the contributions of algal and bacterial groups, and to quantify algal-specific growth rates, thereby enabling modelling and optimization.

5.

Exploring the Impact of Support Media in Column Photobioreactors for Wastewater Treatment[3]

[3] This Chapter has been published in a modified version as:
dos Santos, T.L. *et al.* (2024). Wastewater Treatment in Tubular Photobioreactors: Exploring the Impact of Support Medium. In: Mannina, G., Cosenza, A., Mineo, A. (eds) Resource Recovery from Wastewater Treatment. ICWRR 2024. Lecture Notes in Civil Engineering, vol 524. Springer, Cham. https://doi.org/10.1007/978-3-031-63353-9_44.

ABSTRACT

This study evaluated the use of support media (mini-Biobob) in column photobioreactors inoculated with a native microalgae-bacteria consortium for domestic wastewater treatment. The reactors were tested in biological duplicates under three conditions: without support media (0 BB, control), with ⅓ BB (67.36 ± 0.01 m^2 surface area), and with ½ BB (100.95 ± 0.11 m^2 surface area). Operating semi-continuously with daily feeding of real domestic wastewater at a hydraulic detention time (HRT) of 5 days, the system aimed to assess whether increasing surface area could enhance biomass production and nutrient removal.

While the addition of support media successfully promoted attached biomass growth, this did not improve significantly wastewater treatment performance. Both the ⅓ BB and ½ BB configurations achieved similar removal efficiencies for total nitrogen, total phosphorus and chemical oxygen demand compares to the control. Interestingly, higher surface area appeared to interfere with light penetration, potentially offsetting any benefits of increased biomass attachment.

These findings reveal a key trade-off: although the mini-Biobob increases the available surface for microbial colonisation, its influence on reactor hydrodynamics and light distribution may limit its effectiveness in vertically illuminated PBRs. Nonetheless, the accumulated attached biomass holds potential for reducing HRT or improving biomass separation in future applications. The study concludes that the optimisation of support media concentration must be carefully balanced with operational parameters such as HRT and light availability, underscoring the complexity of attached biomass phenomena and pointing toward practical strategies for enhancing PBR performance.

5.1. INTRODUCTION

The development of wastewater treatment technologies not only provides effective means to addressing effluent pollution but also holds substantial potential to promote environmental and social well-being, significantly contributing to the achievement of the United Nations Sustainable Development Goals (SDGs) (Ossai et al., 2026; WHO & UN-Habitat, 2024). Among the available biological processes, microalgae-based wastewater treatment presents competitive advantages in relation to other biological processes due to the potential for sustainability through the bioremediation of nutrients, the mitigation of greenhouse gases, the closure of nitrogen and phosphorus cycles, carbon sequestration, and the production of value-added biomass (Acién et al., 2016; González et al., 2008; Nishi et al., 2022; Torres-Franco et al., 2021).

In recent years, several studies have suggested that the utilization of reactors incorporating a supporting media for biofilm formation surpasses suspended growth systems in both biomass productivity and effluent treatment efficiency (Mohsenpour et al., 2021; Xu et al., 2024). This superiority is attributed to the relationship between biomass productivity and increased surface area provided by the support material, as well as factors such as reactor design, porosity, and surface roughness, which collectively enhance microbial colonisation and retention (Xiong et al., 2025; Xu et al., 2024; Zhang et al., 2020). Moreover, immobilised microalgae cultures offer practical advantages over suspended growth cultures, as it facilitates the easier separation of biomass and can potentially enhance effluent treatment and the generation of enriched bioproducts (Mohsenpour et al., 2021; Ren et al., 2024; Xu et al., 2024; Zhang et al., 2020). Immobilized microalgae have found applications in various biotechnological processes, and domestic wastewater treatment processes appear to be one of the most promising applications for immobilized microalgae, particularly concerning the removal of heavy metals and nutrients (Mallick, 2002; Mohsenpour et al., 2021; Ren et al., 2024).

Despite these potential benefits, the use of support media for attached biomass in microalgae-bacteria consortia remains underexplored, especially in the context of column photobioreactors (PBRs) treating real domestic wastewater. While several studies have investigated biofilm formation in open systems or flat-panel PBRs, limited information is available on how varying the concentration of a support media affects attached biomass dynamics, nutrient removal, and overall reactor performance in column configurations.

5.2. MATERIALS AND METHODS

5.2.1. MICROALGAL AND BACTERIA CONSORTIUM AND INOCULATION

The microalgal-bacterial consortium used in this study was obtained through the enrichment of the native community of a secondary effluent collected from an UASB at a local municipal wastewater treatment plant (MWTP) in Bauru, São Paulo, Brazil. A 1.5 L sample of the effluent was placed in a 2.0 L Schott® Glass Bottle and incubated in a controlled environment at 24°C with a light intensity of 260 μmol m^{-2} s^{-1} on a 12/12 h light/dark cycle using LED lamps. Once the culture visibly turned green, an aliquot of the native microalgae-bacteria consortium in the early stationary phase was inoculated into the raw effluent at a 10% (v/v) concentration.

5.2.2. EXPERIMENTAL SET-UP

The study was carried out in six column PBRs described in Section 2.3.2, operated under a light intensity of 260 μmol m^{-2} s^{-1} on a 12/12 h light/dark cycle. Room temperature was maintained at 20°C using an air conditioner, but no temperature control was applied directly to the PBRs. The support media employed (mini-Biobob, described in Section 2.3.3) had previously shown promising results for immobilising bacterial biomass in biological processes for treating industrial and municipal wastewater (Roveroto et al., 2021). However, its use in mixed microalgal-bacterial consortia had not yet been explored. To investigate the potential of this support media for enhancing biomass attachment and treatment performance, the present study tested different quantities of mini-Biobob inside the reactors to evaluate the impact of varying the surface area on the performance of PBR in term of both the quality of treated effluent and biomass production.

The reactors were operated in biological duplicates under three conditions: without any support media (0 BB), with a surface area of 67.36 ± 0.01 m^2 (⅓ BB), and with a surface area of 100.95 ± 0.11 m^2 (½ BB) (Figure 41). The experiment was conducted at laboratory scale under controlled light and temperature conditions to minimize external influences.

Figure 41: Schematic diagram of the experimental set-up. Drawing from Biorender and Gemini.

All reactors were inoculated with 1.5 L of the same native consortium of microalgae and bacteria (initial dry weight of 0.41 gDW L^{-1}) and 4.0 L of real domestic wastewater collected from the inlet of the municipal wastewater treatment plant (MWTP), reaching a final working volume of 5.5 L. The characteristics of the wastewater used throughout the experiment are summarised in Table 4.

Table 4: Characterization of domestic wastewater used.

Parameter	Mean value	Methodology
pH	7.09 ± 0.17	4500-HB (measurement by portable probe)
COD (mg L^{-1} O_2)	214.59 ± 43.93	5220-D (APHA, 2012)
TN (mg L^{-1})	35.69 ± 10.49	Tube test total Kjeldahl TKN 16 (Nanocolor)
TP (mg L^{-1})	5.63 ± 2.17	4500-P (APHA, 2012)
Alkalinity (mg $CaCO_3$ L^{-1})	150.33 ± 17.86	2320-B (APHA, 2012)
Dry weight (mg L^{-1})	641.25 ± 95.21	8111-G (APHA, 2012)

Following inoculation, the reactor did not receive or discharge wastewater for the subsequent 5 days allowing the growth and attachment of the consortium. On the sixth day, semi-continuous operation was initiated with daily feeding of real domestic wastewater, maintaining an HRT of 5 days. The reactors were operated for a total of 68 days.

On a daily basis, a sample of each reactor was collected for physical-chemical and biological analyses. The collected samples were promptly analysed for pH, DO, alkalinity, and optical density (OD) measurements at wavelengths of 254 nm, 540 nm, 680 nm, and 750 nm. Twice a week, samples were filtered for the purpose of measuring dissolved nutrients: TN, NO_3^--N, TKN, TP and COD.

5.2.3. ANALYTICAL PROCEDURE

Optical density was measured using a spectrophotometer (DR6000 UV-VIS, HACH) at wavelengths of 254 nm, 540 nm, 680 nm, and 750 nm. Prior to analysis, samples were filtered by a glass fiber membrane (GF5, Ø 0.4µm, Macherey-Nagel, Duren, Germany). TN, NO_3^--N, TKN, TP, COD and dry weight (DW) were determined as described in Section 2.3.4.

5.3. RESULTS AND DISCUSSION

The decision to use domestic wastewater from a MWTP was made to obtain more accurate and applicable results, specifically to enable a direct comparison with the original Biobob® performance in bacterial systems. Although domestic wastewater introduces variability due to its fluctuating composition (Figures 43 and 44), this approach ensures that the findings reflect actual operational conditions, leading to more reliable and practical insights.

At day 0, all reactors shared identical initial conditions, with TSS of 505.0 ± 120.2 mg L^{-1}, TP at 4.4 ± 0.2 mg L^{-1}, TN at 38.8 ± 1.2 mg L^{-1} and COD at 153.4 ± 8.1 mg L^{-1}. The reactors were operated for 64 days in total.

An increase in attached biomass was observed throughout the experiment (Table 5, Figure 42a). However, no clear correlation was found between the DW of the attached biomass or TSS of the suspended biomass and the surface area. Average TSS values for the 0 BB, ⅓ BB, and ½ BB conditions were 852.4 ± 204.9 mg L^{-1}, 794.4 ± 140.7 mg L^{-1}, and 755.4 ± 164.1 mg L^{-1}, respectively, with no statistical difference ($p \geq 0.05$). This result

suggests that the available surface area may not be a critical factor influencing suspended biomass concentration under the tested conditions.

Table 5: Values of biomass concentration attached to support media ($DW_{attached}$).

$DW_{attached}$ (g L^{-1})	0 BB	⅓ BB	½ BB
Initial	N/A	0	0
Final	N/A	181.94 ± 1.02	184.33 ± 0.06

N/A - Not Applicable

At the end of the experiment, the mini-Biobob support media from all conditions were dried to assess the final biomass (Figure 42b). Considering the relationship between attached biomass per unit surface area, the values were 16.50 $g_{biomass}$ m^{-2} for the ⅓ BB and 11.67 $g_{biomass}$ m^{-2} for the ½ BB. This indicates that attachment was not proportional to the surface area, suggesting a limitation in biomass adhesion capacity to the mini-Biobob under the tested conditions.

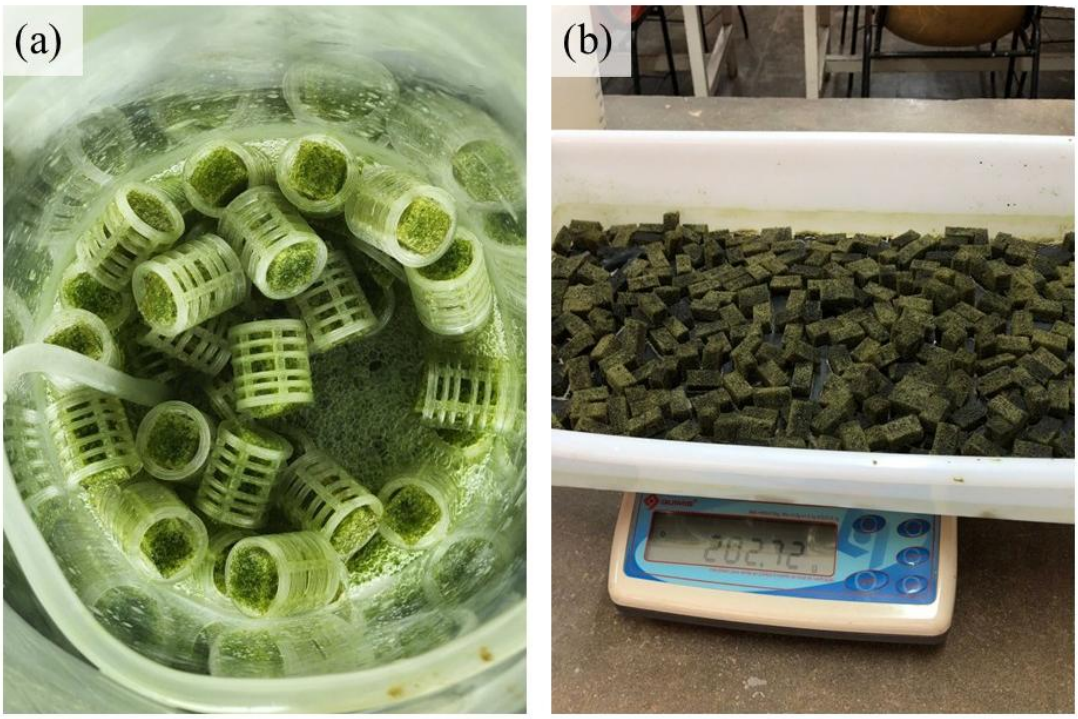

Figure 42: Details of (a) the biomass attached to the support media and (b) dried process of final biomass.

Regarding the quality of treated effluent, no impact of varying the surface area on PBR performance was observed. For nutrient removal, no statistically significant differences occurred between TN concentration and TN removal across the three conditions ($p \geq 0.05$). Notably, TN removal efficiency was marginally higher in 0 BB configuration compared to the reactors with support media, despite comparable overall performance (Figure 43).

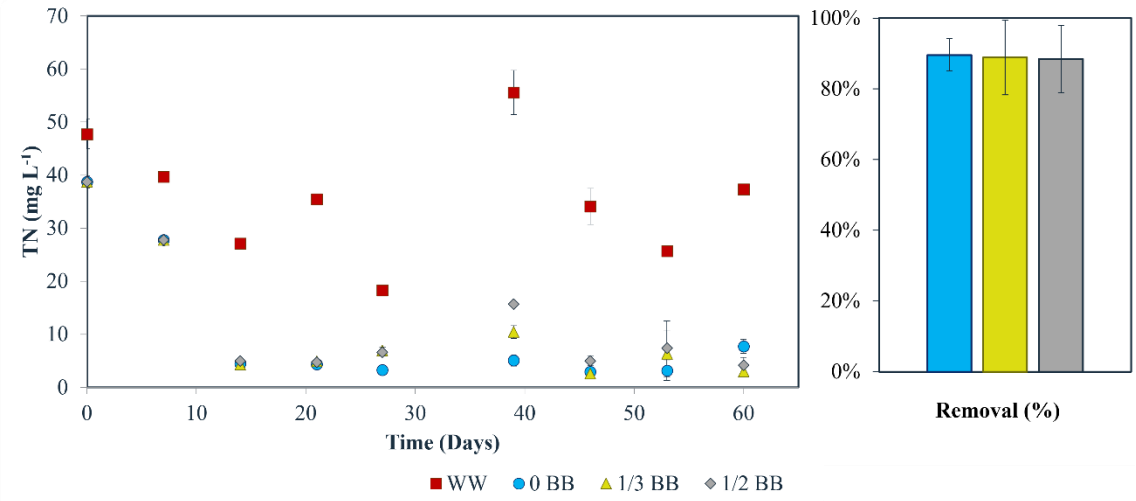

Figure 43: Time course of TN concentration in WW and in the PBRs. The corresponding removal efficiency (%) for each parameter is shown as columns.

The same pattern was observed for TP concentration and removal (Figure 44). Despite the increase in both attached and suspended biomass, the increased surface area did not enhance TP or TN removal rates compared to Control (0 BB).

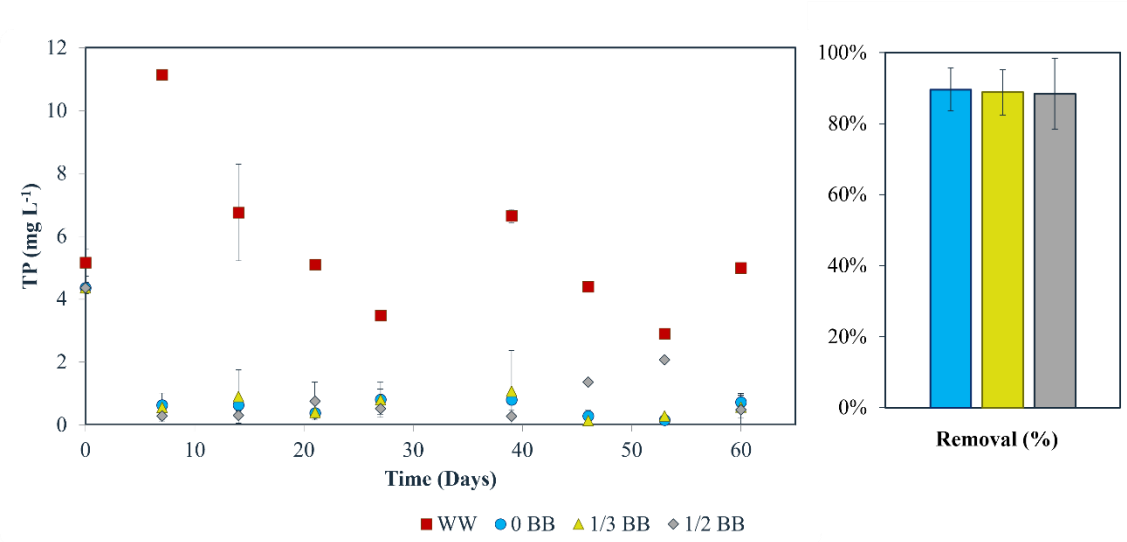

Figure 44: Time course of TP concentration in WW and in the PBRs. The corresponding removal efficiency (%) for each parameter is shown as columns.

The filtered COD concentrations remained stable throughout the experimental period, with mean values of 211.91 ± 36.94 mg L^{-1} in the real wastewater, 138.96 ± 20.12 mg L^{-1} in 0 BB, 138.75 ± 36.04 mg L^{-1} in ⅓ BB, and 140.26 ± 32.85 mg L^{-1} in ½ BB.

These results demonstrate that the incorporation of the mini-Biobob support media into the column PBR did not improve wastewater treatment under the tested conditions. Despite measurable growth in attached biomass, the absence of statistical differences in nutrient removal across configurations indicates that the expected benefits of increased surface area, such as higher nutrient removal rates or greater treatment stability, were not achieved.

This similar performance across all three conditions suggests that factors other than surface area, such as HRT, light distribution, and/or nutrient availability, may exert a stronger influence on treatment performance when using mini-Biobob support media. Furthermore, the non-proportional relationship between available surface area and attached biomass density points to a limited adhesion capacity, potentially due to hydrodynamic constraints, shear forces, or surface saturation.

Moreover, the increase in attached biomass without concurrent improvement in nutrient removal may be explained by mass transfer and light limitations within the attached biomass (Mohsenpour et al., 2021; Xu et al., 2024). As attached biomass accumulated, deeper layers may have experienced limited light penetration, potentially shifting those cells from photosynthetic growth to endogenous respiration (Foladori et al., 2020; Trebuch et al., 2020).

These metabolically inactive cells likely contributed to the increased in total attached biomass but did not actively assimilate nutrients (Mohsenpour et al., 2021). Additionally, the extracellular polymeric substances (EPS) matrix and/or the hydrodynamics at the mini-Biobob surface may have created diffusion resistance, limiting the transport of dissolved nutrients and carbon to the inner layers of the biofilm. Consequently, only a fraction of the total attached biomass likely participated actively in nutrient removal, explaining the lack of correlation between increase of attached biomass and treatment performance (Mohsenpour et al., 2021; Ren et al., 2024; Xu et al., 2024).

From a bioeconomy perspective, however, even though nutrient removal rates remained statistically unchanged, the higher biomass productivity on the support media represents an important resource recovery opportunity. Maximized biomass productivity per unit surface area may enable more compact reactor designs, overcoming one of the bottlenecks of microalgae-based wastewater treatment, while also facilitating easier biomass harvesting. Thus, although the mini-Biobob did not enhance effluent quality under the tested conditions, the system could be envisaged as a platform for value-added biomass production rather than solely as a polishing step for nutrient removal.

Therefore, future work should focus on optimizing the trade-off between attached biomass accumulation and metabolic activity, potentially through periodic biofilm harvesting or controlling the light regime to prevent self-shading, while also evaluating the economic feasibility of biomass valorisation pathways.

5.4. CONCLUSIONS

Despite the accumulation of attached biomass, this phenomenon did not result in significant improvements in domestic wastewater treatment, particularly regarding the removal of nitrogen and phosphorus. The presence of the mini-Biobob support media led to an increase in biomass concentration, yet this did not result in enhanced nutrient removal efficiency.

However, it is imperative to emphasise that this increase in biomass may potentially enable a reduction in the HRT without compromising treatment efficacy. Additionally, the higher biomass concentration achieved with the mini-Biobob could be particularly advantageous when treating effluents with higher nutrient loading rates, potentially leading to

improved removal performance. These possibilities, however, remain to be investigated and experimentally confirmed.

Another noteworthy aspect is that attached biomass may provide substantial advantages in the separation process, one of the biggest current challenges in the use of microalgae for wastewater treatment, indicating promising applications for other purposes. This finding not only underscores the complexity of phenomena associated with attached biomass but also points to promising perspectives and practical implications that warrant further investigation.

Importantly, the interactions between increased surface area with mini-Biobob and key operational parameters, including light penetration, hydrodynamics, and biomass retention, remain not yet well understood. Future investigations should focus on optimising support media concentration in combination with operational variables such as HRT and mixing intensity to fully realise the potential of attached biomass in microalgae-bacteria photobioreactors.

6.

General conclusion

6.1. THESIS CONCLUSION

Conventional wastewater treatment methods, such as activated sludge, have significant economic, energetic and environmental impacts associated with the use of large areas for separated zones (anaerobic, anoxic, and aerobic tanks), high electricity consumption for aeration, and greenhouse gas emissions. Sustainable alternatives based on microalgae have gained attention, yet critical gaps persist in the literature regarding microalgae-bacteria interactions, and the operational parameters impacts in column PBR.

This thesis focused on the development and operation of a single-stage column PBR for recovery of carbon, nitrogen, and phosphorus from domestic wastewater using microalgal-bacterial consortium and biomass production. Throughout the investigation, three axes were explored: (I) the optimization of operational parameters (HRT, SRT, and surface area/volume ratio); (II) the elucidation of the dominant nitrogen removal mechanisms, with emphasis on the balance between microalgal assimilation and bacterial nitrification; and (III) the evaluation of a support media (mini-Biobob) to increase the surface area available for biomass fixation. The single-stage system, which eliminates the need for separate anoxic reactor, not only allowed for advancements in the understanding of algae-bacteria symbiosis but also provided operational guidelines for the decentralized treatment of domestic wastewater.

Therefore, based on the initially proposed objectives and the results obtained, the main conclusions from this work include:

Chapter 3: Operational optimisation.

The optimization of operational parameters provided critical for enhancing treatment performance and understanding the underlying mechanisms of nutrient recovery. The reduction of HRT, essential for making this design competitive with conventional systems, enhanced carbon and nitrogen removal by over 130%. Concurrently, a shorter SRT of 3 days prevented nitrite accumulation and favoured nitrogen assimilation, achieving a rate of 0.55 gN d^{-1}. N_2O emissions remained undetectable when biomass concentrations stayed below 2 gTSS L^{-1}, whereas N_2O emissions reached 0.1% of nitrogen loss at concentrations above this threshold. From a microbiological perspective, *Scenedesmus* sp. (72% relative abundance) outcompeted *Pseudanabaena* sp. under high S/V ratio conditions, indicating that operational parameters directly influence microbial community structure. Together, these

findings demonstrate that careful selection of HRT, SRT, S/V ratio, and biomass concentration can simultaneously optimise carbon and nitrogen removal, minimise greenhouse gas emissions, and favour desirable algal species, advancing the understanding of single-stage photobioreactors for decentralised wastewater treatment.

Chapter 4: Elucidating nitrogen removal pathways.

The role of nitrification in nutrient removal dynamics was investigated using ATU as a selective inhibitor. Phosphate removal remained consistently high across both experimental stages, with efficiencies of 98 ± 4% (Stage I) and 97 ± 7% (Stage II), and no statistical difference between stages ($p > 0.05$). This finding indicated that phosphorus uptake occurs primarily by microalgal assimilation and that nitrification activity had negligible impact on phosphate removal. In terms of nitrogen removal, the single-stage PBR achieved TN removal efficiencies comparable to conventional activated sludge systems. When nitrification was chemically suppressed, 8% of total nitrogen was rerouted towards microalgal assimilation, demonstrating the importance of the balance between nitrification and assimilation balance for nitrogen removal pathway, without compromising overall efficiency. From a microbiological perspective, nitrification suppression induced a clear shift in community structure, altering key microbial functions associated with carbon and nitrogen cycling. The relative abundances of Proteobacteria and Bacteroidota decreased. *Scenedesmus* and *Nodosilinea* became dominant, with *Scenedesmus* emerging as the primary driver of efficient carbon and nitrogen removal following nitrification inhibition. Together, these findings demonstrate that the fundamental pathways for nitrogen removal in this system was predominantly dominated by microalgal assimilation, although in situ bacterial nitrification-denitrification remained necessary to achieve complete nitrogen removal.

Chapter 5: Evaluation of support media.

The use of support media mini-Biobob was evaluated to understand the influence of varying the surface area available for attached biomass on the performance of column PBR treating real domestic wastewater. The presence of the mini-Biobob support media led to an increase in biomass concentration, yet this did not result in enhanced nitrogen and phosphorus removal efficiencies. Importantly, the interactions between increased surface area with mini-

Biobob and key operational parameters, including light penetration, hydrodynamics, and biomass retention, remain not yet well understood , pointing to important directions for future research.

6.1.1. RESEARCH PERSPECTIVES

The present work raised a few issues that could be considered as perspectives for future research.

- **Scale-up and validation with real wastewater.** The single-stage PBR demonstrated promising results for nutrient removal and biomass production under controlled conditions. Following the elucidation of the dominant removal pathways, future studies should validate these findings using real domestic wastewater, considering its inherent variability in composition and influence of dominant biota, and explore the challenges and opportunities of scaling up the system to pilot application.
- **Optimisation of support media performance.** First, from an operational perspective, future studies should focus on evaluating whether the higher biomass concentration obtained with the use of mini-Biobob can be advantageous for reduce HRT and/or the treatment of effluents with higher nutrient loading rates, potentially leading to improved removal performance. Second, from a mechanistic perspective, the interactions between increased surface area and light penetration and hydrodynamics warrant systematic investigation. Third, from a configurational perspective, the performance of this support media should be validated in other PBR geometries to determine whether the observed benefits are robust across different reactor designs. Understanding these photo-hydrodynamic interactions is essential to determine whether, and under what conditions, support media can enhance the performance of column PBRs.

BIBLIOGRAPHY

Abdel-Raouf, N., Al-Homaidan, A. A., & Ibraheem, I. B. M. (2012). Microalgae and wastewater treatment. *Saudi Journal of Biological Sciences*, *19*(3), 257-275. https://doi.org/10.1016/j.sjbs.2012.04.005

Abdur Razzak, S., Bahar, K., Islam, K. M. O., Haniffa, A. K., Faruque, M. O., Hossain, S. M. Z., & Hossain, M. M. (2024). Microalgae cultivation in photobioreactors: Sustainable solutions for a greener future. *Green Chemical Engineering*, *5*(4), 418-439. https://doi.org/10.1016/j.gce.2023.10.004

ABNT, A. B. de N. T. (1986). *NBR 9648:1986—Estudo de concepção de sistemas de esgoto sanitário* (NBR 9648).

Acién, F. G., Gómez-Serrano, C., Morales-Amaral, M. M., Fernández-Sevilla, J. M., & Molina-Grima, E. (2016). Wastewater treatment using microalgae: How realistic a contribution might it be to significant urban wastewater treatment? *Applied Microbiology and Biotechnology*, *100*(21), 9013-9022. https://doi.org/10.1007/s00253-016-7835-7

Alcántara, C., Domínguez, J. M., García, D., Blanco, S., Pérez, R., García-Encina, P. A., & Muñoz, R. (2015). Evaluation of wastewater treatment in a novel anoxic–aerobic algal–bacterial photobioreactor with biomass recycling through carbon and nitrogen mass balances. *Bioresource Technology*, *191*, 173-186. https://doi.org/10.1016/j.biortech.2015.04.125

Alcántara, C., Posadas, E., Guieysse, B., & Muñoz, R. (2015a). *Microalgae-based Wastewater Treatment*. 439-455. https://doi.org/10.1016/b978-0-12-800776-1.00029-7

Alcántara, C., Posadas, E., Guieysse, B., & Muñoz, R. (2015b). Microalgae-based Wastewater Treatment. En S.-K. Kim (Ed.), *Handbook of Marine Microalgae* (pp. 439-455). Academic Press. https://doi.org/10.1016/B978-0-12-800776-1.00029-7

Al-Jabri, H., Das, P., Khan, S., Thaher, M., & AbdulQuadir, M. (2021). Treatment of Wastewaters by Microalgae and the Potential Applications of the Produced Biomass—A Review. *Water*, *13*(1), Article 1. https://doi.org/10.3390/w13010027

Andrade, G. A., Berenguel, M., Guzmán, J. L., Pagano, D. J., & Acién, F. G. (2016). Optimization of biomass production in outdoor tubular photobioreactors. *Journal of Process Control*, *37*, 58-69. https://doi.org/10.1016/j.jprocont.2015.10.001

Aparicio, S., Borrás-Falomir, L., Jiménez-Benítez, A., Seco, A., & Robles, Á. (2024). Urban wastewater treatment at ambient conditions using microalgae-bacteria consortia in a membrane high-rate algal pond (MHRAP): The effect of hydraulic retention time and influent strength. *Environmental Technology & Innovation*, *36*, 103846. https://doi.org/10.1016/j.eti.2024.103846

APHA. (2017). *Standard Methods For the Examination of Water and Wastewater*. American Public Health Association. https://doi.org/10.2105/SMWW.2882

Arango, J., Rojo, A., Casagli, F., Bernard, O., & Jeison, D. (2025). Assessing the impact of biomass retention in membrane-assisted microalgae-bacteria sewage treatment. *Journal of Environmental Chemical Engineering*, *13*(5), 118546. https://doi.org/10.1016/j.jece.2025.118546

Arbib, Z., Ruiz, J., Álvarez-Díaz, P., Garrido-Pérez, C., Barragan, J., & Perales, J. A. (2013a). Effect of pH control by means of flue gas addition on three different photo-bioreactors treating urban wastewater in long-term operation. *Ecological Engineering*, *57*, 226-235. https://doi.org/10.1016/j.ecoleng.2013.04.040

Arbib, Z., Ruiz, J., Álvarez-Díaz, P., Garrido-Pérez, C., Barragan, J., & Perales, J. A. (2013b). Long term outdoor operation of a tubular airlift pilot photobioreactor and a high rate algal pond as tertiary treatment of urban wastewater. *Ecological Engineering*, *52*, 143-153. https://doi.org/10.1016/j.ecoleng.2012.12.089

Bankston, E., Wang, Q., & Higgins, B. T. (2020). Algae support populations of heterotrophic, nitrifying, and phosphate-accumulating bacteria in the treatment of poultry litter anaerobic digestate. *Chemical Engineering Journal*, *398*, 125550. https://doi.org/10.1016/j.cej.2020.125550

Baskaran, V., Patil, P. K., Antony, M. L., Avunje, S., Nagaraju, V. T., Ghate, S. D., Nathamuni, S., Dineshkumar, N., Alavandi, S. V., & Vijayan, K. K. (2020). Microbial community profiling of ammonia and nitrite oxidizing bacterial enrichments from brackishwater ecosystems for mitigating nitrogen species. *Scientific Reports*, *10*(1), 5201. https://doi.org/10.1038/s41598-020-62183-9

Buha, D. M., Atalia, K. R., & Shah, N. K. (2017). Continuous process study on simultaneous nitrification–denitrification of high ammoniacal nitrogen load wastewater in aerobic–anoxic sequencing bioreactors. *International Journal of Environmental Science and Technology*, *14*(11), 2451-2458. https://doi.org/10.1007/s13762-017-1333-z

Bux, F., & Chisti, Y. (2016). Algae biotechnology. Products and processes. *Green Energy and Technology*, (March), 344. https://doi.org/10.1007/978-3-319-12334-9

Chai, W. S., Chew, C. H., Munawaroh, H. S. H., Ashokkumar, V., Cheng, C. K., Park, Y.-K., & Show, P. L. (2021). Microalgae and ammonia: A review on inter-relationship. *Fuel*, *303*, 121303. https://doi.org/10.1016/j.fuel.2021.121303

de Godos, I., Vargas, V. A., Guzmán, H. O., Soto, R., García, B., García, P. A., & Muñoz, R. (2014). Assessing carbon and nitrogen removal in a novel anoxic–aerobic cyanobacterial–bacterial photobioreactor configuration with enhanced biomass sedimentation. *Water Research*, *61*, 77-85. https://doi.org/10.1016/j.watres.2014.04.050

de Haas, D., & Andrews, J. (2022). Nitrous oxide emissions from wastewater treatment—Revisiting the IPCC 2019 refinement guidelines. *Environmental Challenges*, *8*, 100557. https://doi.org/10.1016/j.envc.2022.100557

Deprá, M. C., Mérida, L. G. R., de Menezes, C. R., Zepka, L. Q., & Jacob-Lopes, E. (2019). A new hybrid photobioreactor design for microalgae culture. *Chemical Engineering Research and Design*, *144*, 1-10. https://doi.org/10.1016/j.cherd.2019.01.023

Devos, P., Filali, A., Grau, P., & Gillot, S. (2023). Sidestream characteristics in water resource recovery facilities: A critical review. *Water Research*, *232*, 119620. https://doi.org/10.1016/j.watres.2023.119620

El Wali, M., Golroudbary, S. R., & Kraslawski, A. (2021). Circular economy for phosphorus supply chain and its impact on social sustainable development goals. *Science of The Total Environment*, *777*, 146060. https://doi.org/10.1016/j.scitotenv.2021.146060

Esteves, A. F., Salgado, E. M., Vilar, V. J. P., Gonçalves, A. L., & Pires, J. C. M. (2024). A growth phase analysis on the influence of light intensity on microalgal stress and potential biofuel production. *Energy Conversion and Management*, *311*, 118511. https://doi.org/10.1016/j.enconman.2024.118511

Fallahi, A., Rezvani, F., Asgharnejad, H., Khorshidi Nazloo, E., Hajinajaf, N., & Higgins, B. (2021). Interactions of microalgae-bacteria consortia for nutrient removal from wastewater: A review. *Chemosphere*, *272*, 129878. https://doi.org/10.1016/j.chemosphere.2021.129878

Ferro, L., Colombo, M., Posadas, E., Funk, C., & Muñoz, R. (2019). Elucidating the symbiotic interactions between a locally isolated microalga Chlorella vulgaris and its co-occurring bacterium Rhizobium sp. In synthetic municipal wastewater. *Journal of Applied Phycology*, *31*(4), 2299-2310. https://doi.org/10.1007/s10811-019-1741-1

Foladori, P., Petrini, S., & Andreottola, G. (2020). How suspended solids concentration affects nitrification rate in microalgal-bacterial photobioreactors without external aeration. *Heliyon*, *6*(1), e03088. https://doi.org/10.1016/j.heliyon.2019.e03088

Frutos, O. D., Arvelo, I. A., Pérez, R., Quijano, G., & Muñoz, R. (2015). Continuous nitrous oxide abatement in a novel denitrifying off-gas bioscrubber. *Applied Microbiology and Biotechnology*, *99*(8), 3695-3706. https://doi.org/10.1007/s00253-014-6329-8

García, D., Alcántara, C., Blanco, S., Pérez, R., Bolado, S., & Muñoz, R. (2017). Enhanced carbon, nitrogen and phosphorus removal from domestic wastewater in a novel anoxic-aerobic photobioreactor coupled with biogas upgrading. *Chemical Engineering Journal*, *313*, 424-434. https://doi.org/10.1016/j.cej.2016.12.054

Ginestet, P., Audic, J.-M., Urbain, V., & Block, J.-C. (1998). Estimation of Nitrifying Bacterial Activities by Measuring Oxygen Uptake in the Presence of the Metabolic Inhibitors Allylthiourea and Azide. *Applied and Environmental Microbiology*, *64*(6), 2266-2268. https://doi.org/10.1128/AEM.64.6.2266-2268.1998

Gonçalves, A. L., Pires, J. C. M., & Simões, M. (2017). A review on the use of microalgal consortia for wastewater treatment. *Algal Research, Wastewater and Algae; opportunities, challenges and long term sustainability*, *24*, 403-415. https://doi.org/10.1016/j.algal.2016.11.008

González, C., Marciniak, J., Villaverde, S., León, C., García, P. A., & Muñoz, R. (2008). Efficient nutrient removal from swine manure in a tubular biofilm photo-bioreactor using algae-bacteria consortia. *Water Science and Technology*, *58*(1), 95-102. https://doi.org/10.2166/wst.2008.655

González-Camejo, J., Aparicio, S., Jiménez-Benítez, A., Pachés, M., Ruano, M. V., Borrás, L., Barat, R., & Seco, A. (2020). Improving membrane photobioreactor performance by reducing light path: Operating conditions and key performance indicators. *Water Research*, *172*, 115518. https://doi.org/10.1016/j.watres.2020.115518

González-Camejo, J., Aparicio, S., Pachés, M., Borrás, L., & Seco, A. (2022). Comprehensive assessment of the microalgae-nitrifying bacteria competition in microalgae-based wastewater treatment systems: Relevant factors,

evaluation methods and control strategies. *Algal Research*, *61*, 102563. https://doi.org/10.1016/j.algal.2021.102563

González-Camejo, J., Aparicio, S., Ruano, M. V., Borrás, L., Barat, R., & Ferrer, J. (2019). Effect of ambient temperature variations on an indigenous microalgae-nitrifying bacteria culture dominated by *Chlorella*. *Bioresource Technology*, *290*, 121788. https://doi.org/10.1016/j.biortech.2019.121788

González-Camejo, J., Montero, P., Aparicio, S., Ruano, M. V., Borrás, L., Seco, A., & Barat, R. (2020). Nitrite inhibition of microalgae induced by the competition between microalgae and nitrifying bacteria. *Water Research*, *172*, 115499. https://doi.org/10.1016/j.watres.2020.115499

Han, F., & Zhou, W. (2022). Nitrogen recovery from wastewater by microbial assimilation – A review. *Bioresource Technology*, *363*, 127933. https://doi.org/10.1016/j.biortech.2022.127933

He, P. J., Mao, B., Lü, F., Shao, L. M., Lee, D. J., & Chang, J. S. (2013). The combined effect of bacteria and *Chlorella vulgaris* on the treatment of municipal wastewaters. *Bioresource Technology*, *146*, 562-568. https://doi.org/10.1016/j.biortech.2013.07.111

Hoyos, E. G., Kuri, R., Toda, T., & Muñoz, R. (2024). Innovative design and operational strategies to improve CO2 mass transfer during photosynthetic biogas upgrading. *Bioresource Technology*, *391*, 129955. https://doi.org/10.1016/j.biortech.2023.129955

Jo, Y., Hoyos, E. G., Blanco, S., Kim, S.-H., & Muñoz, R. (2024). Assessing nitrous oxide emissions from algal-bacterial photobioreactors devoted to biogas upgrading and digestate treatment. *Chemosphere*, *361*, 142528. https://doi.org/10.1016/j.chemosphere.2024.142528

Karemore, A., Ramalingam, D., Yadav, G., Subramanian, G., & Sen, R. (2015). Photobioreactors for Improved Algal Biomass Production: Analysis and Design Considerations. En D. Das (Ed.), *Algal Biorefinery: An Integrated Approach*

(pp. 103-124). Springer International Publishing. https://doi.org/10.1007/978-3-319-22813-6_5

Karya, N. G. A. I., van der Steen, N. P., & Lens, P. N. L. (2013). Photo-oxygenation to support nitrification in an algal–bacterial consortium treating artificial wastewater. *Bioresource Technology*, *134*, 244-250. https://doi.org/10.1016/j.biortech.2013.02.005

Kim, S.-W., Miyahara, M., Fushinobu, S., Wakagi, T., & Shoun, H. (2010). Nitrous oxide emission from nitrifying activated sludge dependent on denitrification by ammonia-oxidizing bacteria. *Bioresource Technology*, *101*(11), 3958-3963. https://doi.org/10.1016/j.biortech.2010.01.030

Krustok, I., Odlare, M., Truu, J., & Nehrenheim, E. (2016). Inhibition of nitrification in municipal wastewater-treating photobioreactors: Effect on algal growth and nutrient uptake. *Bioresource Technology*, *202*, 238-243. https://doi.org/10.1016/j.biortech.2015.12.020

Kwon, G., Kim, H., Song, C., & Jahng, D. (2019). Co-culture of microalgae and enriched nitrifying bacteria for energy-efficient nitrification. *Biochemical Engineering Journal*, *152*, 107385. https://doi.org/10.1016/j.bej.2019.107385

Laizu, S. A., Hassan, L. H. S., & Ahmad, I. (2025). *Open and closed photobioreactors for microalgal cultivation and wastewater treatment*. https://doi.org/https://doi.org/10.2166/9781789064100_0121

Langergraber, G., Castellar, J. A. C., Andersen, T. R., Andreucci, M.-B., Baganz, G. F. M., Buttiglieri, G., Canet-Martí, A., Carvalho, P. N., Finger, D. C., Griessler Bulc, T., Junge, R., Megyesi, B., Milošević, D., Oral, H. V., Pearlmutter, D., Pineda-Martos, R., Pucher, B., van Hullebusch, E. D., & Atanasova, N. (2021). Towards a Cross-Sectoral View of Nature-Based Solutions for Enabling Circular Cities. *Water*, *13*(17), 2352. https://doi.org/10.3390/w13172352

Lapébie, P., Lombard, V., Drula, E., Terrapon, N., & Henrissat, B. (2019). Bacteroidetes use thousands of enzyme combinations to break down glycans.

Nature Communications, *10*(1), 2043. https://doi.org/10.1038/s41467-019-10068-5

Li, Q., Xu, Y., Liang, C., Peng, L., & Zhou, Y. (2023). Nitrogen removal by algal-bacterial consortium during mainstream wastewater treatment: Transformation mechanisms and potential N2O mitigation. *Water Research*, *235*, 119890. https://doi.org/10.1016/j.watres.2023.119890

Liu, Q., Lei, X., Li, J., Chu, L., Wang, F., Shan, H., & Hu, F. (2023). Microbial communities and nitrogen cycling in *Litopenaeus vannamei* and *Mercenaria mercenaria* polyculture ponds. *Aquaculture Reports*, *33*, 101769. https://doi.org/10.1016/j.aqrep.2023.101769

Mallick, N. (2002). Biotechnological potential of immobilized algae for wastewater N, P and metal removal: A review. *Biometals*, *15*(4), 377-390. https://doi.org/10.1023/A:1020238520948

Mansfeldt, C., Achermann, S., Men, Y., Walser, J.-C., Villez, K., Joss, A., Johnson, D. R., & Fenner, K. (2019). Microbial residence time is a controlling parameter of the taxonomic composition and functional profile of microbial communities. *The ISME Journal*, *13*(6), 1589-1601. https://doi.org/10.1038/s41396-019-0371-6

Meng, Q., Zeng, W., Zhang, J., Liu, H., Li, S., & Peng, Y. (2024). Combined Phototrophic Simultaneous Nitrification-Endogenous Denitrification with Phosphorus Removal (P-SNDPR) System Treating Low Carbon to Nitrogen Ratio Wastewater for Potential Carbon Neutrality. *Environmental Science & Technology*, *58*(6), 2902-2911. https://doi.org/10.1021/acs.est.3c09351

Metcalf & Eddy Inc, Tchobanoglous, G., Burton, F. L., Tsuchihashi, R. T., & Stensel, H. D. (2013). *Wastewater Engineering: Treatment and Resource Recovery* (5.ª ed.). McGraw Hill.

Mohsenpour, S. F., Hennige, S., Willoughby, N., Adeloye, A., & Gutierrez, T. (2021). Integrating micro-algae into wastewater treatment: A review. *Science of The*

Total Environment, *752*, 142168. https://doi.org/10.1016/j.scitotenv.2020.142168

Morillas-España, A., Sánchez-Zurano, A., Lafarga, T., del Mar Morales-Amaral, M., Gómez-Serrano, C., Acién-Fernández, F. G., & González-López, C. V. (2021). Improvement of wastewater treatment capacity using the microalga *Scenedesmus* sp. And membrane bioreactors. *Algal Research*, *60*, 102516. https://doi.org/10.1016/j.algal.2021.102516

Mustafa, S., Bhatti, H. N., Maqbool, M., & Iqbal, M. (2021). Microalgae biosorption, bioaccumulation and biodegradation efficiency for the remediation of wastewater and carbon dioxide mitigation: Prospects, challenges and opportunities. *Journal of Water Process Engineering*, *41*, 102009. https://doi.org/10.1016/j.jwpe.2021.102009

Ni, B.-J., Ruscalleda, M., Pellicer-Nàcher, C., & Smets, B. F. (2011). Modeling Nitrous Oxide Production during Biological Nitrogen Removal via Nitrification and Denitrification: Extensions to the General ASM Models. *Environmental Science & Technology*, *45*(18), 7768-7776. https://doi.org/10.1021/es201489n

Nishi, K., Akizuki, S., Toda, T., Matsuyama, T., & Ida, J. (2022). Advanced light-tolerant microalgae-nitrifying bacteria consortia for stable ammonia removal under strong light irradiation using light-shielding hydrogel. *Chemosphere*, *297*, 134252. https://doi.org/10.1016/j.chemosphere.2022.134252

Noyola, A., Padilla-Rivera, A., Morgan-Sagastume, J. M., Güereca, L. P., & Hernández-Padilla, F. (2012). Typology of Municipal Wastewater Treatment Technologies in Latin America. *CLEAN – Soil, Air, Water*, *40*(9), 926-932. https://doi.org/10.1002/clen.201100707

Oruganti, R. K., Katam, K., Show, P. L., Gadhamshetty, V., Upadhyayula, V. K. K., & Bhattacharyya, D. (2022). A comprehensive review on the use of algal-bacterial systems for wastewater treatment with emphasis on nutrient and micropollutant removal. *Bioengineered*, *13*(4), 10412-10453. https://doi.org/10.1080/21655979.2022.2056823

Ossai, I. C., Hamid, F. S., Redzwan, G., Aboudi-Mana, S. C., Hassan, A., Emenike, C. U., Okere, K. J., & Ntiamoah-Asare, D. (2026). Progress in wastewater treatment, separation and purification technologies: Mechanisms, benefits, challenges, efficiencies, and sustainability perspectives. *Journal of Environmental Management*, *399*, 128591. https://doi.org/10.1016/j.jenvman.2026.128591

Peng, L., Li, Y., Li, Q., Liang, C., Nasr, M., Xu, Y., Liu, Y., & Zhou, Y. (2023). The effect of free ammonia on ammonium removal and N2O production in a consortium of microalgae and partial nitritation cultures. *Chemical Engineering Journal*, *474*, 145572. https://doi.org/10.1016/j.cej.2023.145572

Phyu, K., Zhi, S., Graham, D. W., Cao, Y., Xu, X., Liu, J., Wang, H., & Zhang, K. (2025). Impact of indigenous vs. Cultivated microalgae strains on biomass accumulation, microbial community composition, and nutrient removal in algae-based dairy wastewater treatment. *Bioresource Technology*, *426*, 132349. https://doi.org/10.1016/j.biortech.2025.132349

Posadas, E., Alcántara, C., García-Encina, P. A., Gouveia, L., Guieysse, B., Norvill, Z., Acién, F. G., Markou, G., Congestri, R., Koreiviene, J., & Muñoz, R. (2017). 3—Microalgae cultivation in wastewater. En C. Gonzalez-Fernandez & R. Muñoz (Eds.), *Microalgae-Based Biofuels and Bioproducts* (pp. 67-91). Woodhead Publishing. https://doi.org/https://doi.org/10.1016/B978-0-08-101023-5.00003-0

Posadas, E., García-Encina, P. A., Domínguez, A., Díaz, I., Becares, E., Blanco, S., & Muñoz, R. (2014). Enclosed tubular and open algal–bacterial biofilm photobioreactors for carbon and nutrient removal from domestic wastewater. *Ecological Engineering*, *67*, 156-164. https://doi.org/10.1016/j.ecoleng.2014.03.007

Posadas, E., García-Encina, P.-A., Soltau, A., Domínguez, A., Díaz, I., & Muñoz, R. (2013). Carbon and nutrient removal from centrates and domestic wastewater using algal-bacterial biofilm bioreactors. *Bioresource Technology*, *139*, 50-58. https://doi.org/10.1016/j.biortech.2013.04.008

Pratap, B., Kumar, S., Nand, S., Azad, I., Bharagava, R. N., Romanholo Ferreira, L. F., & Dutta, V. (2023). Wastewater generation and treatment by various eco-friendly technologies: Possible health hazards and further reuse for environmental safety. *Chemosphere*, *313*, 137547. https://doi.org/10.1016/j.chemosphere.2022.137547

Rada-Ariza, A. M., Fredy, D., Lopez-Vazquez, C. M., Van der Steen, N. P., & Lens, P. N. L. (2019). Ammonium removal mechanisms in a microalgal-bacterial sequencing-batch photobioreactor at different solids retention times. *Algal Research*, *39*, 101468. https://doi.org/10.1016/j.algal.2019.101468

Rahimi, S., Modin, O., & Mijakovic, I. (2020). Technologies for biological removal and recovery of nitrogen from wastewater. *Biotechnology Advances*, *43*, 107570. https://doi.org/10.1016/j.biotechadv.2020.107570

Ren, Z., Li, H., Sun, P., Fu, R., Bai, Z., Zhang, G., Sun, L., & Wei, Y. (2024). Development and challenges of emerging biological technologies for algal-bacterial symbiosis systems: A review. *Bioresource Technology*, *413*, 131459. https://doi.org/10.1016/j.biortech.2024.131459

Rossi, S., Bellucci, M., Marazzi, F., Mezzanotte, V., & Ficara, E. (2018). Activity assessment of microalgal-bacterial consortia based on respirometric tests. *Water Science and Technology*, *78*(1), 207-215. https://doi.org/10.2166/wst.2018.078

Roveroto, G. P., Teles, J. C., Vuitik, G. A., da Silva Batista, J. S., & Barana, A. C. (2021). Craft Brewery Wastewater Treatment: A Fixed-Bed Single-Batch Reactor with Intermittent Aeration to Remove COD and TN. *Brazilian Archives of Biology and Technology*, *64*. https://doi.org/10.1590/1678-4324-75years-2021200613

Sánchez-Zurano, A., Gómez-Serrano, C., Acién-Fernández, F. G., Fernández-Sevilla, J. M., & Molina-Grima, E. (2020). A novel photo-respirometry method to characterize consortia in microalgae-related wastewater treatment processes. *Algal Research*, *47*, 101858. https://doi.org/10.1016/j.algal.2020.101858

Sepúlveda-Muñoz, C. A., de Godos, I., & Muñoz, R. (2023). Wastewater Treatment Using Photosynthetic Microorganisms. *Symmetry*, *15*(2). https://doi.org/10.3390/sym15020525

Shinichi Akizuki, Akizuki, S., Masatoshi Kishi, Kishi, M., Germán Cuevas-Rodríguez, Cuevas-Rodríguez, G., Tatsuki Toda, & Toda, T. (2020). Corrigendum to «Effects of different light conditions on ammonium removal in a consortium of microalgae and partial nitrifying granules» [Water Res. 171 (2020) 115445]. *Water Research*, *175*, 115778. https://doi.org/10.1016/j.watres.2020.115778

Silva, J. A. (2023). Wastewater Treatment and Reuse for Sustainable Water Resources Management: A Systematic Literature Review. *Sustainability*, *15*(14), 10940. https://doi.org/10.3390/su151410940

SINISA, S. N. de I. em S. B. (2025). *Relatório da gestão municipal do saneamento básico*. https://www.gov.br/cidades/pt-br/acesso-a-informacao/acoes-e-programas/saneamento/sinisa/

Solimeno, A., Acíen, F. G., & García, J. (2017). Mechanistic model for design, analysis, operation and control of microalgae cultures: Calibration and application to tubular photobioreactors. *Algal Research*, *21*, 236-246. https://doi.org/10.1016/j.algal.2016.11.023

Sutherland, D. L., Burke, J., Leal, E., & Ralph, P. J. (2020). Effects of nutrient load on microalgal productivity and community composition grown in anaerobically digested food-waste centrate. *Algal Research*, *51*, 102037. https://doi.org/10.1016/j.algal.2020.102037

Sutherland, D. L., & Ralph, P. J. (2019). Microalgal bioremediation of emerging contaminants—Opportunities and challenges. *Water Research*, *164*, 114921. https://doi.org/10.1016/j.watres.2019.114921

Tang, L., Zhang, Y., Gao, M., & Wang, X. (2025). Simultaneous Nitrification–Endogenous Denitrification with Phosphorus Removal Sustained by Aeration-Free Filamentous Microalgal–Bacterial Granular Sludge for Low C/N

Wastewater Treatment. *ACS ES&T Engineering*. https://doi.org/10.1021/acsestengg.4c00833

Toledo-Cervantes, A., Posadas, E., Bertol, I., Turiel, S., Alcoceba, A., & Muñoz, R. (2019). Assessing the influence of the hydraulic retention time and carbon/nitrogen ratio on urban wastewater treatment in a new anoxic-aerobic algal-bacterial photobioreactor configuration. *Algal Research*, *44*, 101672. https://doi.org/10.1016/j.algal.2019.101672

Toledo-Cervantes, A., Serejo, M. L., Blanco, S., Pérez, R., Lebrero, R., & Muñoz, R. (2016). Photosynthetic biogas upgrading to bio-methane: Boosting nutrient recovery via biomass productivity control. *Algal Research*, *17*, 46-52. https://doi.org/10.1016/j.algal.2016.04.017

Torres-Franco, A. F., Zuluaga, M., Hernández-Roldán, D., Leroy-Freitas, D., Sepúlveda-Muñoz, C. A., Blanco, S., Mota, C. R., & Muñoz, R. (2021). Assessment of the performance of an anoxic-aerobic microalgal-bacterial system treating digestate. *Chemosphere*, *270*, 129437. https://doi.org/10.1016/j.chemosphere.2020.129437

Trebuch, L. M., Oyserman, B. O., Janssen, M., Wijffels, R. H., Vet, L. E. M., & Fernandes, T. V. (2020). Impact of hydraulic retention time on community assembly and function of photogranules for wastewater treatment. *Water Research*, *173*, 115506. https://doi.org/10.1016/j.watres.2020.115506

van der Wiel, B. Z., Weijma, J., van Middelaar, C. E., Kleinke, M., Buisman, C. J. N., & Wichern, F. (2019). Restoring nutrient circularity: A review of nutrient stock and flow analyses of local agro-food-waste systems. *Resources, Conservation & Recycling: X*, *3*, 100014. https://doi.org/10.1016/j.rcrx.2019.100014

Vargas, G., Donoso-Bravo, A., Vergara, C., & Ruiz-Filippi, G. (2016). Assessment of microalgae and nitrifiers activity in a consortium in a continuous operation and the effect of oxygen depletion. *Electronic Journal of Biotechnology*, *23*, 63-68. https://doi.org/10.1016/j.ejbt.2016.08.002

Vargas-Estrada, L., Longoria, A., Okoye, P. U., & Sebastian, P. J. (2021). Energy and nutrients recovery from wastewater cultivated microalgae: Assessment of the impact of wastewater dilution on biogas yield. *Bioresource Technology*, *341*, 125755. https://doi.org/10.1016/j.biortech.2021.125755

Von Sperling, M. (2007). *Wastewater Characteristics, Treatment and Disposal*. IWA Publishing. https://doi.org/10.2166/9781780402086

Wali, M. E., Golroudbary, S. R., Andrzej Kraslawski, Andrzej Kraslawski, & Kraslawski, A. (2021). Circular economy for phosphorus supply chain and its impact on social sustainable development goals. *Science of The Total Environment*, *777*, 146060-146060. https://doi.org/10.1016/j.scitotenv.2021.146060

Wang, K., Yan, D., Chen, X., Xu, Z., Cao, W., & Li, H. (2024a). New insight to the enriched microorganisms driven by pollutant concentrations and types for industrial and domestic wastewater via distinguishing the municipal wastewater treatment plants. *Environmental Pollution*, *361*, 124789. https://doi.org/10.1016/j.envpol.2024.124789

Wang, K., Yan, D., Chen, X., Xu, Z., Cao, W., & Li, H. (2024b). New insight to the enriched microorganisms driven by pollutant concentrations and types for industrial and domestic wastewater via distinguishing the municipal wastewater treatment plants. *Environmental Pollution*, *361*, 124789. https://doi.org/10.1016/j.envpol.2024.124789

WHO, (2022). *Guidelines for drinking-water quality: Fourth edition incorporating the first and second addenda*. World Health Organization. https://www.who.int/publications/i/item/9789240045064

WHO, (2025). *WHO water, sanitation, hygiene and waste strategy 2026-2035*. World Health Organization. https://doi.org/10.2471/B09661

WHO & UN-Habitat, (2024). *Progress on the proportion of domestic and industrial wastewater flows safely treated – Mid-term status of SDG Indicator 6.3.1 and*

acceleration needs, with a special focus on climate change, wastewater reuse and health. https://www.who.int/publications/i/item/9789240099081

Xin, L., Hong-ying, H., Ke, G., & Ying-xue, S. (2010). Effects of different nitrogen and phosphorus concentrations on the growth, nutrient uptake, and lipid accumulation of a freshwater microalga *Scenedesmus* sp. *Bioresource Technology*, *101*(14), 5494-5500. https://doi.org/10.1016/j.biortech.2010.02.016

Xiong, C., Zhang, P., Zhu, Y., Gao, X., Wang, Z., Chen, X., & Zhang, P. (2025). Sewage tertiary treatment: Bacterial-algal symbiosis promotes nutrient removal and biofilm stabilization. *Algal Research*, *90*, 104188. https://doi.org/10.1016/j.algal.2025.104188

Xu, S., Li, Z., Yu, S., Chen, Z., Xu, J., Qiu, S., & Ge, S. (2024). Microalgal–Bacteria Biofilm in Wastewater Treatment: Advantages, Principles, and Establishment. *Water*, *16*(18). https://doi.org/10.3390/w16182561

Yadav, S., Anam, G. B., & Ahn, Y.-H. (2021). Influence of Abiotic Factors on the Growth of Cyanobacteria Isolated from Nakdong River, South Korea1. *Journal of Phycology*, *57*(3), 874-885. https://doi.org/10.1111/jpy.13143

Yan, Y., Lu, H., Zhang, J., Zhu, S., Wang, Y., Lei, Y., Zhang, R., & Song, L. (2022). Simultaneous heterotrophic nitrification and aerobic denitrification (SND) for nitrogen removal: A review and future perspectives. *Environmental Advances*, *9*, 100254. https://doi.org/10.1016/j.envadv.2022.100254

Yi, L., Solanki, R., & Strous, M. (2024). In search of the pH limit of growth in halo-alkaliphilic cyanobacteria. *Environmental Microbiology Reports*, *16*(4), e13323. https://doi.org/10.1111/1758-2229.13323

Yi, M., Sheng, Q., Sui, Q., & Lu, H. (2020). β-blockers in the environment: Distribution, transformation, and ecotoxicity. *Environmental Pollution*, *266*, 115269. https://doi.org/10.1016/j.envpol.2020.115269

Yue, X., Xiao, X., Liang, J., Lin, Y., Xiao, K., & Che, K. (2024). Firmicutes and Bacteroidetes as the dominant microorganisms for ammonium nitrogen

wastewater treatment with a low C/N ratio in BCOR. *Journal of Water Process Engineering*, *65*, 105851. https://doi.org/10.1016/j.jwpe.2024.105851

Zhang, B., Li, W., Guo, Y., Zhang, Z., Shi, W., Cui, F., Lens, P. N. L., & Tay, J. H. (2020). Microalgal-bacterial consortia: From interspecies interactions to biotechnological applications. *Renewable and Sustainable Energy Reviews*, *118*, 109563. https://doi.org/10.1016/j.rser.2019.109563

Zhi, M., Zhou, Z., Yang, C., Chen, Y., Xiao, Y., & Meng, F. (2023). Solid retention time regulates partial nitrification by algal-bacterial consortia in wastewater treatment: Performance and mechanism. *Chemical Engineering Journal*, *452*, 139537. https://doi.org/10.1016/j.cej.2022.139537

Zhong, X., Zhao, H., Yue, S., & Fan, J. (2024). Algal-bacterial consortia driven nitrite accumulation and phosphorus removal in partial denitrification. *Journal of Water Process Engineering*, *68*, 106504. https://doi.org/10.1016/j.jwpe.2024.106504

ANEXO A - AUTORIZAÇÃO DA REVISTA PARA SUBMISSÃO EM REPOSITÓRIO INSTITUCIONAL

Jisc Open policy finder

Algal Research:Biomass, Biofuels and Bioproducts

← Back to search results

Report an error

Journal Policy | Open Access Compliance | Transitional Agreement Look-up | Journal Details | Record Informat

Version:

○ Show all ◉ Published ○ Accepted ○ Submitted

Published **Option with associated OA fees, no embargo & CC BY-NC-ND and 1 other licence**

Hide

OA Fee

This option has an Open Access fee associated with it

OA Publishing

We use cookies to give you the best experience and to help improve our website.

Find out more about how we use cookies

Accept cookies

Reject cookies

CC BY-NC

Locations

Named Repository (PubMed Central, Research for Development Repository, ESRC Research Catalogue)

Non-Commercial Repository

Non-Commercial Website

Journal Website

Conditions

Published source must be acknowledged with citation

Published **Option with associated OA fees, no embargo & CC BY licence**

Hide

Jisc Open policy finder

Journal of Water Process Engineering (JWPE)

← Back to search results

Report an error

Journal Policy | Open Access Compliance | Transitional Agreement Look-up | Journal Details | Record Informat

Version:

○ Show all ◉ Published ○ Accepted ○ Submitted

Published

Option with associated OA fees, no embargo & CC BY-NC-ND and 1 other licence

Hide

OA Fee

This option has an Open Access fee associated with it

OA Publishing

CC BY-NC

Locations

Named Repository (PubMed Central, Research for Development Repository, ESRC Research Catalogue)

Non-Commercial Repository

Non-Commercial Website

Journal Website

Conditions

Published source must be acknowledged with citation

Published

Option with associated OA fees, no embargo & CC BY licence

Hide

DADOS CURRICULARES

IDENTIFICAÇÃO	
	Thalita Lacerda dos Santos 09/01/1983
Nacionalidade	Brasileira
Nome em citações bibliográficas:	Santos, Thalita Lacerda dos Dos Santos, Thalita Lacerda Santos, T.L.
Currículo Lattes	https://lattes.cnpq.br/7428165171252274
ORCID	https://orcid.org/0000-0002-6576-1041
FORMAÇÃO ACADÊMICA	
2020/2022	Mestrado em Engenharia Civil e Ambiental. Universidade Estadual Paulista Júlio de Mesquita Filho, UNESP.
2016/2017	Especialização em MBA em Gestão de Projetos. (Carga Horária: 360h). Universidade Federal de Pernambuco, UFPE.
2003/2008	Graduação em Engenharia Química. Universidade Estadual de Campinas, UNICAMP.
PRODUÇÃO BIBLIOGRÁFICA	

dos Santos, Thalita Lacerda; Vargas-Estrada, Laura; Blanco, Saúl; da Silva, Gustavo Henrique Ribeiro; Muñoz, Raúl. Uncovering nitrogen removal in algal-bacterial processes for domestic wastewater treatment. JOURNAL OF WATER PROCESS ENGINEERING, v. 86, p. 109975, 2026.

dos Santos, Thalita Lacerda; Vargas-Estrada, Laura; Blanco, Saúl; da Silva, Gustavo Henrique Ribeiro; Muñoz, Raúl. Influence of operational parameters on the performance of domestic wastewater treatment in a single-stage algal-bacterial column photobioreactor. Algal Research-Biomass Biofuels and Bioproducts, v. 92, p. 104417, 2025.

PRODUÇÃO BIBLIOGRÁFICA

Lima, Pedro Augusto Bertucci; Domingues, Ana Mariele; dos Santos, Thalita Lacerda; de Souza, Fernando Bernardi; Alves, Anabela Carvalho. From postgraduate to undergraduate students: learning about circular economy. International Journal of Information and Operations Management Education, v. 7, p. 348-373, 2024.

Santos, Thalita Lacerda dos; Barbosa, Felipe Teles; Florentino, Anna Patricya; Silva, Gustavo Henrique Ribeiro da. Synergistic nutrient removal by native microalgae-bacteria consortium: key parameter evaluation. Revista Brasileira de Ciências Ambientais (Online), v. 59, p. e1962, 2024.

Lima, Pedro Augusto Bertucci; Delgado, Fernanda Camila Martinez; Santos, Thalita Lacerda dos; Florentino, Anna Patrícya . Medications reverse logistics: A systematic literature review and a method for improving the Brazilian case. Cleaner Logistics and Supply Chain, v. 3, p. 100024, 2022.

Lima, Pedro A. B.; Paião Júnior, Gilberto D.; Santos, Thalita L.; Furlan, Marcelo; Battistelle, Rosane A. G.; Silva, Gustavo H. R.; Ferraz, Diogo; Mariano, Enzo B. . Sustainable Human Development at the Municipal Level: A Data Envelopment Analysis Index. Infrastructures, v. 7, p. 12, 2022.

dos Santos, Thalita Lacerda; Belasco, Gabriela Costa; Pompei, Caroline Moço Erba; Quartaroli, Larissa; Pessi, Bruno Assis; da Silva, Graziele Ruas Lagoas; Silva, Gustavo Henrique Ribeiro. Wastewater Treatment in Tubular Photobioreactors: Exploring the Impact of Support Medium. In: Giorgio Mannina, Alida Cosenza, Antonio Mineo. (Org.). Lecture Notes in Civil Engineering. 1ed.Cham: Springer Nature Switzerland, 2024, v. 1, p. 252-257.

Lima, Pedro Augusto Bertucci; Paião Júnior, Gilberto D.; Santos, Thalita Lacerda dos; Battistelle, Rosane A. G.; Silva, Gustavo H. R.; Mariano, Enzo B. . Municipality human development and sanitation: A Data Envelopment Analysis study in the Brazilian São Paulo State.. In: International Conference Construction, Energy, Environment & Sustainability, 2021, Coimbra. Proceedings of the International Conference Construction, Energy, Environment & Sustainability, 2021.

PRODUÇÃO BIBLIOGRÁFICA

Lima, Pedro Augusto Bertucci; Domingues, A. M.; Santos, Thalita Lacerda dos; Souza, F. B. Desenvolvimento de um curso de introdução à economia circular: Uma pesquisa-ação para graduandos em engenharia de produção. In: XXVIII Simpósio de Engenharia de Produção (SIMPEP, 2021, Bauru. Anais do XXVIII Simpósio de Engenharia de Produção (SIMPEP).

Dias, L. C.; Fattori, J.; Santos, T.L. Síntese de 2-amino-3,5-diois. In: Reunião Anual da Sociedade Brasileira de Química - SBQ 2007, 2007, Águas de Lindóia. Livro de Resumos SBQ 2007, 2007. v. 1. p. QO109.

PARTICIPAÇÃO EM BANCAS E ORIENTAÇÕES

Bancas de trabalhos de conclusão

Santos, T.L.; Pereira, G. M.; Rocha, K. O.. Participação em banca de Gabriel Santos Martins. Adsorção de Bisfenol A por biochar proveniente de pirólise de lodo de tratamento de efluentes de tinturaria têxtil. 2025. Trabalho de Conclusão de Curso (Graduação em Química Tecnológica) - Universidade Estadual Paulista Júlio de Mesquita Filho.

Santos, T.L.; Silveira, M. L. D. C.; Rocha, K. O.. Participação em banca de Renato Pereira Murback Filho. Determinação da isoterma de absorção de diferentes corantes em $CaZrO_3$ preparado pelo método hidrotermal assistido por microondas. 2023. Trabalho de Conclusão de Curso (Graduação em Física) - Universidade Estadual Paulista Júlio de Mesquita Filho.

PARTICIPAÇÃO EM EVENTOS CIENTÍFICOS

International Conference on Wider-Uptake of Water Resource Recovery from Wastewater Treatment (ICWRR2024). Wastewater Treatment in Tubular Photobioreactors: Exploring the Impact of Support Medium. 2024.

Congresso de Pós-graduação da FEB (COPENG). 2023; 2024; 2025.

1o. Fórum de Sustentabilidade Hídrica de Bauru (Fórum Gota d'água). 2019.

7 Encontro Nacional das Águas (ENA). 2018.

VII TALLER de Cianobacterias toxígenas en Argentina. 2018.

Seminário de Saúde Ambiental - Qualidade de água - Abastecimento Público dos Comitês PCJ.Problemas de tratabilidade da água no município de Santa Gertrudes. 2012.

XVI CONEEQ - Congresso Nacional dos Estudantes de Engenharia Química. 2007.

VI CONGRESSO BRASILEIRO DE ENGENHARIA QUÍMICA EM INICIAÇÃO CIENTÍFICA. 2005.